ISSN 0704-2582
ISBN 0-7729-1761-2

THESE TERMS GOVERN YOUR USE OF THIS DOCUMENT

Your use of this Ontario Geological Survey document (the "Content") is governed by the terms set out on this page ("Terms of Use"). By downloading this Content, you (the "User") have accepted, and have agreed to be bound by, the Terms of Use.

Content: This Content is offered by the Province of Ontario's *Ministry of Northern Development and Mines* (MNDM) as a public service, on an "as-is" basis. Recommendations and statements of opinion expressed in the Content are those of the author or authors and are not to be construed as statement of government policy. You are solely responsible for your use of the Content. You should not rely on the Content for legal advice nor as authoritative in your particular circumstances. Users should verify the accuracy and applicability of any Content before acting on it. MNDM does not guarantee, or make any warranty express or implied, that the Content is current, accurate, complete or reliable. MNDM is not responsible for any damage however caused, which results, directly or indirectly, from your use of the Content. MNDM assumes no legal liability or responsibility for the Content whatsoever.

Links to Other Web Sites: This Content may contain links, to Web sites that are not operated by MNDM. Linked Web sites may not be available in French. MNDM neither endorses nor assumes any responsibility for the safety, accuracy or availability of linked Web sites or the information contained on them. The linked Web sites, their operation and content are the responsibility of the person or entity for which they were created or maintained (the "Owner"). Both your use of a linked Web site, and your right to use or reproduce information or materials from a linked Web site, are subject to the terms of use governing that particular Web site. Any comments or inquiries regarding a linked Web site must be directed to its Owner.

Copyright: Canadian and international intellectual property laws protect the Content. Unless otherwise indicated, copyright is held by the Queen's Printer for Ontario.

It is recommended that reference to the Content be made in the following form:

Gupta, V.K. and Wadge, D.R. 1986, Gravity Study of the Birch, Uchi and Red Lakes Area, District of Kenora (Patricia Portion); Ontario Geological Survey, Report 252, 98p.

Use and Reproduction of Content: The Content may be used and reproduced only in accordance with applicable intellectual property laws. *Non-commercial* use of unsubstantial excerpts of the Content is permitted provided that appropriate credit is given and Crown copyright is acknowledged. Any substantial reproduction of the Content or any *commercial* use of all or part of the Content is prohibited without the prior written permission of MNDM. Substantial reproduction includes the reproduction of any illustration or figure, such as, but not limited to graphs, charts and maps. Commercial use includes commercial distribution of the Content, the reproduction of multiple copies of the Content for any purpose whether or not commercial, use of the Content in commercial publications, and the creation of value-added products using the Content.

Contact:

FOR FURTHER INFORMATION ON	PLEASE CONTACT:	BY TELEPHONE:	BY E-MAIL:
The Reproduction of Content	MNDM Publication Services	Local: (705) 670-5691 Toll Free: 1-888-415-9845, ext. 5691 (inside Canada, United States)	pubsales.ndm@ontario.ca
The Purchase of MNDM Publications	MNDM Publication Sales	Local: (705) 670-5691 Toll Free: 1-888-415-9845, ext. 5691 (inside Canada, United States)	pubsales.ndm@ontario.ca
Crown Copyright	Queen's Printer	Local: (416) 326-2678 Toll Free: 1-800-668-9938 (inside Canada, United States)	copyright@gov.on.ca

Mines and Minerals Division

Ontario Geological Survey
Report 252

Gravity Study of the Birch, Uchi, and Red Lakes Area District of Kenora (Patricia Portion)

1986

Ministry of
Northern Development
and Mines

Ontario

Mines and Minerals Division

Ontario Geological Survey
Report 252

Gravity Study of the Birch, Uchi, and Red Lakes Area District of Kenora (Patricia Portion)

by
V.K. Gupta and D.R. Wadge

1986

Ontario
Ministry of
Northern Development
and Mines

Publications of the Ontario Geological Survey, Ministry of Northern Development and Mines, are available from the following sources. Orders for publications should be accompanied by cheque or money order payable to the *Treasurer of Ontario*.

Reports, maps, and price lists (personal shopping or mail order):

Public Information Centre, Ministry of Natural Resources

Room 1640, Whitney Block, Queen's Park

Toronto, Ontario M7A 1W3

Reports and accompanying maps only (personal shopping):

Ontario Government Bookstore

Main Floor, 880 Bay Street

Toronto, Ontario M7A 1N8

Reports and accompanying maps (mail order or telephone orders):

Publications Services Section, Ministry of Government Services

5th Floor, 880 Bay Street

Toronto, Ontario M7A 1N8

Telephone (local calls) 965-6015

Toll-free long distance 1-800-268-7540

Toll-free from Area Code 807 0-ZENITH-67200

Canadian Cataloguing in Publication Data

Gupta, V.K. (Vinod K.), 1942-

Gravity study of the Birch, Uchi and Red Lake areas, district of Kenora (Patricia portion)

(Ontario Geological Survey report, ISSN 0704-2582 ; 252)

ISBN 0-7729-1761-2

1. Gravity--Ontario--Kenora Region. I. Wadge, D.R.

II. Ontario. Ministry of Northern Development and Mines.

III. Ontario Geological Survey. IV. Title. V. Series.

QB335.C3G86 1986 526'.7'097131 C86-099698-0

Critical Reader: R.B. Barlow

Scientific Editor: Guy Kendrick

1000 - 86 - U of T

FOREWORD

This gravity study is partly the result of two summers of field work carried out by staff of the Ontario Geological Survey during the summers of 1975 and 1976. The survey was designed to cover an area of 21 100 km^2, and investigate mineral-rich, near surface metavolcanics as well as large crustal geologic features. Major residual gravity anomalies have been explained in terms of their geological and tectonic significance. Two-dimensional gravity models have been computed to arrive at subsurface configurations of the greenstone belts and the surrounding granitic areas.

It is hoped that the results of this study will provide an important third dimensional constraint to the geoscientists that will assist them in generating realistic tectonic models for the evolution of the Archean greenstone belts.

V.G. Milne
Director
Ontario Geological Survey

Contents

TABLES

FIGURES

GEOPHYSICAL MAPS (back pocket)

CONVERSION FACTORS FOR MEASUREMENTS IN ONTARIO GEOLOGICAL SURVEY PUBLICATIONS

If the reader wishes to convert imperial units to SI (metric) units or SI units to imperial units the following multipliers should be used:

CONVERSION FROM SI TO IMPERIAL			CONVERSION FROM IMPERIAL TO SI		
SI Unit	*Multiplied by*	*Gives*	*Imperial Unit*	*Multiplied by*	*Gives*
			LENGTH		
1 mm	0.039 37	inches	1 inch	**25.4**	mm
1 cm	0.393 70	inches	1 inch	**2.54**	cm
1 m	3.280 84	feet	1 foot	**0.304 8**	m
1 m	0.049 709 7	chains	1 chain	20.116 8	m
1 km	0.621 371	miles (statute)	1 mile (statute)	**1.609 344**	km
			AREA		
1 cm^2	0.155 0	square inches	1 square inch	**6.451 6**	cm^2
1 m^2	10.763 9	square feet	1 square foot	**0.092 903 04**	m^2
1 km^2	0.386 10	square miles	1 square mile	2.589 988	km^2
1 ha	2.471 054	acres	1 acre	0.404 685 6	ha
			VOLUME		
1 cm^3	0.061 02	cubic inches	1 cubic inch	**16.387 064**	cm^3
1 m^3	35.314 7	cubic feet	1 cubic foot	0.028 316 85	m^3
1 m^3	1.308 0	cubic yards	1 cubic yard	0.764 555	m^3
			CAPACITY		
1 L	1.759 755	pints	1 pint	0.568 261	L
1 L	0.879 877	quarts	1 quart	1.136 522	L
1 L	0.219 969	gallons	1 gallon	**4.546 090**	L
			MASS		
1 g	0.035 273 96	ounces (avdp)	1 ounce (avdp)	28.349 523	g
1 g	0.032 150 75	ounces (troy)	1 ounce (troy)	**31.103 476 8**	g
1 kg	2.204 62	pounds (avdp)	1 pound (avdp)	**0.453 592 37**	kg
1 kg	0.001 102 3	tons (short)	1 ton (short)	**907.184 74**	kg
1 t	1.102 311	tons (short)	1 ton (short)	**0.907 184 74**	t
1 kg	0.000 984 21	tons (long)	1 ton (long)	**1016.046 908 8**	kg
1 t	0.984 206 5	tons (long)	1 ton (long)	**1.016 046 908 8**	t
			CONCENTRATION		
1 g/t	0.029 166 6	ounce (troy)/ ton (short)	1 ounce (troy)/ ton (short)	34.285 714 2	g/t
1 g/t	0.583 333 33	pennyweights/ ton (short)	1 pennyweight/ ton (short)	1.714 285 7	g/t

OTHER USEFUL CONVERSION FACTORS

1 ounce (troy)/ton (short)	20.0	pennyweights/ton (short)
1 pennyweight/ton (short)	0.05	ounce (troy)/ton (short)

NOTE–Conversion factors which are in bold type are exact. The conversion factors have been taken from or have been derived from factors given in the Metric Practice Guide for the Canadian Mining and Metallurgical Industries published by The Mining Association of Canada in co-operation with the Coal Association of Canada.

Gravity Study of the Birch, Uchi, and Red Lakes Area District of Kenora (Patricia Portion)

V.K. Gupta and D.R. Wadge

Geophysicists, Geophysics and Geochemistry Section, Ontario Geological Survey, Toronto.

Manuscript accepted for publication by the Chief of the Geophysics and Geochemistry Section, May 15, 1986. This report is published with the consent of V.G. Milne, Director, Ontario Geological Survey.

Abstract

The results of a detailed gravity study of an area of about 21 100 km^2 in Northwestern Ontario, District of Kenora (Patricia Portion) are reported. The area includes parts of the English River, the Uchi, and the Berens River geological Subprovinces, and covers the Red Lake and Birch-Uchi Precambrian Greenstone Belts.

Data from 5180 gravity stations established during the summers of 1975 and 1976 were compiled to produce a map of Bouguer gravity anomalies. A discussion of the density measurements made during the survey on over 2800 fresh rock samples is given for each major rock unit that enables a computation to be made of the gravity models.

The Bouguer gravity anomalies were divided into relatively short (due to shallow, local sources) and long (due to large crustal features) wavelength components by means of spectrum analysis, upward continuation, and graphical smoothing techniques. A comparison of the filtered maps with the local geology showed that the spectrum and 16.09 km upward continuation based maps were unable to satisfactorily isolate the two components of the Bouguer gravity field.

Thus, graphically smoothed regional and residual maps with a bias towards the geology were prepared for two-dimensional gravity modeling purposes. A vertical second derivative map of the gravity field is found to be useful in lithological identification and with resolution of stratigraphic problems.

The residual Bouguer anomaly map shows numerous positive and negative anomalies which are usually associated with high density metavolcanics and low density granitic rocks, respectively. Two-dimensional gravity modeling carried out along 26 gravity profiles suggests that the modeled greenstone belts generally indicate broad synformal basin-like shape with varying thicknesses. The depth extent of greenstones averages 4 km in the Red Lake Belt, between 3.5 to 4 km in the Birch-Uchi Belt, 2.3 km in the Dixie Lake Belt, and about 1 km in the Coli Lake Belt. The felsic to intermediate metavolcanics and metasediments (Uchi Subprovince) are less than 1.5 km thick. The bottom topography of the models sometimes reflects typical synclinal, anticlinal, or homoclinal structures whose vertical projection onto the surface in many instances coincide with mapped structures. The gravity modeling suggests that most granitic batholiths are relatively thin, sheet-like, or flat sill-like, usually between 4 to 7 km depth-extent, with relatively inhomogeneous phases near the greenstone/granite boundary. Exceptions are the Gull Lake (about 13 to 16 km deep), the Rosen Lake (about 10 to 12 km deep), and the Trout River (about 9 km deep) Batholiths.

The 12 to 15 mgal amplitude residual positive anomaly associated with the boundary between the Uchi and English River Subprovinces indicates the existence of an east-west trending Archean metasedimentary trough which dips steeply to the south reaching depths varying between 8.5 to 10 km.

The regional gravity model, which compares with the seismic depths, has been explained by undulations on the Riel and Mohorovičić discontinuities.

Gravity Study of the Birch, Uchi, and Red Lakes Area, District of Kenora (Patricia Portion), by V.K. Gupta and D.R. Wadge, Ontario Geological Survey Report 252, 98p. Accompanied by Maps 2492, 2493, 2494 and 2495, scale 1:250 000. Published 1986. ISBN 0-7729-1761-2.

RESUME

On trouvera décrits ici les résultats d'une étude détaillée sur la gravité d'une région couvrant près de 21 000 km^2 dans le Nord-Ouest de l'Ontario, district de Kenora (Section de Patricia). Cette région englobe certaines parties de la rivière English, l'Uchi, les sept sous-provinces géologiques de la rivière Berens et s'étend sur les ceintures de roches vertes précambriennes de Red Lake et de Birch-Uchi.

Les données recueillies par 5180 stations de gravité créées au cours des étés 1975 et 1976 ont été rassemblées pour produire une carte des anomalies de gravité de Bouguer. Chaque grande unité de roches fait l'objet d'explications sur les mesures de densité prises au cours de l'enquête effectuée sur plus de 2800 nouveaux échantillons de roches, qui permet de calculer les modèles de gravité.

Les anomalies de gravité de Bouguer ont été séparées en composantes de longueurs d'ondes relativement courtes (en raison de sources locales peu profondes) et longues (en raison des caractéristiques de l'écorce terrestre) par le recours à des techniques d'analyse spectrale, de continuation verticale et d'aplanissement graphique. La comparaison des cartes filtrées avec la géologie de la région a révélé que les cartes s'appuyant sur l'analyse spectrale et la continuation verticale sur 16,09 km ne permettaient pas d'isoler de manière satisfaisante les deux composantes du champ de gravité de Bouguer.

On a donc préparé des cartes régionales et résiduelles graphiquement aplanies, avec une orientation géologique pour façonner des modèles de gravité bi-dimensionnelle. On a trouvé utile de disposer de la carte verticale à une deuxième deuxième dérivée du champ de gravité pour l'identification lithologique et la solution des problèmes stratigraphiques.

La carte des anomalies résiduelles de Bouguer révèle de nombreuses anomalies positives et négatives que l'on associe généralement à la présence respective de roches métavolcaniques de haute densité et de roches granitiques de basse densité. Le façonnement des modèles de gavité bi-dimensionnelle effectué à partir de 26 profils de gravité indique que les ceintures de roches vertes prennant habituellement la forme d'un vaste bassin synformal de plusieurs épaisseurs. La profondeur des roches vertes varie entre 4 et 1 km dans la ceinture du lac Red et entre 3,5 et 4 km dans la ceinture de Birch-Uchi, elle avoisine 2,3 km dans la ceinture du lac Dixie et 1 km dans la ceinture du lac Coli. Les roches métavolcaniques et métasédimentaires felsiques à intermédiaires (sous-province d'Uchi) ont moins d'1,5 km d'épaisseur. La topographie du fond des modèles reflète parfois des structures synclinales, anticlinales ou homoclinales typiques dont la projection verticale sur la surface coincide souvent avec des structures indiquées sur les cartes. Le façonnement des modèles de gravité révèle que la plupart des batholites granitiques sont relativement fins, comme des feuilles, ou plats, comme des filons-couches, et ont habituellement entre 4 et 7 km de profondeur, avec des phases relativement inhomogènes près de la limite entre les roches vertes et le granit. Les batholites du lac Gull (qui a près de 13 à 16 km de profondeur), du lac Rosen (près de 10 à 12 km de profondeur) et de la rivière Trout (près de 9 km de profondeur) font exception à la règle.

L'anomalie positive résiduelle d'une amplitude de 12 à 15 mgal associée à la limite entre les sous-provinces d'Uchi et de la rivière English révèle l'existence d'un pli synclinal, formé de roches métasédimentaires archéennes, orienté vers l'est-ouest et qui plonge abruptement vers le sud pour atteindre des profondeurs variant entre 8,5 et 10 km.

On a expliqué le modèle de gravité de la région, comparable aux profondeurs sismiques, par des accidents de terrain sur les discontinuités de Riel et de Mohorovicic.

Introduction

The results presented in this report form part of the Ontario Geological Survey's systematic detailed gravity survey of the Precambrian metavolcanic-metasedimentary belts of Ontario. Geological studies in many of these belts have shown that they are lithologically and structurally complex with significant density contrasts. Gravity survey is, therefore, one of the few feasible methods for determining the deeper geological and structural characteristics of the relatively flat and often inaccessible Precambrian terrain of Ontario. The present study considers the implications of the gravity field for the structure and geometry of the Birch-Uchi and Red Lake Greenstone Belts in the Uchi Subprovince of Northwestern Ontario.

The area of investigation (Figure 1), situated within the Superior Province of the Precambrian Shield, includes parts of three geological subprovinces. These are: the Uchi Subprovince in the middle which is bounded on the north by the Berens River Subprovince, and on the south by the English River Subprovince (Figure 1). Numerous metavolcanic-metasedimentary belts and distinct felsic intrusive rocks are located throughout the survey area. In the Uchi Subprovince, the study area of this report includes two economically important and structurally complex metavolcanic-metasedimentary belts, namely the Birch-Uchi and Red Lake Belts. These two belts are important for gold, silver, and base metals and have several past and producing mines.

The gravity survey was undertaken during the summer months of 1975 and 1976. The survey was designed to cover a vast area (21 100 km^2) since both the short wavelength (shallow supracrustal rocks) as well as long wavelength (deep crustal) geological features were of interest. Emphasis in the field was placed on a closer spacing of gravity stations over the known metavolcanic metasedimentary areas. A total of 5180 gravity stations were established using four LaCoste-Romberg model G gravimeters. During the course of the survey, over 2800 fresh rock samples were collected from outcrops of various lithologic units. As a result of this work, two preliminary Bouguer gravity maps have already been published (Gupta and Wadge 1978; Barlow *et al.* 1976). For final publication, these two maps were combined to produce a Bouguer gravity map at 1:250 000 scale (Map 2492, back pocket). Geological maps for the survey area are available from the Ontario Geological Survey at scales varying from 1:12 000 to 1:253 440.

The interpretation of the local (near surface) geological features, usually represented by small wavelength "residual anomalies", is best carried out by removing the long wavelength "regional anomalies" from the observed gravity field. As this study is primarily concerned with residual gravity features, a variety of regional-residual separation methods were applied to the Bouguer gravity map. These are upward continuation filters, optimum filters designed from an analysis of the energy spectrum, and visual graphical smoothing. The filtered maps obtained were compared with the mapped geology. To enhance anomalies originating from shallow sources, an optimum second derivative map was also computed.

Quantitative two-dimensional model analysis of the graphically smoothed residual gravity field has been carried out along 26 profiles covering most of the prominent anomalies. Computed gravity models have been compared with the mapped geology. For certain strike limited anomalies, a strike correction has been applied to the two dimensional models. A crustal gravity model was also computed across the broad long wavelength regional gravity low of the survey area to investigate the configuration of the deep crustal boundaries, that is, of the Riel and Mohorovicic discontinuities. The regional gravity interpretation is compared with the seismic results of Hall and Hajnal (1969).

The object of this study has been:

1. To study the relationship of the gravity field with the geology
2. To obtain the geometry and depth of infolding of the various greenstone belts and to investigate their contact relationship with the surrounding granitic terrain
3. To determine the nature and configuration of those metasedimentary and igneous rocks that have a gravity expression
4. To study the large scale deep crustal structures of the area.

Location and Accessibility

The map area is bounded by Latitudes 50°30'N to 51°45'N, and by Longitudes 91°45'W to 94°30'W. The main access to the area is provided by Highway 105 (Vermilion Bay to Ear Falls to Red Lake) which originates from Trans-Canada Highway 17. An all season gravel road extends from Ear Falls to the South Bay Mine on Confederation Lake. The Nungesser northern resources gravel road, which joins with Highway 125 just northeast of Red Lake, cuts across the northwestern section of the map area and runs northward about 120 km to the Berens River bridge. A network of lumber, mining, and resource access roads provides access to various interconnecting lake systems. Remote areas are normally reached by float-equipped fixed wing aircraft and helicopters.

Previous Gravity Studies

Until recently, little gravity work had been done in this area. The first regional gravity interpretation was by Innes (1960) who suggested, based on meagre gravity data, that the depth-extent of the basic rocks in the Red Lake area is between 1.9 and 4.1 km. Later, Grant *et al.* (1965) established 108 gravity stations along two traverses in the Red Lake area and suggested a depth extent of 7.6 km for the metavolcanic rocks. The first systematic regional gravity survey of the Red Lake

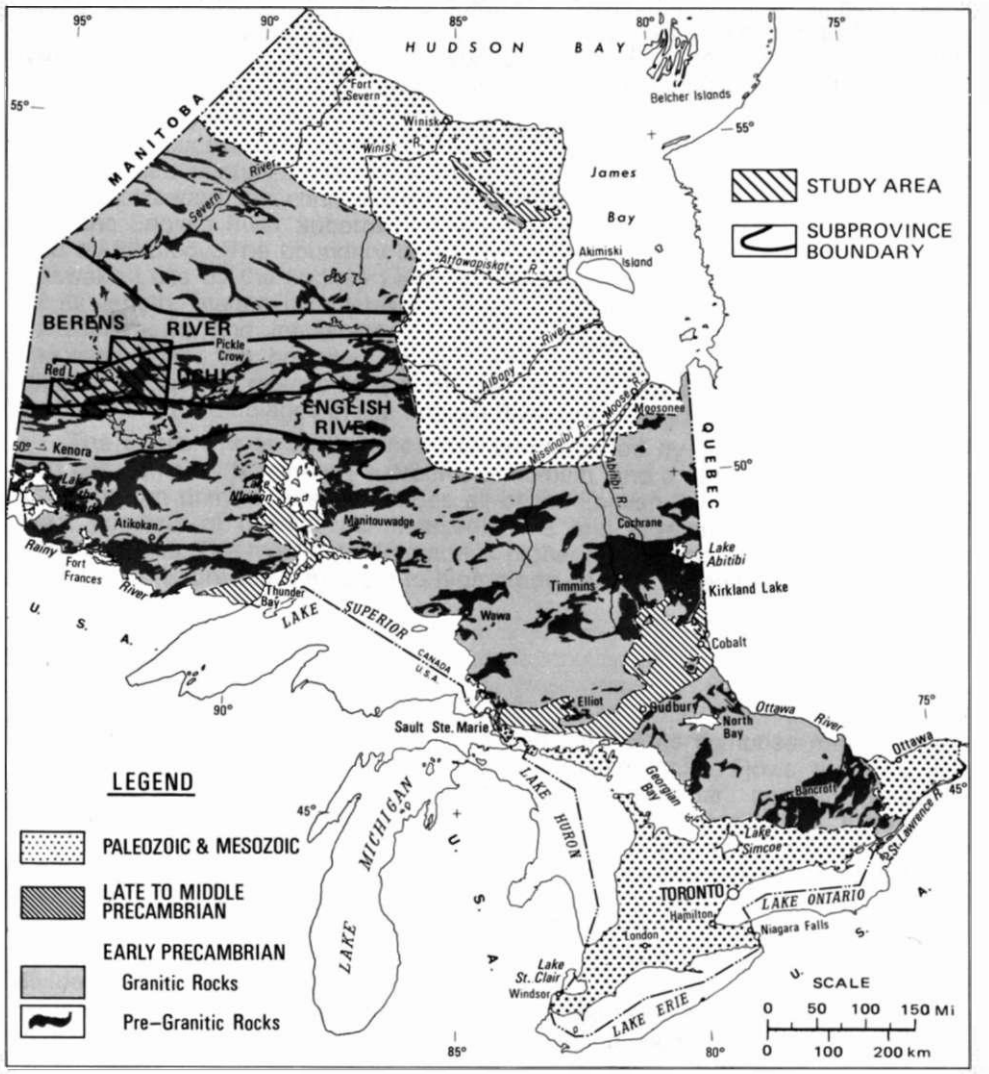

Figure 1. *Location of the study area*

and Birch-Uchi Lakes areas was undertaken by the Earth Physics Branch, Ottawa. They established 160 gravity stations in a grid-like pattern, approximately 13 km apart. The results were released as a series of Bouguer anomaly maps, contoured at 5 mgal intervals, at a scale of 1:500 000 (Observatories Branch, 1967, 1973). Recently, a quantitative interpretation study, involving two and three dimensional gravity models, was carried out in the Red Lake region by Runnalls (1978).

Acknowledgments

The authors acknowledge the contributions made by the assistants in collecting the field data. The authors were fortunate in having the services of D. Kinvig, R. Hinds, A. Jurkevics, R. Runnalls, I. MacLeod, J. Buchanan, J. Bedrij, and B. Chamberlain. R.B. Barlow served as leader for the 1975 field season and was instrumental in the planning and organization of the field program. Gratitude is also extended to P. Mark for his able assistance both in the office and in carrying out field work. K.D. Card and P. Nunes gave their valuable time in rechecking many of the rock sample identifications at the base camp. Many local residents, tourist operators, and government agencies too numerous to mention, provided valuable information and services. Discussions with numerous individuals especially, P.C. Thurston, J. Pirie, A.C. Colvine, W.D. Bond, F.W. Breaks, B. Wilson, J. Misner, and F.S. Grant have been valuable. N. Ramani assisted with the processing, computational, and plotting stages of this project. His assistance is sincerely acknowledged. Finally, the authors would like to thank T.H. Dusanowskyj, who, in the summer of 1978, assisted with the interpretation and computer modeling of the data.

General Geology

INTRODUCTION

The study area lies within the Superior Province of the Canadian Shield, and contains Archean supracrustal and plutonic rocks covered for the most part by Pleistocene and Recent unconsolidated sediments. The map area (Figure 2) includes parts of three subprovinces (Ayres *et al.* 1971). The Berens River Subprovince occurs along the northern edge of the map area, the English River Subprovince occurs along the southern edge and between them is the Uchi Subprovince.

The Berens River Subprovince is composed of low to high grade massive and gneissic plutonic rocks and scattered small, generally highly metamorphosed metavolcanic metasedimentary remnants. The boundary with the Uchi Subprovince is irregular and poorly defined, and may be chosen, somewhat arbitrarily, as the northern contact of recognizable Uchi metavolcanic rocks (Schwerdtner and Goodwin 1977). It has been proposed that the Berens River Subprovince in Ontario represents a zone of deeper and more intense plutonic activity than the adjacent Uchi Subprovince (Ayres *et al.* 1973).

The Uchi Subprovince comprises isoclinally folded, metavolcanic-metasedimentary sequences (greenstone belts) that are intruded by composite granitoid batholiths ranging in composition from diorite to granite; the average composition being granodiorite (Ayres 1978).

In the study area, the Uchi Subprovince is dominated by the Red Lake and Birch-Uchi supracrustal belts. Numerous small supracrustal belts are quasi-continuous with the Birch-Uchi Belt. The grade of metamorphism is lower than in the Berens River Subprovince, with characteristic low pressure, very low to low grade, and occasionally medium grade mineral assemblages in the metavolcanic and metasedimentary rocks. In the two larger belts, the grade of metamorphism increases toward the contact with the surrounding plutonic rocks. The boundary with the English River Subprovince is better defined, in part by structure, and in part by lithology. The boundary is delineated from the western edge of the map to Pakwash Lake by the Sydney Lake cataclastic zone which separates, along much of its length, metatexitic metasedimentary migmatite on the southern side from metasediments and metavolcanics on the northern side (Stone 1977). East of Pakwash Lake, the boundary is less well defined, marking the transition from distally deposited metavolcanics of the Uchi Subprovince to wacke mudstone sedimentary assemblages of the English River Subprovince (Breaks *et al.* 1978).

The English River Subprovince has been divided by Breaks and Bond (1977) into two domains: a northern supracrustal domain, and a southern plutonic domain. The northern domain, which includes all of the English River rocks within the map area, consists of migmatized metasediments and a relatively low proportion of plutonic rocks. The metamorphic grade is higher than in the Uchi Subprovince, with slightly higher pressure, medium to high grade mineral assemblages (Thurston and Breaks 1978).

SUPRACRUSTAL ROCKS

Metavolcanics

Metavolcanics within the Birch-Uchi and Red Lake Belts comprise mafic to felsic flows, pyroclastic rocks, and subvolcanic intrusive rocks. Flows are frequently composed of pillowed, brecciated, porphyritic amygdular, and spherulitic, or variolitic rocks. Pyroclastic rocks include tuff, lapilli tuff, lapillistone, tuff-breccia, and volcanic breccia. Wherever possible, mafic, intermediate, and felsic metavolcanic rocks, corresponding roughly to basaltic to andesitic, andesitic to rhyodacitic, and rhyodacitic to rhyolitic rocks (Ayres 1974), respectively, have been differentiated on the map. (*See* Maps 2492, 2493, 2494, and 2495, back pocket).

In the southern part of the Birch-Uchi Belt, the metavolcanics have been divided by Thurston (1976, 1985) into three volcanic cycles (Ayres 1974; Anhaeusser 1971). These cycles each began with the extrusion of massive and pillowed mafic flows followed by dominantly explosive intermediate to felsic volcanism.

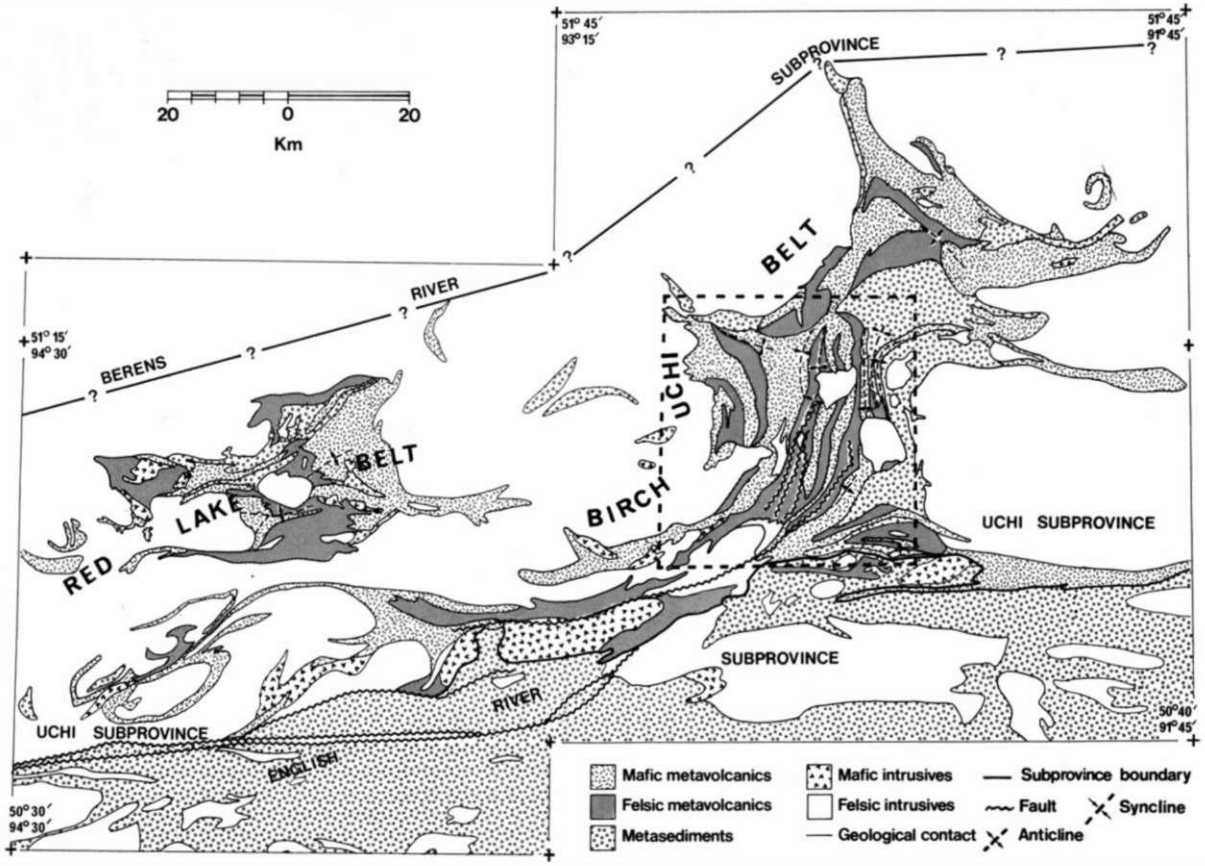

Figure 2. *Generalized geological map*

Metasediments are common within, and between the volcanic cycles. The stratigraphy delineated in this area by Thurston has not been successfully traced into the northern part of the Birch-Uchi Belt (Thurston 1977, 1985).

The nature of volcanic cyclicity elsewhere in the Red Lake-Uchi Lake region is not well defined. Work by Ferguson (1972) in the Red Lake Belt implies one or possibly two cycles, while more recent mapping by Riley (1975, 1976, 1978a, 1978b), Pirie and Sawitzky (1977), and Pirie and Grant (1978a, 1978b) suggests two or possibly three cycles. Other metavolcanic belts, including those at Longlegged, Dixie, Slate, and Papaonga Lakes (Breaks *et al.* 1978) may represent parts of one or more cycles.

Metasediments

The bulk of the metasediments in the Red Lake and Birch-Uchi region are clastic, though significant proportions of chemical metasediments have been mapped. The clastic rocks comprise mainly wackes, lesser amounts of arenites and mudstones, and metamorphosed equivalents of all these rocks. Conglomerate occurs in relatively minor amounts. These metasediments are dominantly volcanic in origin although other sources, especially granitoid terrains, may be locally important.

Chert is the predominant chemical rock. Iron oxides, sulphides, and silicates are common, occasionally forming oxide or sulphide facies iron formation. Carbonate facies iron formation is rarely found. Other metamorphosed precipitates occurring in a few locations include calc-silicates and marble.

Sediments within the northern supracrustal domain of the English River Subprovince have been metamorphosed to form metatexitic and diatexitic metasedimentary migmatite (Breaks *et al.* 1978). Metatexite, representing the commonest migmatite in the map area, consists of rock produced by a process of segregation, generally of quartz and feldspar, to form alternating layers of wacke and 10 percent to 60 percent granitoid to pegmatitic mobilizate. Diatexite lacks continuous migmatitic banding and is composed of 60 percent to 90 percent mobilizate.

INTRUSIVE ROCKS

Intermediate to Ultramafic Intrusive Rocks

Intermediate to ultramafic intrusive rocks range in composition from quartz diorite, diorite, anorthosite, gabbro, and diabase to pyroxenite, peridotite, and dunite and their altered equivalents, notably serpentinite. Most of the ultramafic intrusive rocks are partly or wholly carbonitized or serpentinized (Riley 1975, 1978a). In generalizing rock units for the map, (*see* maps 2492, 2493, 2494, and 2495, in back pocket) many small intermediate to ultramafic intrusions have been omitted. Where gabbroic bodies have intruded mafic metavolcanics, rocks of equivalent composition and density, even large gabbroic plutons have been left off the map.

Subvolcanic Intrusive Rocks

Subvolcanic intrusive rocks occur throughout the map area and form an integral part of the supracrustal succession. Rocks of probable subvolcanic origin include abundant small dikes and sills of various compositions, gabbroic dikes and sills which are often indistinguishable from coarse-grained massive mafic flows, and quartz-feldspar porphyry which is occasionally difficult to distinguish from rhyolitic flows and pyroclastic rocks. Large bodies of felsic subvolcanic intrusive rocks are shown on the map (Map 2492, back pocket) and are grouped, using a separate code, with the felsic to intermediate intrusive rocks.

Felsic to Intermediate Intrusive Rocks

There exists, within the map area, a great diversity of felsic to intermediate intrusive rocks. Numerous variants of granite *sensu stricto* through granodiorite, trondhjemite, quartz monzonite, and syenodiorite (monzonite) occur as aplitic to pegmatitic plutons. The multifarious granitoid phases and the lack of detailed

mapping in many parts of the region preclude the drawing of contacts between phases on the map.

STRUCTURE

Folds

The regional structure within the map area has not been completely determined, but considerable detail has been described in the southern part of the Birch-Uchi Belt (Thurston 1976, 1978, 1985; Thurston and Jackson 1978). A cross-section drawn through the centres of Corless, Dent, Agnew, and Costello Townships would show a central syncline cored by Cycle III metavolcanics and, to the east, an anticline-syncline-anticline triplet folding metavolcanics of Cycle I. Although these folds may be traced to the north and south through adjoining townships, probably reflecting the dominant fold pattern, the complete picture must be more complex as is indicated by bedding top reversals in Honeywell (Johns and Thurston 1975) and Earngey (Thurston *et al.* 1974) Townships. Other folds, those through Goodall and Skinner Townships, at Shabumeni Lake, and at Birch Lake, are based on available stratigraphic and bedding top data.

A syncline-anticline pair has been traced through the Red Lake Belt by Riley (1978a, 1978b), Pirie and Sawitzky (1977), and Pirie and Grant (1978a, 1978b). Other major folds, anticlines similar to those shown on the map (*see* back pocket), must pass through Baird and Heyson Townships, and Dome, Balmer, and Bateman Townships to account for bedding top reversals shown by Ferguson (1965a, 1965b), and Pirie and Grant (1978b).

Faults

Minor faults, displaying little or no offset in stratigraphy, are abundant throughout the Birch-Uchi and Red Lake region. For simplicity, only a few larger faults have been drawn on the map. Faults shown in the south-central part of the Birch-Uchi Belt are from a compilation by Thurston and Jackson (1978).

By far the largest fault is represented by the Sydney Lake cataclastic zone, which has been shown to be continuous from the Ontario-Manitoba border west of the map area to Pakwash Lake (Breaks *et al.* 1978). East of Pakwash Lake, the zone is discontinuous, probably deflecting northward into the metavolcanics of the Birch-Uchi Belt (Breaks *et al.* 1978). The cataclastic zone is a region of extreme strain generally marked by a 1 to 2 km wide band of protomylonitic to mylonitic rocks (Stone 1977). Offset on the fault is right-handed with a possible strike separation in the order of 10s of kms and a dip separation; the south side was uplifted about 2 km relative to the north side (Stone 1981).

GRAVITY SURVEY

SURVEY METHODS

The following primary data are recorded at each station in a land gravity survey: the time of observation in Greenwich Mean Time (GMT), the observed gravimeter scale value, the elevation of the station with reference to mean sea level, and the grid coordinates. During the summers of 1975 and 1976, a total of 5180 gravity stations were established, utilizing fixed wing De Havilland Beaver aircraft, a Bell G-4 helicopter, and four-wheel drive vehicles. Transportation on lakes was by means of outboard motor-equipped canoes and boats.

Four LaCoste-Romberg model G gravimeters, numbers G-28, G-294, G-329, and G-417 were used during the survey. The gravity station sites were preselected on topographic maps at convenient locations to enable a uniform density of coverage. The gravity station distribution varied from 1 station per 2 km^2 in areas of known metavolcanics to 1 station per 6 km^2 in areas of granitic rocks and metasediments. The average station distribution over the entire area was one gravity station per 4.1 km^2.

The gravity observations were tied to control stations established by the Earth Physics Branch, Ottawa, at Red Lake, Ear Falls, and Vermilion Bay. These stations form part of the national gravity network which is tied to the International Gravity Standardization Net 1971.

During the present survey, 14 gravity base stations were established to an order of precision somewhat comparable with that of the Earth Physics Branch, Ottawa. The location of most of these base stations in the field is permanently marked by placing an aluminum disc on the ground. Both the survey stations and the base stations are marked on the gravity maps (Gupta and Wadge 1978; Barlow *et al.* 1976). The LaCoste-Romberg gravimeters which are relatively drift-free were read at control stations every day at the beginning and end of each traverse to check for instrument drift which averaged about 0.03 mgal per day (1 mgal = 10^{-5} Nkg^{-1} = 10 Gravity Units).

ELEVATION CONTROL

Survey elevation control was provided by bench marks of the Geodetic Survey of Canada, Ontario Ministry of Transportation and Communications, and Ontario Hydro.

For gravity stations near the lakeshores, the elevations were recorded relative to water surface elevations of lakes, which in turn were determined either by precise levelling from nearby bench marks, or by using Wallace and Tiernan altimeters in pair. Highway and railroad elevations were also used in some instances. Altimeters were read at a known elevation approximately every one to two hours in order to correct elevations of the intermediate stations for variations in barometric pressure. Wet and dry bulb temperatures were recorded using a psychrometer for temperature and humidity corrections.

HORIZONTAL CONTROL

The gravity stations were established at identifiable sites and were located on 1:57 420 scale air photographs. The station positions were then transferred onto base maps (scale 1:63 360) which were compiled in Transverse Mercator Projection with a three degree grid superimposed. The gravity stations were digitized with a precision of ±40 m.

ERRORS IN THE GRAVITY ANOMALIES

The accuracy of the final Bouguer anomaly values, which were reduced to the datum of the mean sea level using a uniform crustal density of 2.67 g/cm^3, is limited by the following sources of error.

Elevation Errors

The principal source of error in a gravity survey comes from the uncertainty in elevation measurements using altimeters. In this area, the elevations are accurate to within ±0.3 m for 993 gravity stations, while 1508 gravity station elevations are accurate to within ±1 m. The remaining 2679 gravity station elevations are accurate to within ±3 m. The average deviation of the altimeter elevations calculated from 200 independently repeated altimeter measurements of 62 sites was ±2.1 m. This is equivalent to an error of ±0.4 mgal in the Bouguer anomalies.

Location Errors

Gravity station positions were located correctly to within ±40 m. This imprecision is equivalent to errors of about ±0.03 mgal in the latitude correction.

Terrain Correction Errors

The average elevation for all the gravity stations is 386 m (from mean sea level) with a standard deviation of ±23 m. The gravity stations were located on flat ground to minimize the gravity effect of local terrain. Terrain corrections are not

calculated since the relief of the area is relatively flat; the maximum relief is 65 m over a distance of 24 km. It is estimated that the maximum error from irregular topography would not exceed 0.1 mgal.

Instrument Errors

An error may arise due to the assumption of a linear gravimeter drift between the control readings. This average error due to the instrument drift is approximately ±0.035 mgal.

Observational errors arising from factors such as poor levelling of the gravimeter would not exceed ±0.02 mgal.

Error Summary

The resulting maximum expected error, defined as the square root of the sum of the squares of the individual errors, in the Bouguer anomaly due to the above listed sources will be about ±0.42 mgal for any gravity station.

PRESENTATION OF BOUGUER ANOMALY MAP

The Bouguer anomaly map (Figure 3, and Map 2492 in back pocket) was compiled using a gridding and contouring program developed specifically for random data location. The randomly spaced observed gravity data were interpolated to a 1.609 km grid cell size. A nine point smoothing on the final Bouguer contours was also applied. The gravity data superimposed on generalized geology are presented on the Bouguer anomaly map (Map 2492, back pocket) at a scale of 1:250 000; the contour interval is 20 gravity units which is equivalent to 2 mgal.

The principal facts of all gravity stations, descriptions of control station locations, and detailed density data are available at cost from the Geophysics/Geochemistry Section, Ontario Geological Survey, Ontario Ministry of Northern Development and Mines, 77 Grenville Street, Toronto, Ontario, M7A 1W4.

ROCK DENSITIES

INTRODUCTION

During the course of the gravity survey, 2813 fresh rock samples were collected at or near gravity station sites. Hand samples were chosen in a manner as to be representative of the whole outcrop, so that mean density values might be assigned to the major rock types in the survey area. Density values were obtained in the field by weighing dry and saturated specimen of rocks in air and water, respectively. These results, considered to be accurate to 0.01 g/cm^3, were averaged to assign mean representative values for each of the major rock types. The mean, standard deviation, and the range of densities are listed in Table 1. Density histograms for major rock types are shown in Figure 4.

METAVOLCANICS

The metavolcanics were classified into two general groups, mafic to intermediate, and felsic to intermediate types. The mafic to intermediate metavolcanics exhibit a broad range in density (2.71 to 3.28 g/cm^3). This suggests that a number of rock samples belonging to the lighter felsic to intermediate classification have been included into the mafic to intermediate group. This is due to the limitations imposed in classifying dark coloured hand specimens of limited size without the benefit of chemical analysis, study of the whole outcrop, or microscopic work.

The histogram obtained from 376 samples of the mafic to intermediate metavolcanics is negatively skewed about a mean density of 2.93 g/cm^3. This density is close to the value 2.94 g/cm^3 which was obtained from 14 basalt samples. Among all the rocks, the density contrast with respect to the background is the largest for the mafic to intermediate metavolcanics and thus they contribute substantially to the Bouguer gravity field of the area.

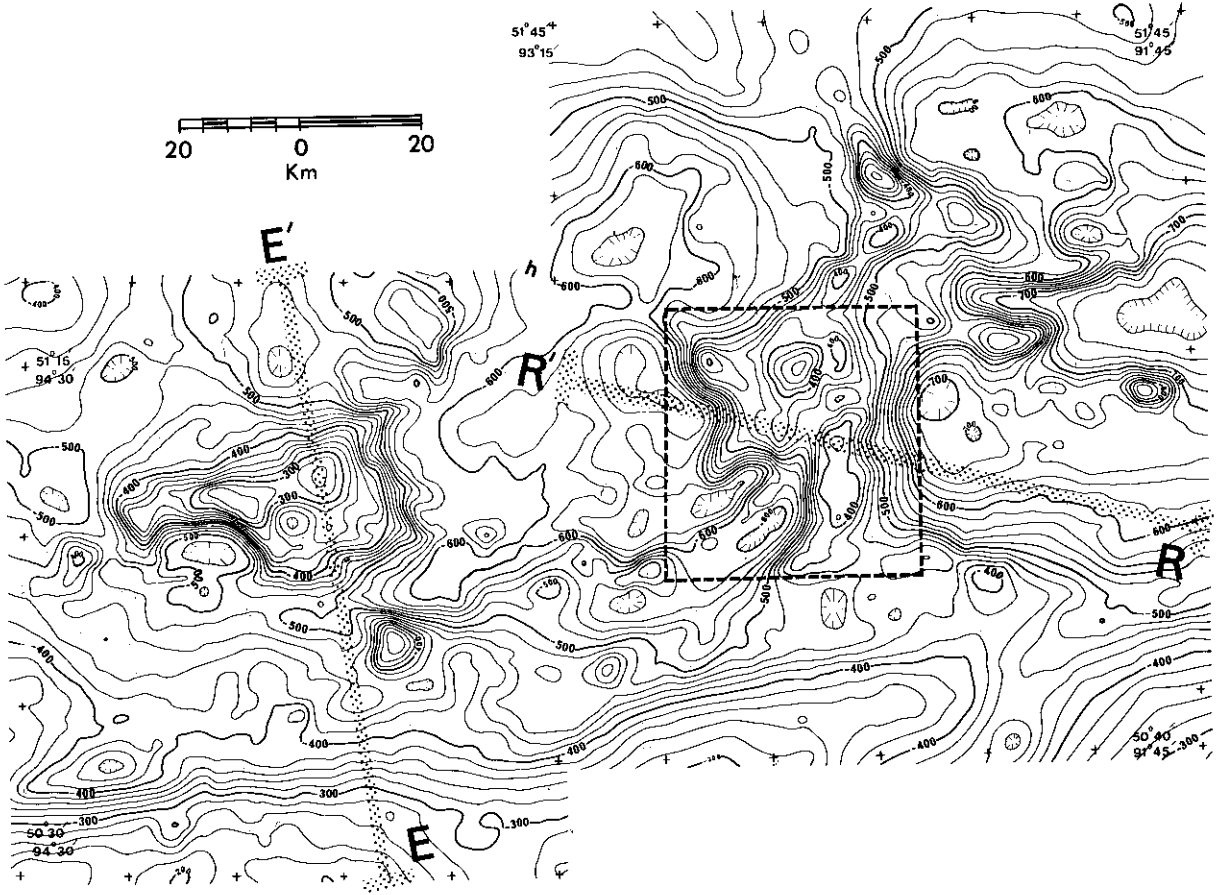

Figure 3. *Bouguer gravity anomaly contour map. Contour interval is 2 mgal. The locations of Profiles EE' and RR' are also shown.*

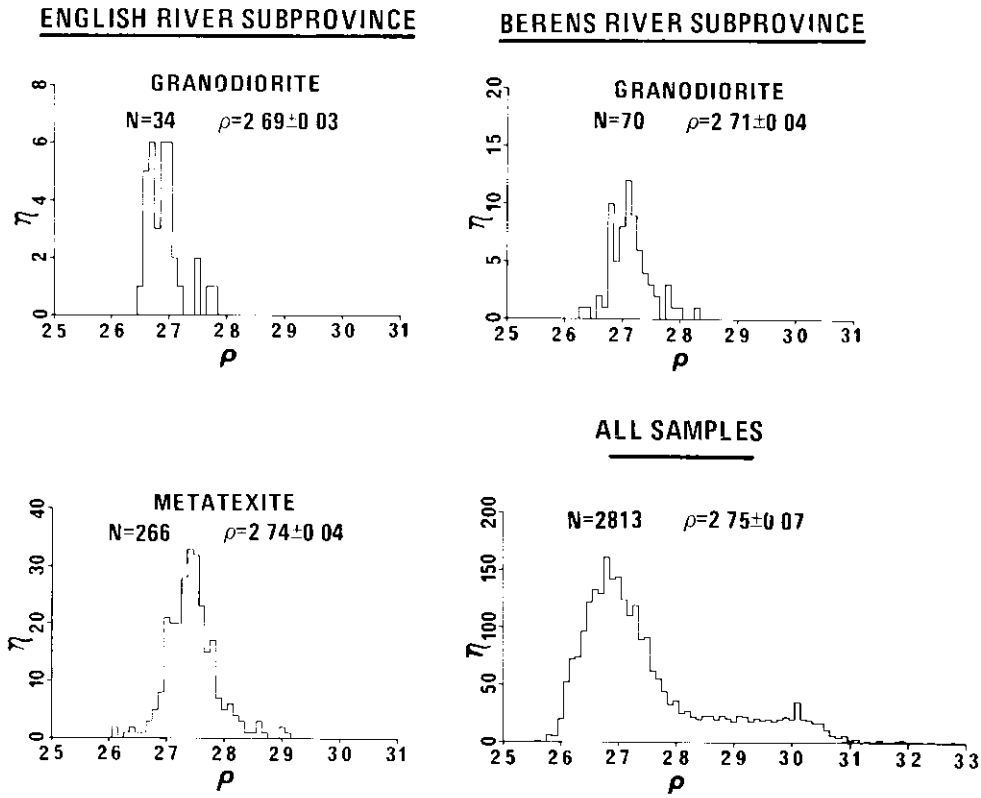

Figure 4 Density histograms

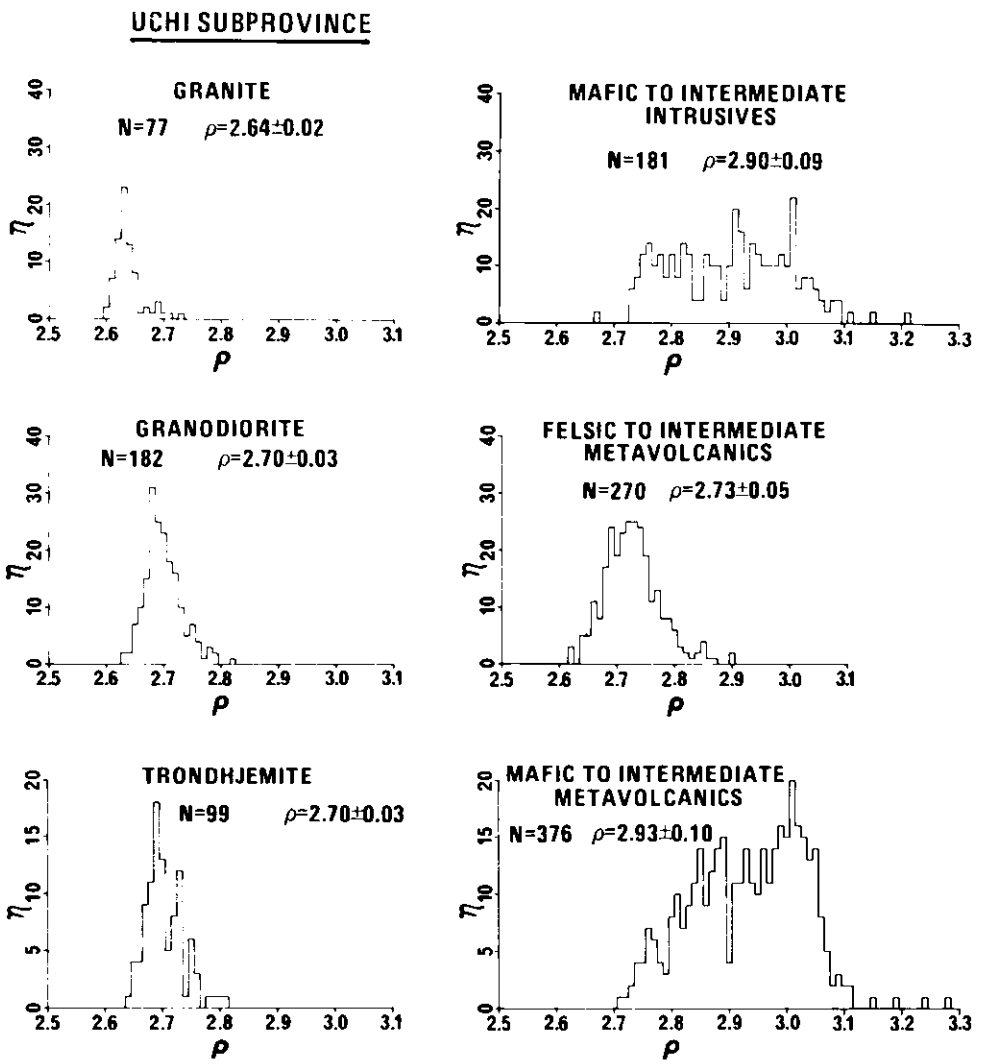

Figure 4 *(continued). Density histograms*

TABLE 1. SUMMARY OF DENSITY MEASUREMENTS (g/cm^3).

Rock Type	N	R	$\rho \pm s$
Uchi Subprovince			
Felsic to Intermediate Intrusive Rocks			
All Samples (not weighted)	914	2.58-2.89	2.68±0.05
Granite	77	2.60-2.73	2.64±0.02
Quartz Monzonite	105	2.61-2.72	2.66±0.02
Granitic Gneiss	75	2.63-2.78	2.68±0.03
Granodiorite	182	2.63-2.82	2.70±0.03
Trondhjemite	99	2.64-2.81	2.70±0.03
Quartz Diorite	28	2.67-2.84	2.75±0.04
Mafic to Intermediate Intrusive Rocks			
All Samples (not weighted)	181	2.67-3.21	2.90±0.09
Diorite	88	2.67-2.96	2.83±0.06
Gabbro	82	2.86-3.21	2.98±0.07
Ultramafic Intrusive Rocks			
All Samples (not weighted)	25	2.60-3.01	2.80±0.11
Metasediments			
All Samples (not weighted)	154	2.58-3.02	2.75±0.07
Wacke	50	2.68-2.84	2.75±0.04
Metavolcanics			
Felsic Metavolcanics	38	2.62-2.76	2.68±0.03
Felsic to Intermediate Metavolcanics	270	2.62-2.90	2.73±0.05
Intermediate Metavolcanics	85	2.67-2.90	2.77±0.05
Mafic to Intermediate Metavolcanics	376	2.71-3.28	2.93±0.10
Basalt	14	2.81-3.06	2.94±0.08
Berens River Subprovince			
Felsic to Intermediate Intrusive Rocks			
All samples (not weighted)	181	2.60-2.83	2.69±0.04
Granite	33	2.60-2.71	2.63±0.03
Quartz Monzonite	34	2.63-2.70	2.67±0.02
Granodiorite	70	2.63-2.83	2.71±0.04
Mafic to Intermediate Intrusive Rocks			
Diorite	14	2.71-2.94	2.81±0.05
English River Subprovince			
Felsic to Intermediate Intrusive Rocks			
All samples (not weighted)	207	2.58-2.84	2.67±0.04
Granite	15	2.58-2.66	2.62±0.02
Quartz Monzonite	63	2.59-2.70	2.64±0.02
Granitic Gneiss	25	2.62-2.83	2.68±0.05
Granodiorite	34	2.65-2.78	2.69±0.03
Trondhjemite	70	2.63-2.84	2.69±0.04
Mafic to Intermediate Intrusive Rocks			
Diorite	6	2.76-2.96	2.87±0.07
Metasediments			
All samples (not weighted)	348	2.60-2.91	2.72±0.10
Diatexite	31	2.61-2.64	2.63±0.01
Metatexite	266	2.61-2.91	2.74±0.04
Total of all Samples (not weighted)	2813	2.58-3.28	2.75±0.07

N = number of samples; R = density range in g/cm^3; ρ = mean density in g/cm^3; s = standard deviation in g/cm^3

A unimodel distribution is obtained for 270 samples of the felsic to intermediate metavolcanics, the calculated mean density being 2.73 g/cm^3. The mean density of 85 samples recognized as intermediate metavolcanics is 2.77 g/cm^3.

METASEDIMENTS

The density evaluation of the metasediments is based on their location whether they are in the Uchi Subprovince or whether they are in the English River Subprovince. In general, the metasediments of the two subprovinces have almost similar average densities.

The mean density of all the Uchi Subprovince metasediments is 2.75 g/cm^3 which is calculated from 154 samples (*see* Table 1). The dominant metasediments are the wackes with a mean density of 2.75 g/cm^3, based on 50 samples.

In the English River Subprovince, the metatexites and the wackes have been combined in one group for density purposes and the diatexite densities are listed separately. The histogram (Figure 4) for 266 metatexite and wacke samples shows a unimodel distribution with a calculated mean density of 2.74 g/cm^3. The calculated mean density of diatexites is 2.63 g/cm^3.

GRANITOID AND INTRUSIVE ROCKS

A mean density of 2.64 g/cm^3 has been obtained for 77 granite samples from the Uchi Subprovince. Their histogram (Figure 4) is unimodel with a slight positive skew. Densities of 33 granite samples belonging to the Berens River Subprovince (?) average 2.63 g/cm^3. Thus, the granites, having the largest negative density contrast with the background, will produce negative Bouguer anomalies.

The mafic to intermediate intrusive rocks of the Uchi Subprovince have a mean density of 2.90 g/cm^{3}which is based on 181 samples. The histogram of these rocks show a wide density variation and have a bell-shaped curve.

BACKGROUND DENSITY

An overall mean of 2.75 g/cm^3, using all the densities measured in the survey region, has been obtained for the Precambrian rocks as a whole. Due to a higher than usual proportion of metavolcanic units in the sample, however, it is felt that this value is on the high side, and is not representative of the true mean density of the upper crustal rocks in the region. Thurston (1978) and Breaks and Bond (1977) proposed that the average upper crustal composition in the region ranges from tonalite-granodiorite to trondhjemite.

An examination of Table 1 reveals that granodiorites sampled by subprovinces show that their mean densities are 2.71 g/cm^3 (70 samples), 2.70 g/cm^3 (182 samples), and 2.69 g/cm^3 (34 samples) from Berens River, Uchi, and English River Subprovinces, respectively. Similarly, the trondhjemites have mean densities of 2.70 g/cm^3 (99 samples) and 2.69 g/cm^3 (70 samples) from the Uchi and English River Subprovinces, respectively. The granitic gneisses belonging to both the Uchi and English River Subprovinces have a mean density of 2.68 g/cm^3 (100 samples).

Based on the above density data, a value of 2.69 g/cm^3 has been chosen to represent the mean density for the upper crustal rocks of the survey region, approximating that of granite-gneiss, granodiorite, and trondhjemite. The value 2.69 g/cm^3 has thus been considered to be the "background density" having zero density contrast for the purpose of gravity modeling and interpretation.

DENSITIES USED IN GRAVITY MODELING

The average densities used in gravity modeling were chosen either directly from the summary of density measurements shown in Table 1 for relatively homogeneous areas, or were calculated directly from a plot of density values. The density values from this density plot were then averaged over a 8 x 8 km grid for relatively inhomogeneous areas. In many instances, to facilitate gravity modeling, narrow and small geological units were grouped together to form a single unit.

Such units were assigned weighted average densities which were calculated from an areal proportion of all the units used in the formation of the single unit.

A weighted mean density was also computed for the mafic, intermediate, and felsic metavolcanics as a whole. The areal proportions used in the estimation of a single weighted density are those given by Thurston (1978) and Goodwin (1972, 1977) for the "greenstone" rocks of the Uchi Subprovince. A weighted mean density of 2.87 g/cm^3 was calculated for the metavolcanics of the Uchi Subprovince based on these proposed ratios and by adopting the densities shown in Table 1.

The appropriate density values used in the construction and interpretation of two-dimensional gravity models are given along the modeled gravity profiles.

PATTERN RECOGNITION AND DATA TREATMENT

INTRODUCTION

The separation of a Bouguer gravity field into its regional and residual components is often an ambiguous and relatively troublesome task. In recent years, the application of digital filters has become increasingly popular with the geophysicist to achieve this regional residual separation. The effectiveness of these mathematically derived maps from the viewpoint of quantitative gravity modeling is, however, still debatable. An attempt is made in this study to evaluate the use of digital filtering together with various other separation techniques by using them on the actual field data of the study area. A brief description of the filtering techniques applied to the present data is also presented. The filtered maps have been compared with the mapped geology and critically examined from the view point of gravity modeling and interpretation.

The different steps in the analysis of the potential field data using frequency domain techniques are as follows:

1. calculation of the Fourier transform
2. estimation of the power spectrum
3. separation of the power spectrum into different components: regional, residual, and noise
4. design of suitable filters to separate the field into signals due to these components
5. obtaining the filtered map by multiplying the Fourier transform by the filter transfer function and calculating the inverse Fourier transform.

In this study, the computer software system MAGMAP of Patterson, Grant and Watson Limited, was used for most of the computations.

OPTIMUM FILTERS

The term 'regional-residual analysis' is used to describe the process of isolating anomaly patterns of the kinds in which one is interested (residual), from the remainder of the field (regional). The most common example is where the geologist, interested in the surface features, wishes to remove the effect of deeper sources. Until recently, regional-residual separation was done using co-efficient sets approximating the desired operator, or by using trend surface analysis, the techniques being mathematically somewhat arbitrary. With the advent of the fast Fourier transform (Cooley and Tukey 1965), it is convenient at present to use mathematically defined operators in the frequency domain for the filtering operations (Clarke 1969; Spector and Grant 1970; Ku *et al.* 1971; Meyer 1974). Here, one first computes the power spectrum of the map and looks for a separation of power that can be ascribed to signal and noise. Optimum matched filters are then designed to separate the components or to enhance or suppress effects of specific wave lengths which correspond to certain geological features (Gupta and Ramani 1978, 1980).

Wiener's filter theory (1949) provided the method for designing the required filters. The mapped data t is assumed to be the sum of a signal s and a noise

component n. One wishes to design a linear filter whose output d approximates s in some statistical sense. Under certain assumptions, the optimum filter which minimizes the mean square error between d and s is given by (in the frequency domain):

$$H_{opt}(f) = P_s(f)/P_t(f) \quad (1)$$

where $P_s(f)$ is the signal power and $P_t(f)$ is the total power. Thus the procedure involves:

1. obtaining the two-dimensional Fourier transform of the input data
2. computing the power spectrum
3. estimating the regional, residual, and noise parts of the data from the power spectrum.

The Fourier Transform

Consider a field F (x,y) known only on a regular grid of finite size. In order to use Fourier techniques, one assumes that this measured data is repeated outside the recorded range. Thus, if M x N values are known with x and y, the grid spacings in the x and y directions, respectively, the two dimensional discrete Fourier transform can be defined as:

$$F(u,v) = \frac{1}{MN} \sum_{m=o}^{M-1} \sum_{n=o}^{N-1} f(m\Delta x, n\Delta y)\, e^{-2\pi i (um\Delta x + vn\Delta y)}$$

$$u = \frac{k}{M\Delta x} \; ; \qquad v = \frac{\ell}{N\Delta y} \, , \quad (2)$$

$$k = 0 \text{ ---- } M-1 \qquad \ell = 0 \text{ ---- } N-1$$

The use of this transform for filtering applications results in distortions because of the windowing effect due to the finite map size. In an attempt to minimize these distortions, the above transform is sometimes refined using two-dimensional window functions. The MAGMAP computer package uses a prediction operator to extrapolate the data outside the map area and thus the edge effect is minimized.

Estimation of the Power Spectrum

In general, power spectra of gravity data can be roughly divided into three segment signals. The part at the low-frequency (long wavelength) end of the spectrum with a steep slope in power is termed regional, that is, due to sources that are deep and/or broad. At high frequencies (short wavelengths), the residual part has a flatter slope and is due to relatively shallow sources. Spector and Grant (1970) showed that a single straight line fitted to a part of the spectrum corresponds to a single average depth. At very high frequencies, the spectrum is dominated by the effects due to measurement errors, digitizing errors, etc.

The two-dimensional power spectrum is simply the square of the absolute value of the Fourier Transform, that is,

$$E(u,v) = F(u,v).\, F^*(u,v) \quad (3)$$

where * denotes the complex conjugate.

Following Spector and Grant (1970), a radially averaged spectrum P(f) was computed for further analysis, where $f = (u^2 + v^2)^{1/2}$. The use of a radial average

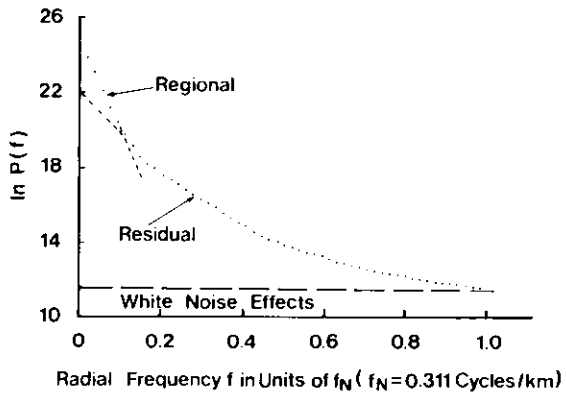

Figure 5. *Radial component of the power spectrum of the Bouguer gravity map.*

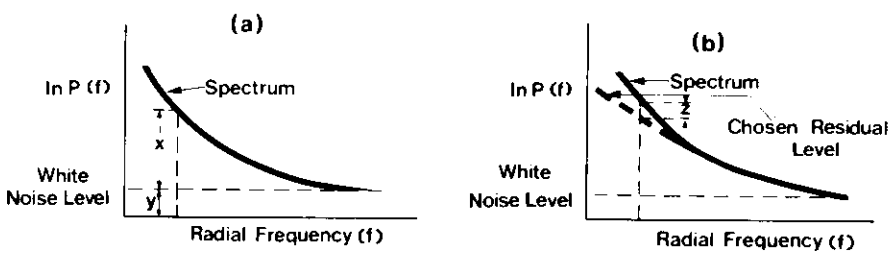

Figure 6. *Calculation of the optimum filters from the spectrum.*

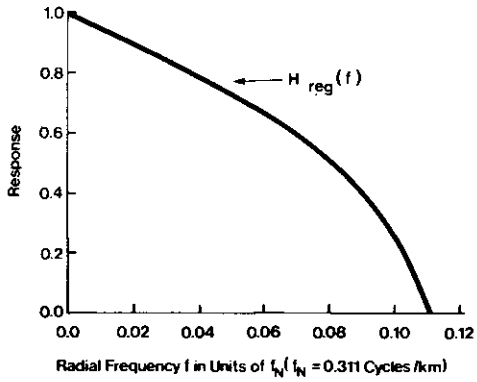

Figure 7. *Radial frequency domain response of the optimum regional filter $H_{reg}(f)$.*

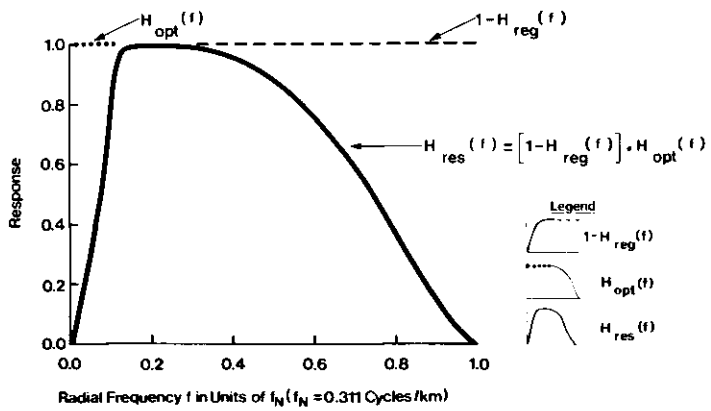

Figure 8. *Radial frequency domain response of the optimum residual filter $H_{res}(f)$.*

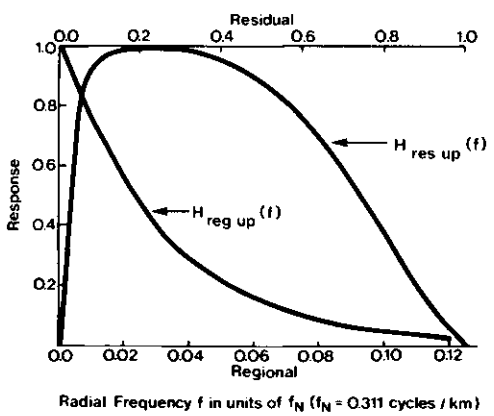

Figure 9. *Radial frequency domain response of the upward continued regional $H_{reg,up}(f)$ and residual $H_{res,up}(f)$ filters.*

spectrum has a smoothing effect on the spectrum and also simplifies the design of the filters.

The spectrum was calculated for a digitizing interval of 1.609 km. and was plotted on a logarithmic scale (Figure 5). Straight-line asymptotes were drawn on the spectral plot at the lower and higher frequency ends. The two lines were connected by a smooth curve to allow for the overlap of the component powers. The part of the spectrum below 0.034 (i.e. 0.11 f_N) cycles/km was called 'regional' and the part from 0.034 (i.e. $0.11f_N$) to 0.311 (i.e. $1.0f_N$) cycles/km was called 'residual', where f_N is the Nyquist frequency (0.311 cycles/km). The high frequency end of the spectrum was extrapolated smoothly until it flattened out and the white noise level was taken as ln (P_n) = 11.5. Figure 5 shows the spectrum divided, subjectively, into its regional, residual, and noise components.

Design of Optimum Filters

The Wiener (1949) filter theory provides a method for designing the required filters. Consider a field t consisting of a signal s and noise n, then

$$t = s + n \tag{4}$$

and one wishes to extract the signal s from t by a linear filtering process. Since this is in general impossible, one aims to design a filter whose output d approximates s in some statistical sense. Under certain assumptions, the optimum Wiener filter, having a response Hopt (f) minimizes the mean-square error between the desired filter output s and the actual filter output d. The transfer function of such a filter is given by (Weiner 1949).

$$H_{opt}(f) = \frac{P_s(f)}{P_t(f)} = \frac{P_s(f)}{P_s(f) + P_n(f)} \tag{5}$$

where f is the frequency, $P_s(f)$ is the power of the signal, $P_n(f)$ is the noise power, and $P_t(f)$ is the total power.

The optimum filters can be calculated quite easily from the spectrum as follows. In Figure 6a at a particular frequency f, let x(f) be the signal power and y(f) the white noise power, then from equation (5.5):

$$\begin{aligned} H_{opt}(f) &= \frac{P_s(f)}{P_t(f)} \\ &= 1 - \frac{P_n(f)}{P_t(f)} \\ &= 1 - \frac{e^{y(f)}}{e^{[x(f) + y(f)]}} \\ &= 1 - e^{-x(f)} \end{aligned} \tag{6}$$

Similarly, if z(f) is the logarithmic distance between the chosen residual level and the spectrum (Figure 6b), the optimum regional filter is given by

$$H_{reg}(f) = 1 - e^{-z(f)} \quad (7)$$

and the optimum residual filter is given by

$$H_{res}(f) = [1-H_{reg}(f)].\ H_{opt}(f) \quad (8)$$

In the current study, $H_{reg}(0)$ was set equal to unity (Figure 7) to include all the low frequency components in the regional. This requires slight adjustment in the response curve in the zero-frequency region.

The responses of the regional and residual filters designed are shown in Figures 7 and 8, respectively. The regional filter is a low-pass filter which falls off to 0 at 0.034 ($0.11f_N$) cycles/km and has a cut-off at 0.031 ($0.1f_N$) cycles/km. The cut-off being defined as the frequency at which the gain falls to 20 percent of the peak (Figure 7). The residual filter is a band-pass filter with a low frequency cut-off at 0.012 ($0.04\ f_N$) cycles/km and a high frequency cut-off at 0.274 ($0.88\ f_N$) cycles/km (Figure 8).

From the radial filter, the equivalent two-dimensional filter is first calculated. The filtered map is then obtained as the inverse Fourier transform of the product of the filter and the Fourier transform of the original map.

UPWARD CONTINUATION

Analytical continuation of the potential field map vertically upwards had been used often to approximate a regional map (Fuller 1967; Henderson 1960; Peters 1949). Once the Fourier transform of the mapped data is known, it is a simple matter to obtain the continued maps, the upward continuation filter being given by (Dean 1958)

$$H_{reg,up}(f) = e^{-2\pi hf} \quad (9)$$

where h is the continuation height. The map continued to a height of 16.09 km (that is, 10 grid units) was taken to be the regional gravity field. The residual field was obtained by applying to the Bouguer field an upward continued based residual filter.

$$H_{res,up}(f) = [1 - H_{reg,up}(f)].\ H_{opt}(f) \quad (10)$$

The radial frequency responses of both the regional and residual upward continuation filters are shown in Figure 9.

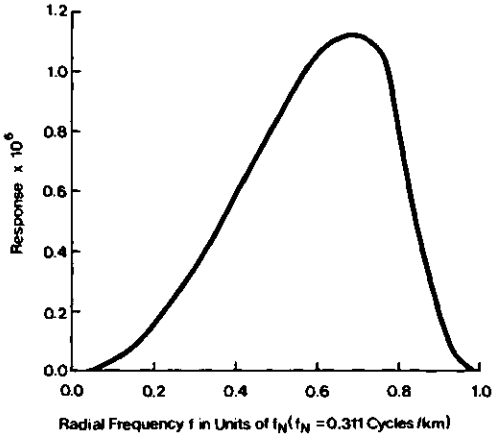

Figure 10. *Radial frequency domain response of the optimum second derivative filter $H_{drv}(f)$ used.*

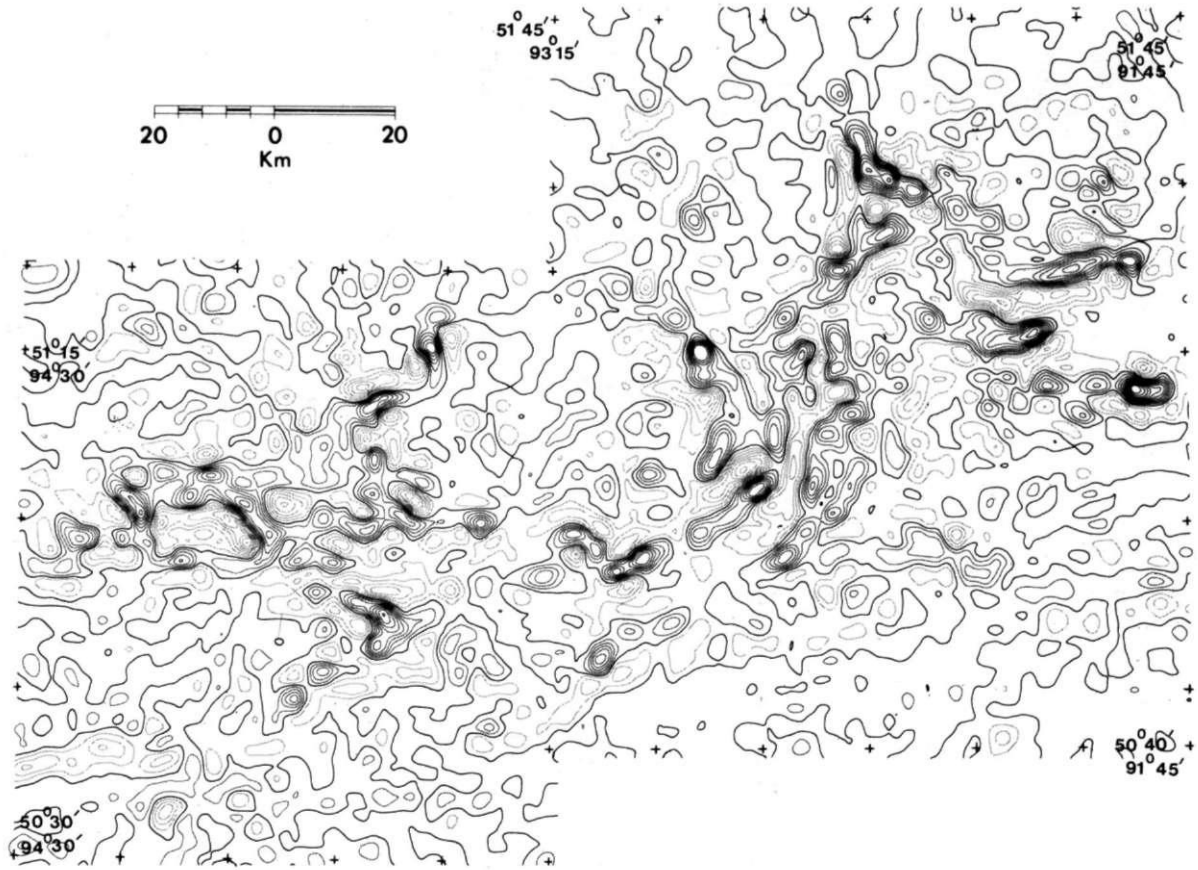

Figure 11. *Second vertical derivative of the Bouguer anomaly map. Contour interval 0.5 mgal/km^2. Positive contours are shown in dark, negative contours are shown in light, and zero contour is shown by solid black line.*

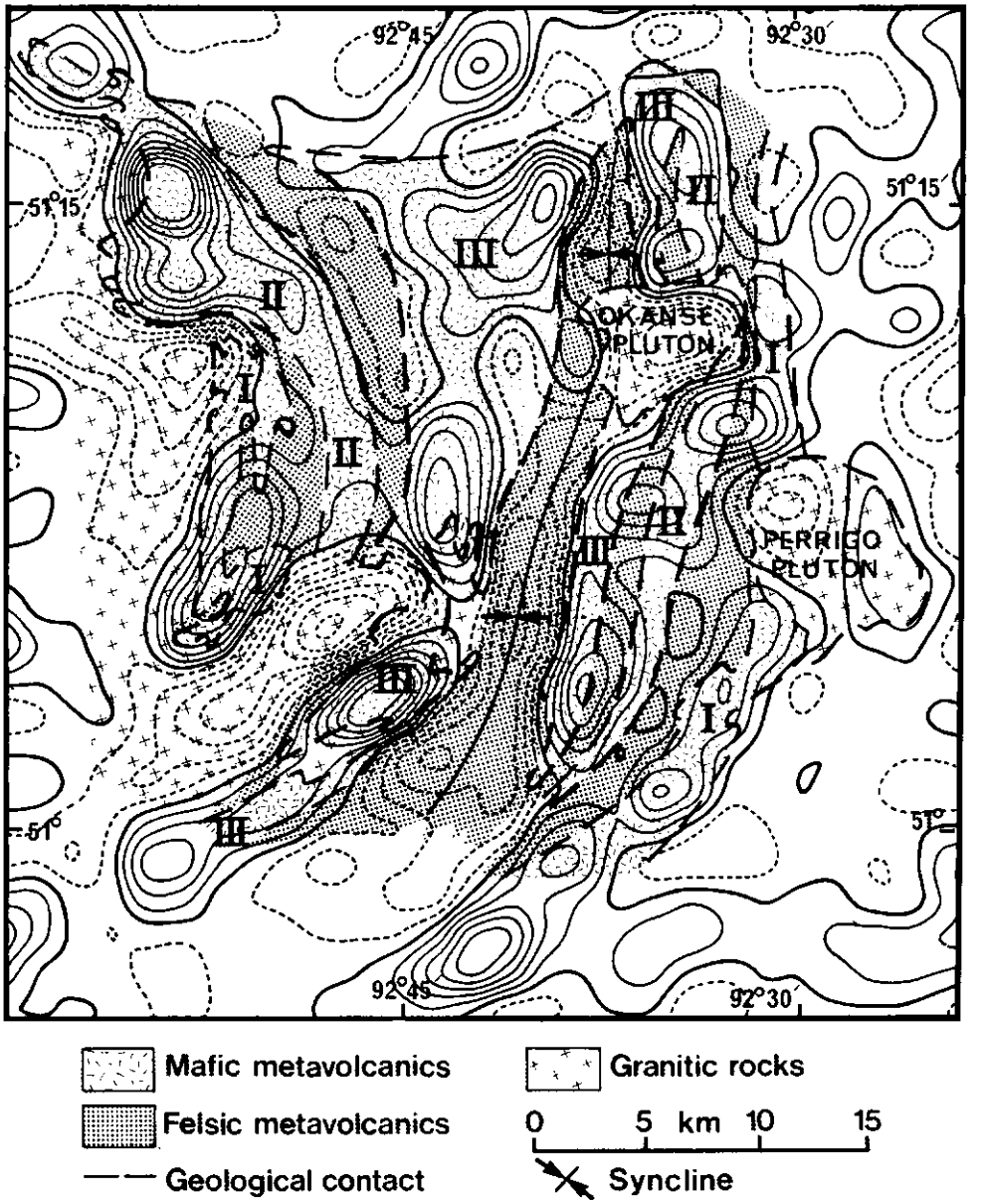

Figure 12. Second vertical derivative of the Bouguer anomaly map for the central part of the Birch-Uchi Greenstone Belt. Contour interval is 0.5 mgal/km^2. Positive contours are shown in dark, negative contours are shown in light, and zero contour is shown by solid black line. The surface geology and the mapped positions of mafic volcanic cycles I, II, and III are superimposed. Geology after Thurston (Thurston 1985).

GRAPHICAL SEPARATION

To estimate the regional gravity field, 25 north-south and 18 east-west Bouguer gravity profiles were drawn at 8.045 km (5 mile) intervals. On each profile, the level of the regional field was visually estimated by considering the influence on the gravity field brought about by local geology. The value of the regional field kept the same at profile intersections. Trondhjemitic and granodioritic areas were considered to represent the background gravity field. The resulting regional gravity field was hand digitized at an 8.045 km (5 mile) grid interval from which a 1.609 km (1 mile) grid was generated for automatic contouring of the regional field. The 1.609 km regional grid values were then automatically subtracted from the Bouguer gravity map to obtain a residual gravity map.

Positive residual anomalies were obtained in areas where their cause was obvious from the surface rocks or from measured density values. Similarly, negative residual anomalies were obtained where the observed field was producing a definite gravity low against the background that could be explained by surface rocks.

SECOND DERIVATIVE MAP

A second derivative gravity map has been computed to enhance the local variations of gravity field so that a correlation could be made between the second derivative anomalies and the surface geological features. A second derivative gravity field is more sensitive to weak anomalies arising from shallow sources and can be used effectively to delineate the boundaries of anomaly sources. In general, a second derivative gravity map can be considered equivalent to a special kind of residual gravity map which is devoid of any regional gravity component.

The second derivative map has been computed on a 1.609 km by 1.609 km (1 mile by 1 mile) grid by designing optimum second derivative filters. The radial frequency response of the optimum Weiner (1949) filter is given by

$$H_{dr.}\ (f) = (2\pi f)^2.\ H_{opt}(f) \qquad 11$$

This filter had a sharp cut-off at high frequencies and therefore a cosine-squared roll-off from 0.375 to 0.5 cycles/grid interval was applied to smooth the response. The filter used is shown in Figure 10. It has a peak at 0.217 (that is $0.7f_N$) cycles/km and low and high frequency cut-offs at 0.074 (that is 0.237 f_N) and 0.276 (that is 0.889 fN) cycles/km, respectively. The second derivative map which was obtained using the above optimum filter was contoured at an interval of 0.5 mgal/km^2 and is presented as Map 2495 (*in* back pocket) and Figure 11.

In general, the correlation of the second derivative positive and negative anomalies (Figure 11) is much more consistent with the surface geology than that of the residual anomalies. Many localized shallow geological features which are barely visible on Bouguer or residual gravity maps are intensified on the second derivative map. Strong positive and negative anomalies (Figure 11) correspond remarkably well with the surface exposures of the mafic and felsic metavolcanic units, respectively. In certain regions, the zero trace of the second derivative map near the "greenstone"- granite contact marks their boundary. A linear zone of negative second derivative anomalies near the southern edge of the map coincides with a mapped zone of cataclastic rocks. This zone is barely identifiable from the Bouguer anomaly field. Phases of mafic intrusive activity within the large plutonic bodies are distinguishable from the second derivative map. Overall, it is reasonable to propose that the stratigraphy may be delineated from an examination of the second-derivative map by identifying contrasting mafic and felsic metavolcanic anomaly sources.

In the present study, the usefulness of the second derivative map in terms of stratigraphic mapping can be assessed mainly in the central part of the Birch-Uchi Greenstone Belt where the geology has been mapped in detail by Thurston (1978). The north-trending central part of the Birch-Uchi Greenstone Belt (Figures 2 and 12) is isoclinally folded about a synclinorial axis. The metavolcanics of the belt consist of three basalt-to -rhyolite volcanic cycles — I, II and III — each with their mafic and felsic members (Goodwin 1967; Prystak 1971; Thurston *et al.* 1978). The

trace of the axial plane of the north-south trending syncline lies in the upper felsic metavolcanics of cycle III. In the central part of this belt, the narrow, linear zones of positive second derivative anomalies show excellent correlation with the mafic members of the volcanic cycles (Figure 12). Similarly, a linear 50 km long zone of negative second derivative anomalies coincides with the upper felsic metavolcanics of cycle III and follows the mapped synclinorial axis about which the metavolcanics of the Birch-Uchi Belt are folded. The second derivative of gravity thus clearly delineates the boundaries between the three basalt-to-rhyolite volcanic cycles.

The second derivative map is also useful in delineating structures which are obscure or poorly known. For example, some of the arcuate anomalies in the northern part of the Birch-Uchi Belt (near Casummit and Blondin gravity highs) and the western part of the Red Lake Belt (west of the Todd Fairlie gravity high) may correspond with local or regional fold-like structures. The second derivative map is a tool capable of delineating stratigraphy which in turn can be used in the resolution of structural problems.

EVALUATION OF COMPUTED MAPS

In this section, an evaluation of various regional and residual maps is considered in terms of their geological significance.

Regional Maps

In the spectrum-based regional map (Figure 13), broad circular gravity highs are obtained over both the Red Lake and Birch-Uchi greenstone belts and lows over the granitic plutons. Near the southern border of the map area, the east-west trending linear gravity contours coincide with the boundary between the Uchi and English River Subprovinces. Also, the total crust is considered to be thin along this boundary. The map retains anomalies >32 km in width. The upward continued regional map (Figure 14) shows a similarity to the spectrum based regional map except that the regional highs over the greenstone belts are less pronounced and are no longer delineated by close contours. These regional highs centred over the greenstone belts are probably due to the existence of relatively high density upper crustal greenstone rocks of this region. The graphically constructed regional map (Figure 15) shows an east-west trending gravity low where the contours take the form of concentric ellipses, occupying the entire map area. The regional field has been explained entirely by the undulations on the Riel and Mohorovicic discontinuities.

Residual Maps

The spectrum-based residual map (Figure 16) shows negative residual anomalies, in certain locations, that coincide with terrain of higher than background density material, namely, intermediate intrusive rocks (areas 1 and 6), metasediments (areas 2, 4 and 5), and mafic metavolcanics (areas 2 and 3).

These areas of poor correlation mentioned above show only a slight improvement in the upward continuation based residual map (Figure 17). The graphical residual anomalies are shown in Figure 18.

The correlation of the residual anomalies with surface geology is studied along two Bouguer gravity profiles EE′ and RR′ (Figure 19), onto which the regional fields were drawn from the appropriate maps. On profile EE′ (Figure 19a) between locations A to B and D to F, the negative residual anomalies produced from spectrum and upward continuation methods correspond with anomalously high-density areas. Similarly, in the region B to C they coincide with outcrops of predominantly trondhjemitic and granodioritic rocks which are considered to represent the background density, 2.69 g/cm^3, of the upper crust in this area. On profile RR′ (Figure 19b), between the location I to J and K to L, the negative residual anomalies of the spectrum and upward continuation based residual field correspond on the surface to the known anomalously high density rocks. On both

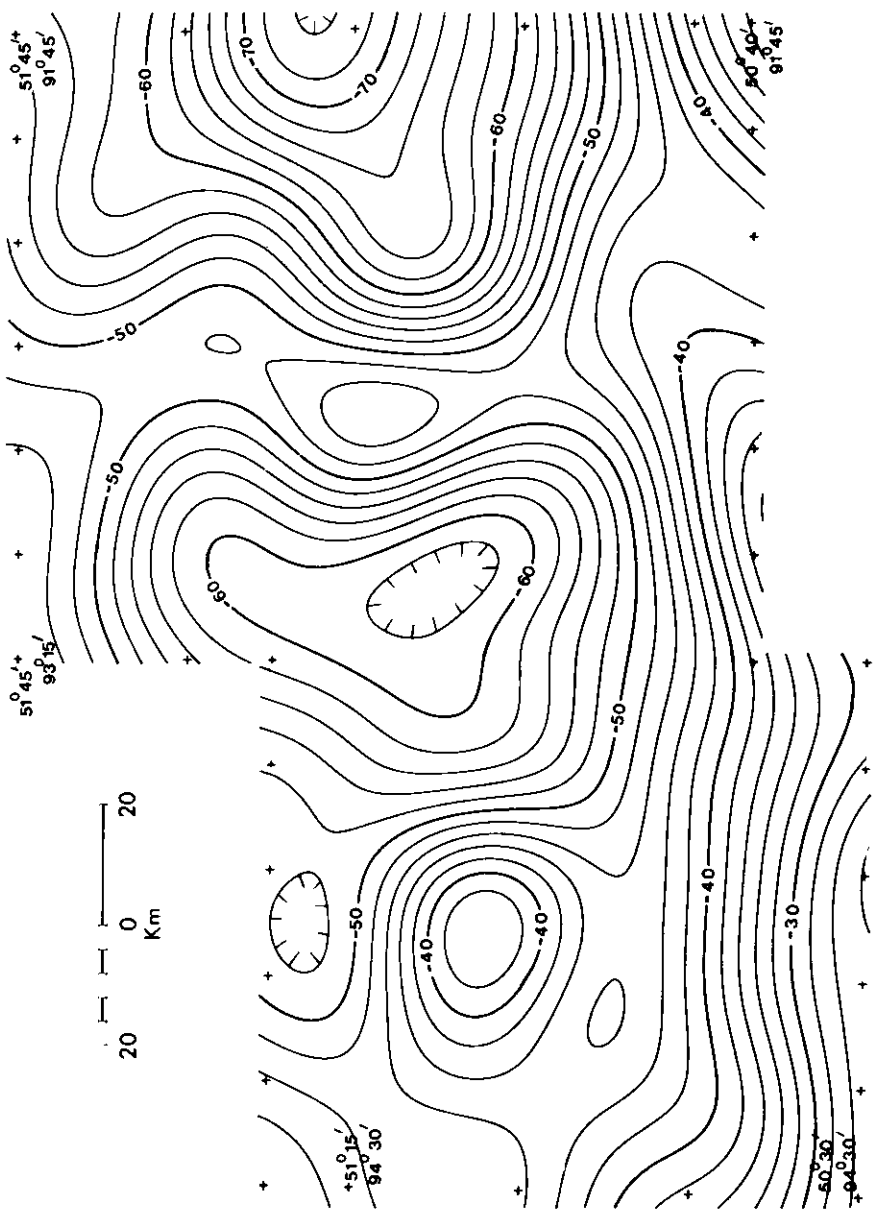

Figure 13. *Spectrum-based regional component of the Bouguer gravity map. Contour interval is 2 mgal.*

Figure 14. Regional component of the Bouguer gravity map obtained from an upward continuation to a height of 16.09 km (10 grid units). Contour interval is 2 mgal.

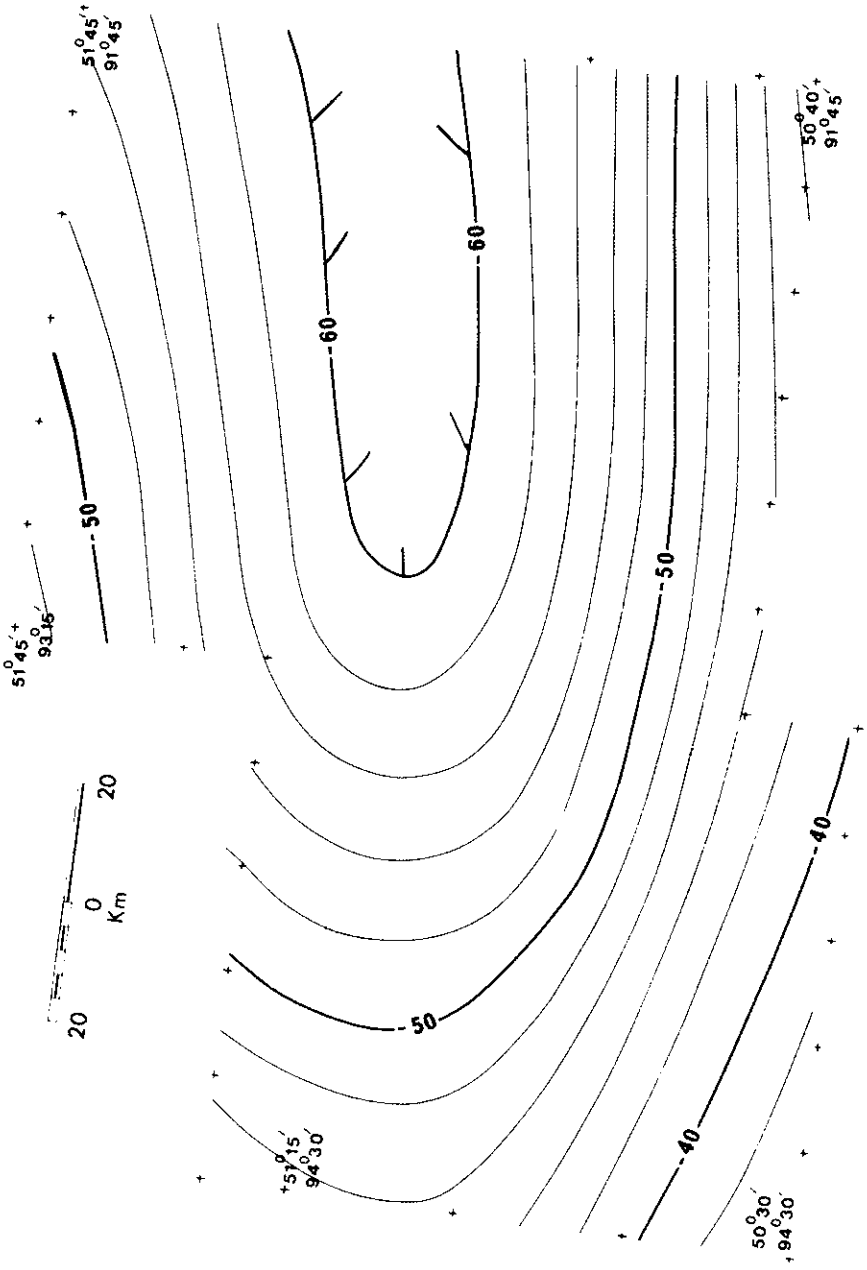

Figure 15. *Graphically separated regional component of the Bouguer gravity map. Contour interval is 2 mgal.*

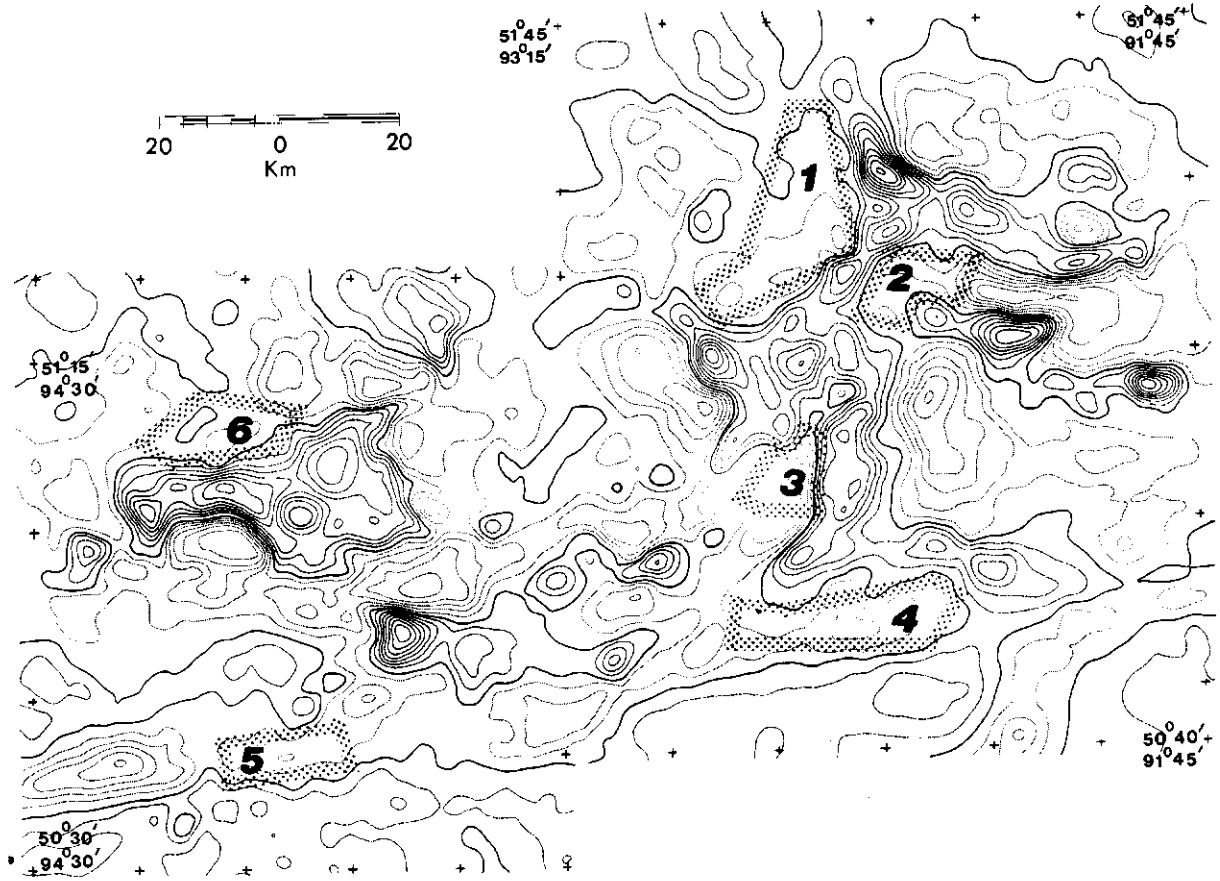

Figure 16. *Spectrum-based residual component of the Bouguer gravity map. Contour interval 2 mgal. Positive contours are shown in dark, negative contours are shown in light, and zero contour is shown by solid black line. Areas 1 to 6 referred to in the text are also shown.*

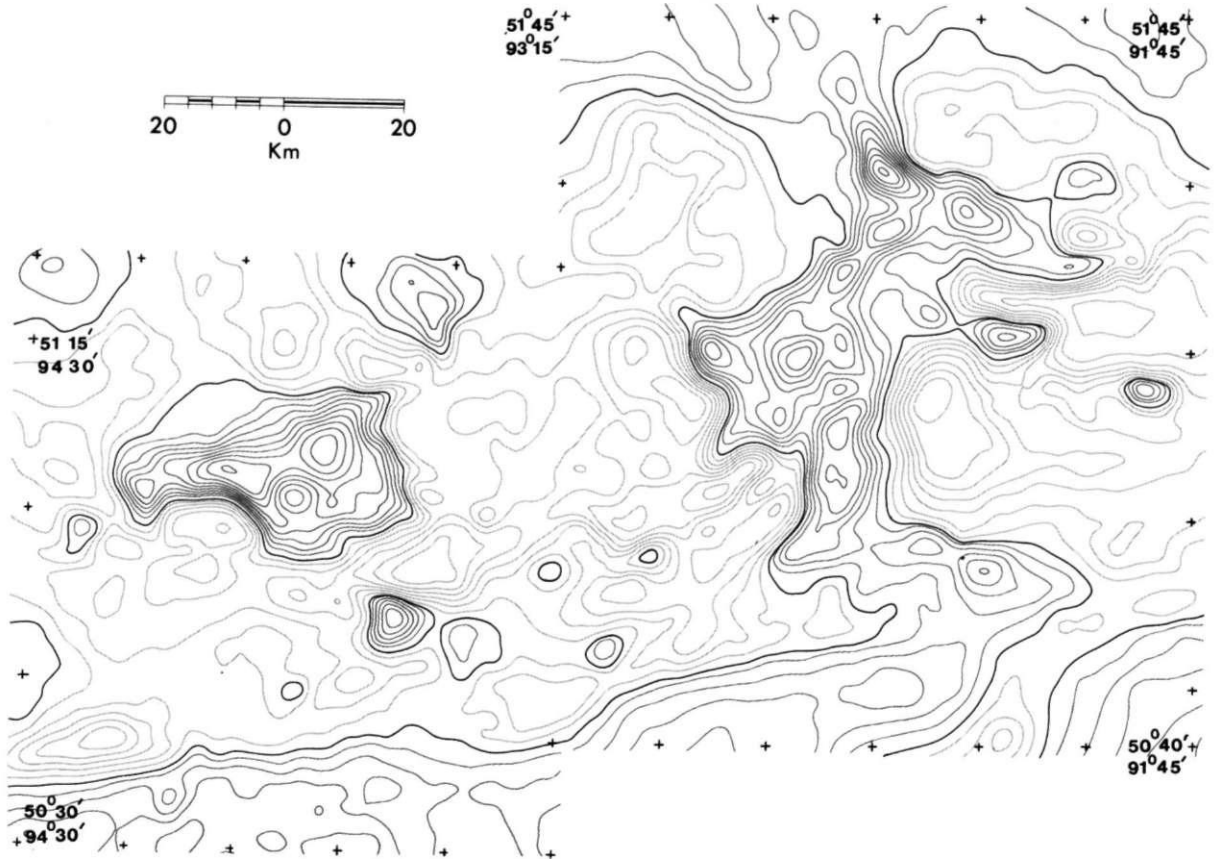

Figure 17. *Residual component of the Bouguer gravity map obtained from an upward continuation to a height of 16.09 km (10 grid unit). Contour* ***interval 2 mgal****.* ***Positive*** *contours are shown in dark, negative contours are shown in light, and zero contour is shown by solid black line.*

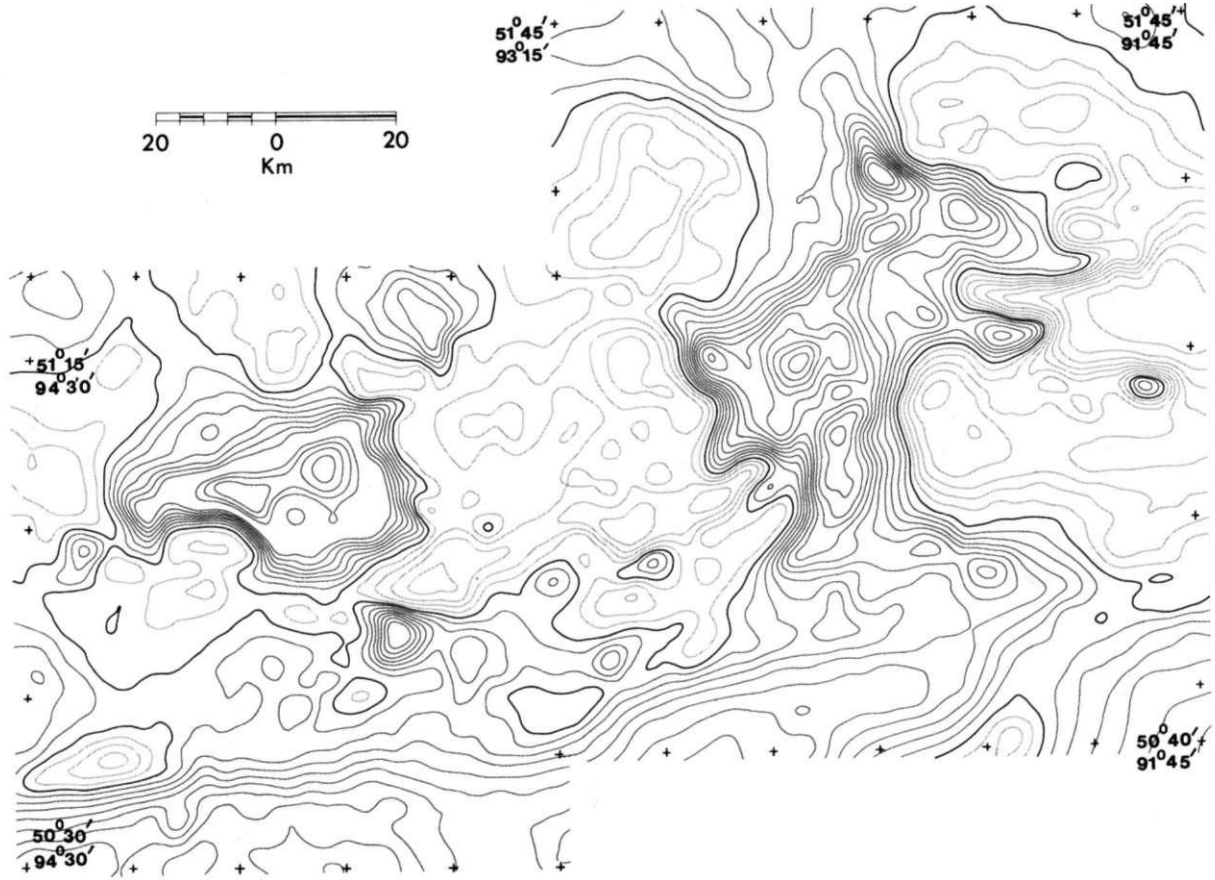

Figure 18. *Graphically separated residual component of the Bouguer gravity map. Contour interval 2 mgal. Positive contours are shown in dark, negative contours are shown in light, and zero contour is shown by solid black line.*

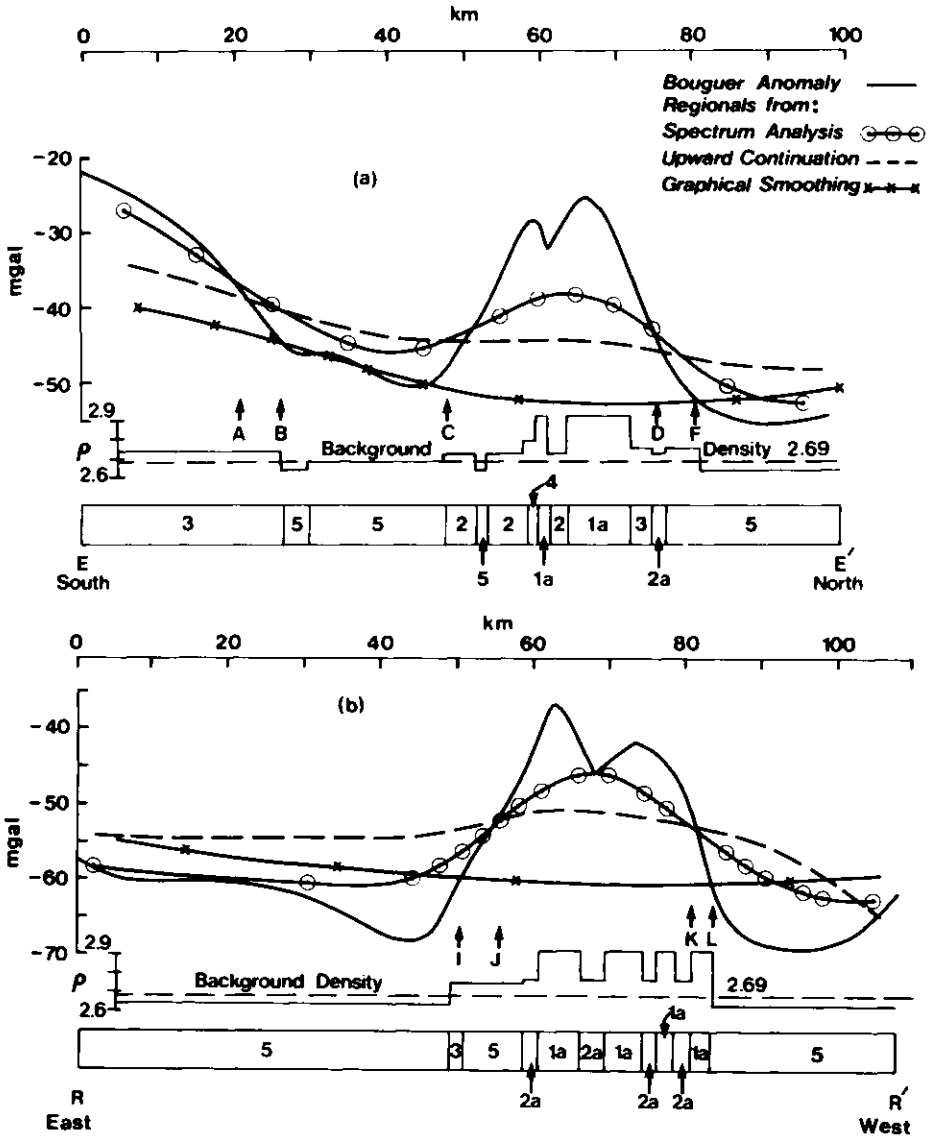

Figure 19. Profiles EE' and RR' showing the Bouguer anomaly (for location see Figure 3); the spectrum-based, upward continuation based and graphically smoothed regional fields. A plot of the mean densities and the surface geology is also shown. See Table 3 for explanation of geological legend.

profiles, the graphical residual anomalies are positive over all the problem locations.

Thus, it is noted that for both the spectrum-based and upward continuation residual maps, the highs and lows and their spatial extent are unrelated to observed geology and densities. It is possible that a shift in the datum (-5 to -10 mgal) of the spectrum and upward-based residual fields will improve their correlation with surface geology, especially in the earlier mentioned problem areas 1 to 6.

The amplitudes of the residual anomalies along profiles EE' and RR' have been compared in Table 2, over greenstone areas. From this comparison of the residual maps, it is observed that for the spectrum and upward-based residual

TABLE 2. RESIDUAL ANOMALY AMPLITUDES ON PROFILES E-E' AND R-R'.

	Residual Amplitude (mgal)		
Profile	Spectrum	Upward	Graphical
EE'	11	18	27
RR'	10	13	23

maps, the amplitude of the positive residual anomalies decreases considerably over the greenstone areas. Conversely, the amplitudes are increased over the granitic areas compared with the graphical residuals.

This will result in underestimating the thickness of the greenstone bodies and overestimating the granitic bodies, if spectrum and upward continued residual maps are used for quantitative modeling.

SUMMARY

To determine the advantages of using one set of regional-residual maps over the other for the purpose of quantitative gravity modeling, two separate criteria were established for the regional and residual maps.

Assessment Criteria for a Regional Map

The regional field should contain only smooth large wavelength components that are related to the deep crustal features and must not include greenstone belts which are known to have a limited depth-extent, but in some cases are fairly broad.

Based on this criteria, the spectrum-based regional (*see* Figure 13) was considered least applicable. The two regional gravity highs which are centred over the greenstone belts can be explained better by upper crustal greenstone densities rather than by undulations at the Riel and Mohorovicic discontinuities. This substantiates the point that the usefulness of filters based upon the spectra depends considerably upon the distribution of the bodies causing the gravity anomalies. In this case, because of the presence of broad and shallow greenstone masses (up to 40 km wide) the regional-residual separation is not very effective. The matched regional filter having a cut-off wavelength of approximately 32 km (0.031 cycles/km) allows the wavelengths due to the greenstone anomalies to be retained in the regional map.

The upward continuation based regional shows (*see* Figure 14) less correlation with the surface geology than the spectrum-based regional, but the greenstone belts are still discernable.

The graphical regional field, (*see* Figure 15, and Map 2493), which produces a gravity low for the entire area, is found to be the most satisfactory as it seems to represent variations at the Riel and Mohorovicic discontinuities. The east-trending regional anomaly is in good agreement with the regional Bouguer map which was prepared by Innes (1960) from the regionally spaced gravity stations established in granitic terrain only. Innes (1960) explained the regional field in terms of varying crustal thicknesses and density variations in the granitic rocks themselves.

Assessment Criteria for a Residual Map

The residual map should contain the effects of local and near-surface masses. Also, in plan view, in mapped areas, it should be possible to explain most of the highs and lows by the geology already mapped on the ground together with density measurements. This map would be used to model quantitatively the subsurface geometry of exposed geological units.

For the spectrum-based technique, the difficulty encountered is related to the lack of a clear-cut break in the power spectrum (*see* Figure 5). The separation of

power required for the design of the filters thus becomes subjective. Also the problem is complicated by the presence of very few points on the spectrum curve in the low frequency region.

The upward continuation technique is also subjective because of the continuation height which must be selected by trial and error.

The occurrence of negative residual anomalies in many areas of spectrum (*see* Figure 16) and upward-based (*see* Figure 17) residual maps correspond on the surface with areas of high density rocks. This will make modeling of the residual anomalies a problem thus lacking in geological control. Artificial bodies of low density would be buried to account for the regional-residual separation discrepancy of negative anomalies, where the surface evidence clearly indicates high density rocks. The problem can be avoided in the graphical technique where local geology is considered by the geophysicist at the time of regional-residual separation. It is considered unrealistic to ignore the surface geology.

It has been shown that the amplitudes of the positive and negative residual anomalies from spectrum and upward continuation based residual maps are greatly reduced over the greenstone areas and increased over the granitoid areas when compared to the graphically separated anomalies. The reduction in amplitude is as much as 40 percent. This has the effect that the spectrum and upward continuation based residual dual anomalies produce too shallow and too deep thicknesses for the greenstone and granitic bodies, respectively, that are unrealistic from a geological viewpoint.

Thus, it is suggested that in the area under discussion, regional and residual maps based on spectrum and upward continuation methods should not be used for the purpose of quantitative gravity modeling. However, there is no doubt that these maps are excellent tools for qualitative interpretation. Overall, the graphical method (*see* Figure 18) which has a certain bias towards the local geology, is considered to be more suitable to provide maps for quantitative gravity modeling.

The second derivative map (*see* Figure 11) shows a much more sharp and close relationship to the surface geology as is evident in the centre of the Birch-Uchi Belt, where the geology is best known. The bands of positive and negative second derivative anomalies in the centre of the Birch-Uchi Belt (*see* Figure 12) are clearly associated with the contrasting mafic to felsic cycles of volcanism. The second derivative map has thus been shown to have merits as an aid to geological mapping in poorly exposed areas.

Residual Anomaly Map

GENERAL DESCRIPTION OF RESIDUAL ANOMALIES

A number of positive and negative residual anomalies, isolated by the graphical technique (Map 2494), having different shapes, sizes, trends, and amplitudes, occur throughout the region (*see* Figure 18). The greenstone belts of the survey area are characterized by distinct zones of positive residual anomalies caused by supracrustal rocks which are surrounded by negative residual anomalies caused by oval-shaped granitoid plutons and batholiths. The margins of these anomalous positive zones are dominated by steep gravity gradients that coincide remarkably well with the greenstone-granite boundaries. This distinct pattern is, generally, evident among all the greenstone belts of the area and is believed to be caused in part by large density contrasts at the contacts. However, in certain locations, for example, the Alford Lake area and the Berens River area (Figure 20), the gravity field is gentle near the greenstone-granite boundary (*see* Figure 18, and Map 2492). This is possibly caused by the presence of rocks of intermediate composition (for example quartz diorite, metasediments, and so on) between the greenstone and the low density plutons.

There is good correlation between most of the residual gravity anomalies and the surface geology (*see* Map 2494). This suggests that both the anomalies and the geology are closely related to the upper crustal structure. For example, a majority of the positive residual anomalies are associated with the mafic to intermediate metavolcanics (mean density 2.93 g/cm^3, *see* Table 1) which constitute about 66 percent of the greenstone area. In addition, gabbro (mean density 2.94 g/cm^3), ultramafic rocks (mean density 2.80 g/cm^3), diorite (mean density 2.75 g/cm^3), and metasediments (mean density 2.75 g/cm^3 and 2.74 g/cm^3 in Uchi and English River Subprovinces, respectively) also undoubtedly contribute to the overall shape and amplitude of the positive residual anomalies.

Most of the negative residual anomalies occur over diapiric granitoid intrusive rocks (ranging in density from 2.63 to 2.65 g/cm^3) and lighter diatexite units (mean density 2.63 g/cm^3). Many negative anomaly closures are associated with intrusive bodies of batholithic proportions, for example, the Killala-Medicine Stone Lake and Gull Lake Batholiths (*see* Figures 18, 20, and Map 2494). In many greenstone belts, the positive residual anomalies associated with mafic metavolcanics are sometimes distinctly interrupted or separated by relative negative closures that are associated with small plutonic bodies, for example, the Dome Stock and the Okanse Pluton.

The absence of gravity anomalies in well-defined structures of intermediate to mafic metavolcanics, for example, Longlegged Lake Dome area (*see* Profile BB', Figure 22), can be explained in terms of it being narrow and relatively thin. Thus, such units are lacking sufficient volume to generate appreciable anomalies. The absence of positive gravity effects over smaller ultramafic bodies can be explained by their being very thin and/or highly serpentinized and thus reducing the density. Similarly, the iron formations which are very narrow and thin are incapable of generating enough gravity effect to be detected at the size of the present survey.

UCHI SUBPROVINCE

On the basis of distinct gravity features, the residual gravity map of the Uchi Subprovince can be divided into four characteristic segments:

1. the Red Lake Belt to the west
2. the Dixie Lake Belt to the south
3. the Birch-Uchi Belt to the east
4. the intervening areas of widely distributed granitic plutons and batholiths (Map 2494, back pocket)

Red Lake Belt

The Red Lake Metavolcanic-Metasedimentary Belt which also includes the Telescope and Embryo Lakes area, is a dominant gravity anomaly characterized by positive anomaly contours depicting individual closures (*see* Figure 20, Map 2494).

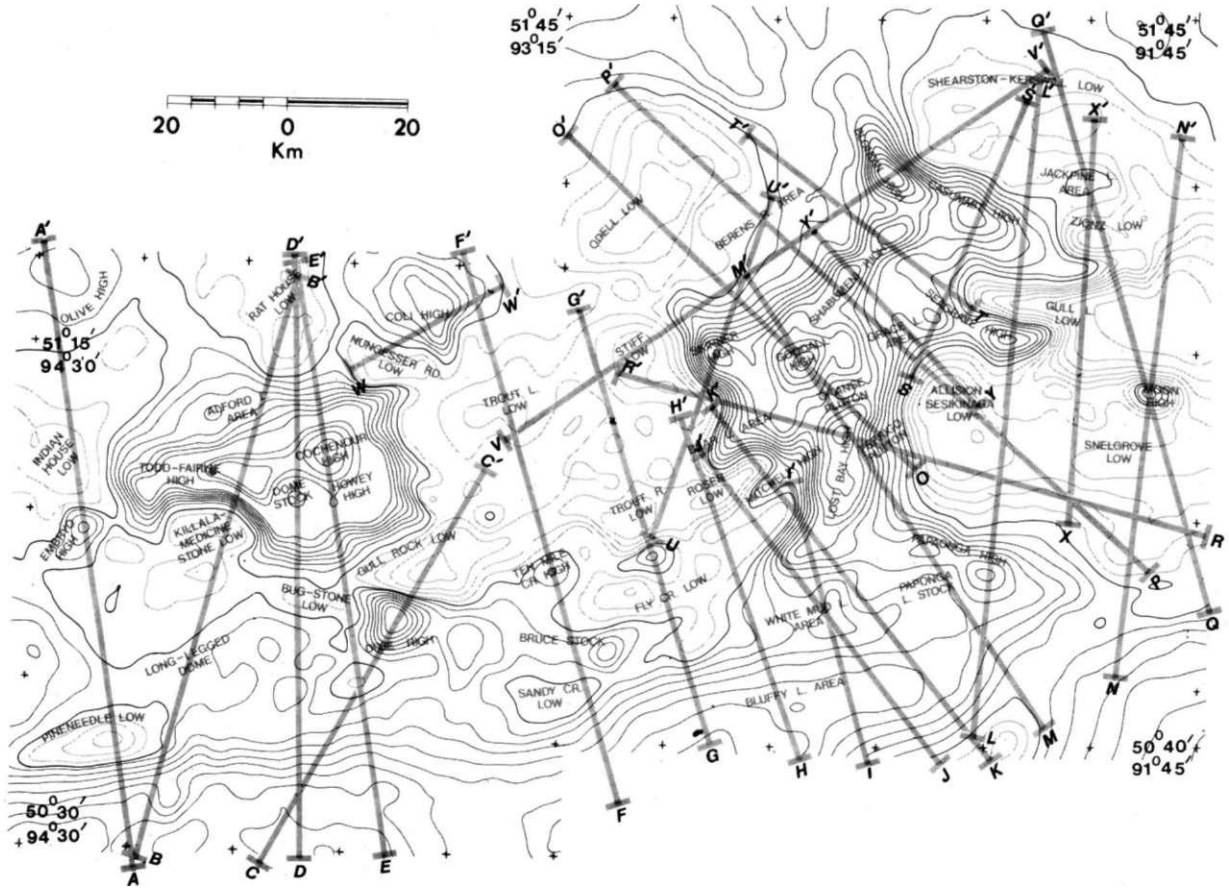

Figure 20. *Locations of gravity profiles AA′ to YY′ and various anomaly names referred to in the text.*

The belt is more than 64 km long and between 8 to 32 km wide. The trend of the residual gravity anomalies varies from near northwest to north-northeast to almost east. In general, there is a good correlation between the outcropping mafic to intermediate metavolcanics and positive residual anomalies.

Along the east-west part of the Red Lake Belt, the Cochenour and Todd Fairlie gravity highs, associated with the mafic metavolcanics, are separated by a circular gravity low caused by the Dome Stock (*see* Figure 20, Map 2494, back pocket). The positive residual gravity anomalies of the Red Lake Belt are elongate in shape and range in amplitude from 15 to 25 mgal. The presence of extensive outcrops of mafic to intermediate metavolcanics with high density contrast suggest that they are the principal contributor to the positive gravity effect. The steepened gravity gradients that border the Red Lake Belt on all sides flatten somewhat in the Alford Lake area where limited dioritic outcrops have been mapped by Pirie and Sawitzky (1977).

The Red Lake anomalous positive zone is surrounded to the east by the Gullrock Lake (*see* Profile CC', Figure 23) and the Trout Lake gravity lows and to the west by the Indian House Lake gravity low (*see* Profile AA', Figure 21). The Rathouse Lake and the Linge Lake Batholiths associated with negative residual closures border the north of the anomalous Red Lake Belt (*see* Profiles BB', DD', and EE', Figure 22, 24b, and 25). Similarly, the southern boundary of the Red Lake Belt comes into contact with a dominant negative residual anomaly associated with the Killala-Medicine Stone Lakes Batholith (*see* Profile BB', Figure 22) which is responsible for producing at the contact the sharpest gravity gradient (8.0 mgal/km) of the entire area.

Within the Red Lake Belt, many small to medium size stocks have been outlined by geological mapping (Ferguson 1972). The largest is the Dome Stock (*see* Profile DD', Figure 24) which has a maximum diameter in plan of about 8 to 10 km. The stock is composed of porphyritic quartz diorite, granodiorite, and trondhjemite (Pirie 1978) and coincides with a circular negative residual anomaly. The small McKenzie Island and Faulkenhan Lake Stocks cannot be isolated by gravity alone, perhaps due to a lack of density contrast. Just east of the Dome Stock, the mafic metavolcanics are intruded by an intermediate composition intrusive complex known locally as the Howey Diorite (Pirie 1978). The complex produces a weak 2 to 3 mgal positive residual anomaly (*see* Profile EE', Figure 25).

Four gravity profiles (AA', BB', DD', and EE'; Figure 21, 22, 24 and 25) passing through major gravity anomalies of the Red Lake Belt were modeled to compute the shape and thickness of the greenstone belt of the Red Lake area.

Dixie Lake Belt

The Dixie Lake Metavolcanic-Metasedimentary Belt, located south of Red Lake, is defined by a dominant, oval-shaped positive residual gravity anomaly (*see* Figure 20, Map 2494). This anomaly has an amplitude of more than 16 mgal with surface dimensions of 11 x 13 km. It is centred over Dixie Creek where intermediate to mafic metavolcanics outcrop. Profile CC', which passes through the centre, was used for two-dimensional gravity modeling of the Dixie Lake gravity high.

Coli Lake Belt

The Coli Lake Metavolcanic-Metasedimentary Belt is characterized by an elongate northwest trending 8 mgal positive residual anomaly approximately 20 km long and 12 km wide (Figure 20, and Map 2494, back pocket). The steepened gravity gradient that defines the southern margin of the anomaly is quite typical of the gradient found at greenstone-granite contacts. This style is, however, lacking near the northern border of the anomaly where extensive glacial cover is known to exist which may mask or reduce the observed gravity effect. It is also possible that under the northern part of the anomaly, high density intrusive rocks or metasediments are buried under the glacial cover. From profile WW' passing through the centre of the anomaly, three two-dimensional gravity models were computed. These show some of the range of acceptable structures attainable by varying the

shape of the metavolcanics and their densities. An additional gravity model has been computed from profile FF′ which passes through the northern tail of the Coli Lake gravity high.

Birch Uchi Belt

The Birch-Uchi Greenstone Belt underlies extensive positive residual gravity anomalies which range in amplitude between 15 to 25 mgal (Map 2494, back pocket). The anomalous zone has a north-south extent of more than 90 km and is 6 to 33 km wide. Throughout its entire length, the various arms of the Birch-Uchi Belt are recognizable on the basis of residual anomalies which follow them. Along the belt, the gravity anomaly trends are found to be consistent with the reported geological trends.

By virtue of higher amplitudes of the gravity anomalies in this belt, deeper accumulations of mafic metavolcanics are supported. In general, the greenstone-granite contacts are marked by steep gravity gradients with slopes varying from 6 mgal/km to 1 mgal/km. In the area just east of the Casummit gravity high, and in the Berens River and Papaonga Lake areas, however, moderate gravity gradients extend the positive anomalies several kilometres (into granitic terrain) beyond the boundaries of the metavolcanic units with which they are thought to be primarily associated (Figure 20, Map 2494). In the Berens River area and in the area just east of the Casummit gravity high, these extensions can qualitatively, at least, be accounted for by denser (2.73 g/cm^3) surface rocks. In the Papaonga Lake area, however, the extended gravity field does not correlate with the surface geology. This suggests that the anomalous region may be explained by the metavolcanics having more significant lateral extend at depth than the geological mapping indicates.

To the east and west, the Birch-Uchi Greenstone Belt is bounded by extensive granitic areas which are characterized by generally negative residual closures. The most prominent is a -17 mgal negative residual anomaly centred over Gull Lake which is situated east of the Birch-Uchi Greenstone Belt (Map 2494). The anomaly is bounded to the north and south by the Springpole Lake and Moon Lake arms of the belt, respectively. This anomaly is underlain by a uniform, low density granite and appears to represent a single major batholith which underlies, at least partly, the Springpole Lake and Seagrave Lake areas of the Birch-Uchi metavolcanic belt (*see* Profiles NN′, QQ′, and XX′, Figure 20, 34, 37 and 44).

The remaining negative anomaly areas are more complex. The Allison-Sesikinaga Lake Batholith (Figure 20, Map 2494) is considered to constitute a major part of the granitic area to the east-southeast of the Birch-Uchi Greenstone Belt. The batholith dimensions have been estimated at 15 km wide and 30 km long. The corresponding residual anomaly, however, averages only about -8 mgal, with a minimum of -11 mgal occurring less than 5 km from the greenstone-granite contact. The actual batholith, therefore, appears to be located to the north of Allison Lake, while the Sesikinaga Lake area represents a shallower marginal structure (*see* Profiles LL′, PP′, RR′, and YY′, Figures 20, 32, 36, 38 and 45).

The Trout Lake granitic area (*see* Profile FF′, Figure 26) which lies between the Red Lake and the Birch-Uchi Greenstone Belts contains several local minima which may mark the actual centres of intrusions (Figure 20, Map 2494). As in the Allison Lake Area, these lows occur near the greenstonegranite contacts rather than in the centre of the granitic terrain. In addition, the lows do not appear to correspond to any discreet, clearly defined geological structures. Both the Stiff Lake and Rosen Lake lows are fairly narrow, elongated anomalies which reach a minimum of about -9 mgals (*see* Profiles RR′, VV′, HH′, and II′ respectively, (Figures 38, 42, 28, and 28)).

The Fly Creek low, which extends some 15 km into the Birch-Uchi Greenstone Belt possibly marks a major feeder, as would be indicated by the graben structure along the main synclinal axis of the Birch-Uchi Belt (*see* Profile GG′; Figure 27).

The Odell Lake gravity low (*see* Profiles OO′ and PP′; Figures 35 and 36) to the northwest of the Birch-Uchi Greenstone Belt, correlates approximately with a

low-density (2.64 g/cm^3) granitic unit which underlies the centre of the anomaly (Figure 20, Map 2494). The contacts of this body with the surrounding higher density rocks, however, are poorly defined and the shallow gravity gradients make an accurate regional-residual separation difficult to make. The present residual map indicates, that the granitic unit has significantly greater lateral extent at depth than is given by the density sampling.

The Shearstone-Kerswill Lake gravity low (*see* Profiles LL', QQ', SS', and VV'; Figures 32, 37, 39, and 42) to the northeast of the Birch-Uchi Greenstone Belt is a broad elongated anomaly underlain by a complex granitic terrain which ranges in density from 2.64 to 2.73 g/cm^3.

With the exception of the Okanse Lake Pluton (*see* Profiles MM' and OO'; Figures 33 and 35), none of the smaller plutons or batholiths which intrude the Birch-Uchi Greenstone Belt show any noticeable correlation with gravity because their densities are very similar to the rocks (dominantly metasediments) that they intrude.

Numerous gravity profiles (HH', II', JJ', KK', LL', MM', OO', PP', RR', SS', TT', UU', VV', XX', and YY'; Figures 28, 29, 30, 31, 32, 33, 35, 36, 38, 39, 40, 41, 42, 44, and 45), have been drawn across the Birch-Uchi Greenstone Belt and surrounding granitic areas. Significant residual anomalies have been modeled to extrapolate the shape and to establish the thickness of the causative anomaly sources.

ENGLISH RIVER SUBPROVINCE

In general, the gravity field increases southward as the English River Subprovince is approached from the Uchi Subprovince (Map 2494). A 145 km long linear gravity zone, having a steep gravity gradient, reaches a residual gravity maxima of 16 mgal over the northern supracrustal domain of the English River Subprovince. The linear zone trends almost east-west from the western edge of the map to Ear Falls and then swings to an east-northeast direction. This linear zone perhaps reflects, completely or in part, the northern boundary of the metasedimentary trough (mean density 2.74 g/cm^3) of the northern supracrustal domain. This zone also coincides with the Sydney Lake Fault System which outcrops at various places as a zone composed of cataclastic rocks. The subprovince boundary is marked by a fairly uniform, southerly increasing rise of 1.2 mgal/km over most of its length.

A characteristic of the gravity anomaly over the English River metasediments is its almost total lack of response to the numerous, intrusive, trondhjemite-granodiorite bodies, the largest of which is the Bluffy Lake Batholith which is 12 km wide and 60 km long. The Bluffy Lake Batholith (Figure 20, Map 2494) has a very distinct aeromagnetic character. One would expect its 0.05 g/cm^3 density contrast with the surrounding metasediments to be significant. Only in the immediate vicinity of Bluffy Lake is it associated with a gravity low. This suggests that these bodies are extremely shallow, sheet-like features (*see* Profiles II', JJ' and KK'; Figures 29, 30, and 31). Numerous gravity profiles across the English River Subprovince have been modeled to show the geometry and configuration of the linear gravity zone and other associated anomalies of this subprovince (*see* Profiles AA' to MM').

BERENS RIVER SUBPROVINCE

The boundary between the Uchi and Berens River Subprovince is poorly defined in the survey area. For example, this boundary, as shown on many Ontario Geological Survey maps divides many batholiths of the survey area into half, including the Coli Lake Metavolcanic-Metasedimentary Belt. For this reason, the description of the gravity anomalies which may belong to the Berens River Subprovince have been given under the Uchi Subprovince.

Gravity Models of the Residual Anomalies

INTRODUCTION

For quantitative, two-dimensional gravity analysis, 25 residual profiles, AA′ to YY′ (Figures 21 to 45), were selected from the graphically separated residual anomaly map. The profiles (for locations *see* Figure 20) are spread throughout the survey area and their selection was guided by anomaly resolution, amplitude, dimension, and the geological environment. The generalized geology shown underneath each gravity profile has been adopted from the geology shown on Map 2494. A description of the geological legend is given in Table 3. On each profile, the estimate of standard deviation ( ) and the coefficient of correlation (c) between the residual and computed gravity anomalies is shown. All the profiles are described from south to north except RR′ (Figure 38), which is from east to west.

GENERAL ASSUMPTIONS, LIMITATIONS, AND PROBLEMS

The following basic assumptions were made in the two-dimensional model analysis of the gravitational field:

1. the causative body has a uniform density
2. the causative body has infinite strike length
3. the bodies are flat topped.

In model interpretation, the two-dimensionality of the anomaly is generally assumed if the anomaly strike length is more than several times larger than the width of the more than several times larger than the width of the anomaly. Darracott (1976) has suggested that the above criterion is arbitrary and the choice between a two-dimensional or three-dimensional model should be based on the criterion of depth of burial of the top surface and the depth extent of the body. Using Darracott's type curves both criteria hold good for a majority of the anomalies in the study gravity high (*see* Profile CC′; Figure 23), end corrections were applied using a lamina model (Milsom and Worthington 1977) to the two-dimensional formula. In this method, a body is approximated by a number of straight-sided slabs where the gravity field of a slab is calculated due to a rectangular horizontal lamina.

Unlike more direct exploration techniques, the interpretation of gravity fields potentially gives an infinite number of model solutions. In order to limit the number of possible models, discreet boundary conditions, that is, knowledge of the surface geology and rock density are required. The major geological boundaries in the greenstone belts and English River Subprovince are fairly well mapped. The detail available for the surrounding granitic areas, however, is sparse. The density sampling is very valuable in revealing phases of varying density in areas which are uniformly designated as trondhjemitegranodiorite on the geological maps. In most surveys, the sampling intervals, however, are rarely sufficient to accurately delineate the boundaries. As a result many areas must be assigned an average density which consequently reduces the accuracy of the model (*see* Profile DD; Figure 24).

The contouring interval of the Bouguer further limits interpretation. A comparison was made of a test profile (contour interval = 2 mgal) using actual gravity station values over a geological section with alternating lithologies (that is, successive mafic-felsic cycles). Discrepancies were found that were appreciably greater than the ±0.5 mgal expected error in individual values. Since the corresponding second vertical derivative shows remarkably good correlation with the individual units, it must be assumed that not all the gravity detail is transmitted to the final contoured Bouguer map. Thus, discrete units cannot be interpreted with any confidence.

Where fold axes can be inferred from the geological configuration, but no other structural control is available, gravity interpretation becomes indecisive because of the ambiguity of horizontal layering. Therefore, a best possible model that then can be obtained is a "geologically acceptable" model. Gravity interpretation also becomes problematic where two different adjacent lithologies show no density

TABLE 3. GEOLOGICAL LEGEND FOR PROFILES AA' TO YY'

PRECAMBRIAN*

EARLY PRECAMBRIAN

INTRUSIVE ROCKS

FELSIC TO INTERMEDIATE ROCKS

5 Undifferentiated
5a Granite (ss)
5b Granodiorite
5c Trondhjemite
5d Quartz Monzonite
5e Syenodiorite
5f Subvolcanic intrusive rocks

INTRUSIVE CONTACT

INTERMEDIATE TO ULTRAMAFIC INTRUSIVE ROCKS

4a Intermediate to mafic intrusive rocks
4b Serpentinized or carbonatized ultramafic intrusive rocks

INTRUSIVE CONTACT

METASEDIMENTS

3a Metasediments
3b Metatexitic metasedimentary migmatite
3c Diatexitic metasedimentary migmatite

METAVOLCANICS

FELSIC AND INTERMEDIATE METAVOLCANICS

2 Undifferentiated
2a Intermediate metavolcanics
2b Felsic metavolcanics

INTERMEDIATE AND MAFIC METAVOLCANICS

1 Undifferentiated
1a Mafic metavolcanics

*These rock units are grouped litholigically and the order does not necessarily imply age relationship between groups.

A	Anticline
S	Syncline
ERSP	English River Subprovince
BRSP	Berens River Subprovince
σ	Estimate of Standard Deviation
C	Coefficient of Correlation

contrast, for example, the Perrigo Pluton intruding the metasediments of nearly the same density (*see* Profile RR'; Figure 38).

Finally, the residual anomalies should all, ideally, show a correlation with the surface geology. In areas where the residual anomaly requires the introduction of a buried body, the interpretation can, at best, be guided by the surrounding geology. Even with all these inherent limitations, it must be emphasized that gravity modeling, assisted by second vertical derivative and aeromagnetic maps, provides valuable and valid criteria for evaluating any proposed structural model.

Gravity Modeling Procedure

The anomaly modeling was carried out by using a computer program which calculates the gravitational effect of two-dimensional masses of arbitrary cross-section (Nagy 1964). The modeling program is fully interchangeable between an iterative non-linear optimization mode and a simple forward (trial and error) mode. In the iterative mode, the modeling program is used in conjunction with a non-linear optimization computer package MINUIT (James and Roos 1976) which allows a user to minimize a function of several independent variables. The function f to be minimized is determined through the subroutine of the modeling program and a two-dimensional body model that will best fit an observed gravity anomaly is calculated. The parameters (x and z coordinates of the body, the background gravity of the form R0 +R1x and the density) can be bounded within a lower and upper limit, or kept constant if their values are known (from surface geology, drilling, or seismic data, and so on).

The initial shape of the causative bodies at the beginning of the computation were constructed using geological information. Where the outcrop limit of the geological units were known, the boundaries of the model body points at the surface were kept fixed. The surface dips, wherever known, were also used in model interpretation. The appropriate densities used in the modeling procedure are shown for each unit along the profile.

The estimate of the standard deviation and the coefficient of correlation were used to determine the goodness-of-fit between a set of residual and computed gravity anomalies. The standard deviation (σ) is given by:

$$\sigma = \left[\frac{\Sigma\,(x-y)^2}{n-1}\right]^{1/2} \qquad (12)$$

where, the indicated summations are over a total of n observations (x) and corresponding computed values (y). A standard deviation of 1 mgal or less was considered a good fit. The coefficient of correlation C is given by:

$$C = \frac{\Sigma\,(x-\bar{x})\cdot(y-\bar{y})}{[\Sigma\,(x-\bar{x})^2\cdot(y-\bar{y})^2]^{1/2}} \qquad (13)$$

The coefficient of correlation ranges in value from 0 to 1, (1>C>0), and a value of C equal to 1 shows a perfect agreement between a set of residual and computed anomalies.

PROFILE INTERPRETATION

Profile AA'

Profile AA' (Figure 21) near the western edge of the map, extends in a north-northwest direction across the Northern Supracrustal Domain to north of the Red Lake Belt. The profile is >100 km long and has several prominent positive and negative residual anomalies. They are the Northern Supracrustal Domain gravity high in the vicinity of Sydney Lake Fault, the Pineneedle Lake Pluton gravity low, the Embyro Lake gravity high, and the Indian House Lake Pluton gravity low. The computed two-dimensional shapes of the causative bodies are shown in Figure 21.

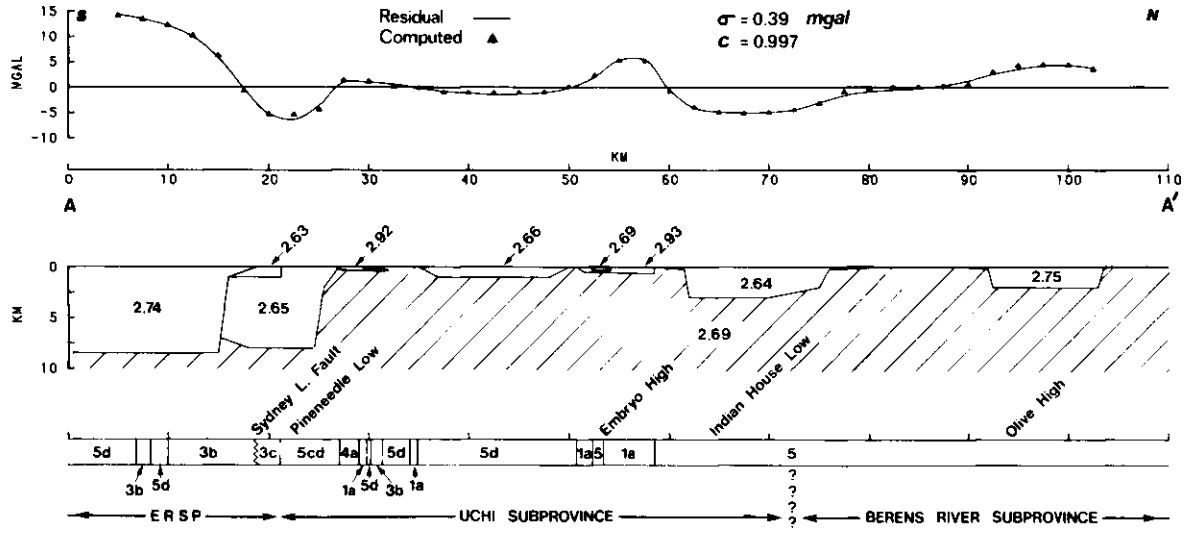

Figure 21. *Profile AA', showing the graphical residual and computed gravity anomalies, interpreted gravity models and surface geology. Densities in g/cm³. For profile location see Figure 20. See Table 3 for explanation of geological legend.*

The coefficient of correlation between the observed and computed anomalies is 0.997 and the estimate of standard deviation is 0.39 mgal.

The metasedimentary trough of the Northern Supracrustal Domain of the English River Subprovince consists mainly of metatexites of mean density 2.74 g/cm^3. The metatexites coincide with a residual positive anomaly, 14 mgal in amplitude. The northern edge of the trough in the vicinity of the Sydney Lake Fault System has a calculated dip of 25°S. Approximately 5 km south of the fault, the dip, however, becomes almost vertical, and the basin assumes a depth extent of 8.5 km.

North of the Sydney Lake Fault lies the Pineneedle Lake quartz monzonitic pluton of mean density 2.65 g/cm^3. The pluton gives a 6.5 mgal amplitude, elliptically shaped, negative residual anomaly of dimensions 27 km x 8 km. The sides of the pluton are south-dipping and extend to a subsurface depth of 8 km.

The outcropping mafic metavolcanics of the Red Lake Belt in the Embryo-Telescope Lakes area correlate with a 6 mgal positive residual anomaly. A mean density of 2.93 g/cm^3 has been used in the model calculations. The calculated model indicates a synclinal structure with gentle dips that may extend to 0.6 km depth. The model, therefore, suggests that the western end of the Red Lake metavolcanic belt is <1 km thick.

North of the Embryo Lake gravity high a 5 mgal negative residual anomaly correlates with the Indian House Lake Pluton. An average density of 2.64 g/cm^3 has been used for this pluton which has inward sloping surfaces that extend to a depth of 3 km.

From the profile it is clear that the positive and negative residual anomalies are closely connected with the denser and lighter outcropping rocks, respectively.

Profile BB'

This north-northeast running profile (Figure 22) is more than 90 km long and cuts across both the Northern Supracrustal Domain and the Red Lake Belt. The major anomalies under this profile are the Northern Supracrustal Domain gravity high, the Killala-Medicine Stone Lakes Batholith gravity low, the Todd-Fairlie gravity high, the Alford Lake area gravity high, and finally, the Rathouse Lake gravity low. The observed and calculated anomalies have a coefficient of correlation of 0.998 and a standard deviation of 0.54 mgal.

The Northern Supracrustal Domain region is characterized here by a 15 mgal positive residual anomaly. The northern boundary of the metasedimentary basin, having a mean density of 2.74 g/cm^3, again has a gentle dip near the Sydney Lake Fault zone and a steep dip about 6 km south of the fault. On this profile, the trough is calculated to have a depth extent of 9 km which is slightly deeper than in Profile AA'.

The diatexite unit (3C), centred at kilometre 20, has been modeled with a mean density of 2.63 g/cm^3. The causative funnel-shaped body is dipping to the south and has a depth extent of 3 km.

In the Longlegged Lake Dome area, between kilometres 25 to 40, the residual gravity field is too insignificant to warrant any modeling of the various units. The mean density of the surface rocks in this area is 2.75 g/cm^3 that is, a density contrast of +0.06 with the background. This contrast is sufficient enough to cause gravity anomalies. However, the lack of significant gravitational field suggests that the outcropping narrow units are of limited depth extent.

The Killala-Medicine Stone Lakes Batholith of mean density 2.66 g/cm^3 correlates with a 4 mgal negative residual anomaly. On the surface, the Medicine Stone Lake portion of the batholith appears to be separated from the Killala part by a thin east-trending felsic to intermediate metavolcanic unit. However, these batholiths having inward sloping sides are joined at depth. The intervening metavolcanics of mean density 2.73 g/cm^3 near kilometre 55, are modeled to a 1 km depth. The southern side of the batholith extends to a depth of 6 km,

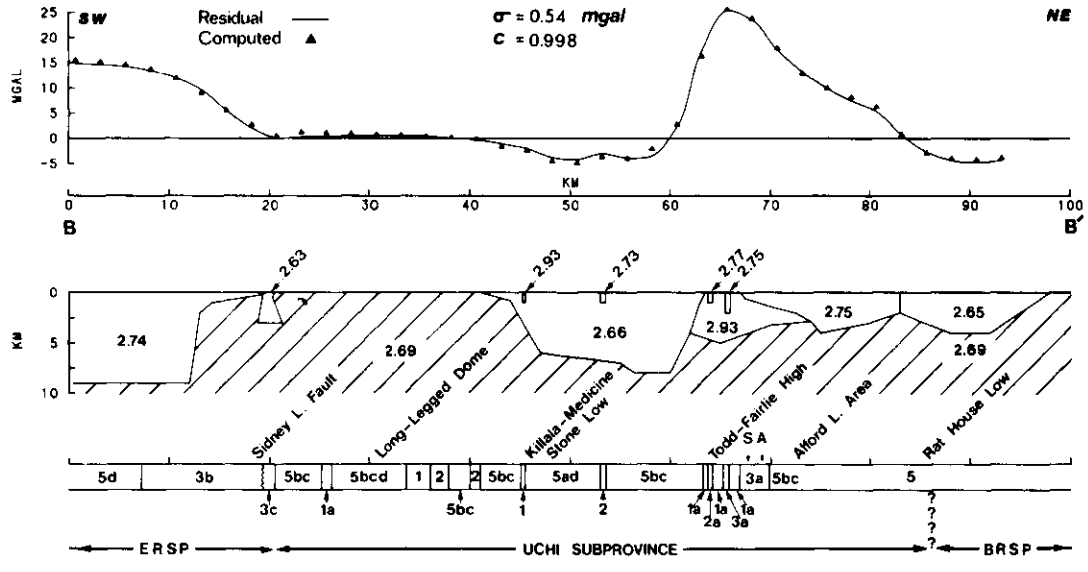

Figure 22. *Profile BB', showing the graphical residual and computed gravity anomalies, interpreted gravity models and surface geology. Densities in g/cm³. For profile location see Figure 20. See Table 3 for explanation of geological legend.*

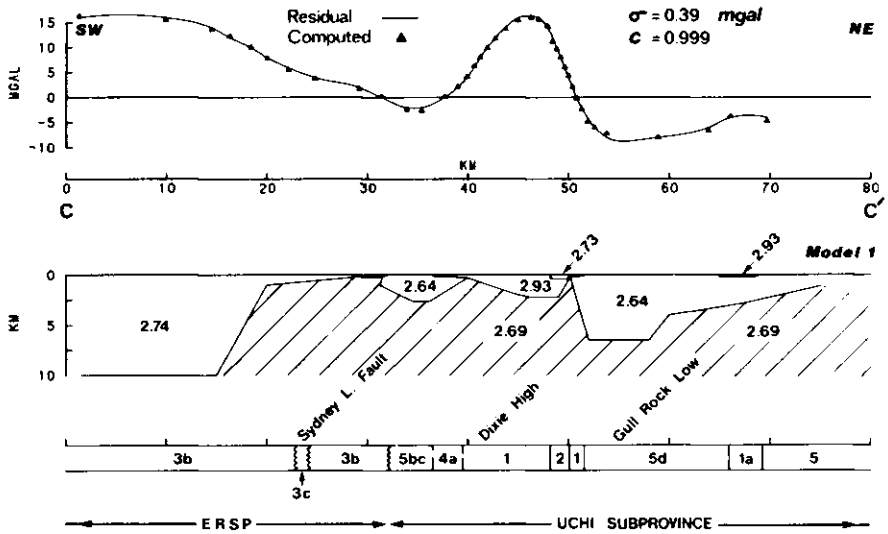

Figure 23a. *Profile CC' (Model 1), showing the graphical residual and computed gravity anomalies, interpreted gravity models and surface geology. Densities in g/cm³. For profile location see Figure 20. See Table 3 for explanation of geological legend.*

whereas the north side, which comes into contact with the Red Lake metavolcanic belt, dips steeply to the south and has a depth extent of 8 km.

The 25 mgal positive residual anomaly called the Todd- Fairlie gravity high is caused by outcropping mafic metavolcanics of mean density 2.93 g/cm and the metasedimentary and quartz diorite rocks of mean density 2.75 g/cm³. The mafic metavolcanics, which have been modeled to a thickness of 5 km, partly underlie the metasediments and 2.75 g/cm³ density rocks of the Alford Lake area between kilometres 67 to 74. The metasediments dip to the north and have a depth extent of about 2 km. Within the Todd-Fairlie metavolcanic body, two metasedimentary units have been modeled with a 1 km and 2 km depth extent. A part of the north flank of the Todd-Fairlie gravity anomaly coincides with the rocks of the Alford Lake area. The density sampling in this area shows that a mean density of 2.75 g/cm³ is representative of the exposed rocks. Using this density, the Alford Lake causative body extends to a depth extent of 4 km.

The gravity field over the Rathouse Lake Batholith is characterized by a 4 mgal negative residual anomaly. The anomaly is modeled with a mean density of 2.65 g/cm³ and the density contrast extends to a depth of about 4 km.

Profile CC'

This 70 km long profile (Figure 23) runs in a northeast direction across the Northern Supracrustal Domain to the Dixie Lake Metavolcanic-Metasedimentary Belt and terminates past the Gullrock Lake gravity low. Two models have been calculated for this profile: a two-dimensional model (Model 1) and a strike-limited model (Model 2) which is calculated only for the Dixie Lake gravity high region.

Model 1 The steeply dipping metasedimentary trough of the Northern Supracrustal Domain is calculated to be 10 km thick (*see* Figure 23a). A gravity low centred around kilometre 35 is attributed to a granitic pluton of mean density 2.64 g/cm³. The pluton underlies the southern edge of the Dixie Lake Greenstone Belt and has a depth extent of 2.6 km. The northern contact of this pluton which comes into contact with the Dixie Lake Greenstone Belt is shown to be shallow dipping.

The Dixie Lake gravity high represented by a 16 mgal positive residual anomaly coincides with outcrops of mafic metavolcanics of mean density 2.93 g/cm^3. The mafic metavolcanics calculated to have a depth extend of 2.2 km show a synformal shape. This belt thus appears to be shallower than the other belts in the area.

Farther north along this profile, the Gull Rock Lake Pluton has a coinciding 8 mgal negative residual anomaly. The anomaly has been explained by a quartz monzonitic pluton of mean density 2.64 g/cm^3. This pluton has inward sloping interfaces which extend to a depth of about 6.5 km. The southern edge of the pluton is steeply dipping, whilst the northern edge takes the form of a shallow-dipping sheet.

The smaller narrow tongue of the Red Lake mafic metavolcanic unit, near kilometre 65, appears to be contained as a remnant within the Gullrock Lake Pluton. The remnants of the mafic metavolcanics are <0.5 km thick and probably dip to the south.

Model 2 In this model (Figure 23b) , the anomaly underlying the Dixie Lake metavolcanics, between kilometres 36 to 52, was modeled using bodies of limited strike length. End corrections were thus calculated for two-dimensional models using the algorithm of Milsom and Worthington (1977). In this method, a body is approximated by a number of straight-sided slabs where the gravity field of a slab is calculated due to a rectangular horizontal lamina. The bodies were approximated by 10 laminae of equal thicknesses each having a half-strike length of 6 km. After applying the strike correction, the calculated depth extent of the mafic metavolcanic increased by about 10 percent (2.4 km) compared to that obtained in Model 1 (2.2 km) where infinite strike length was assumed. Since the difference between the two depths was minimal, end corrections were not attempted in other profiles.

Profile DD'

Profile DD', 85 km in length, runs approximately northerly across the Northern Supracrustal Domain and the Red Lake Belt. The prominent gravity anomalies along this profile are the Northern Supracrustal Domain gravity high, the Bug Lake-Stone

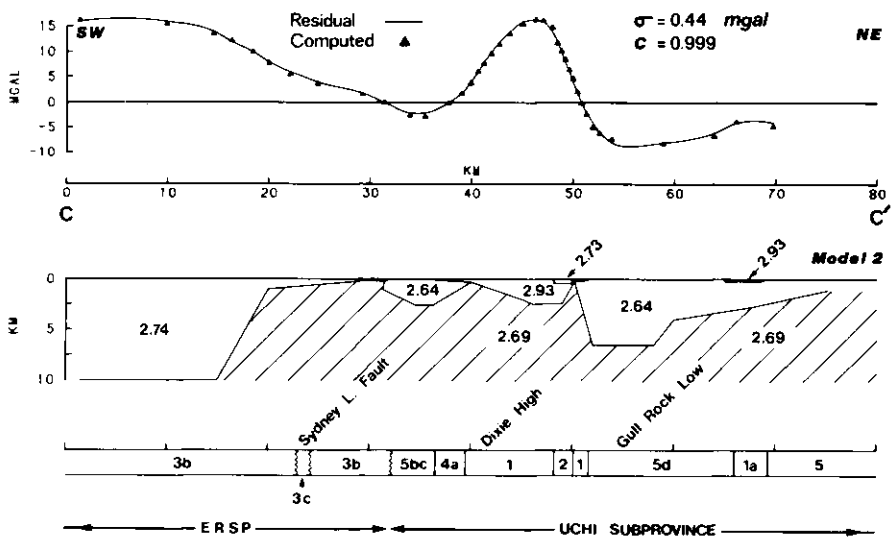

Figure 23b. *Profile CC' (Model 2), showing the graphical residual and computed gravity anomalies, interpreted gravity models and surface geology. Densities in g/cm^3. For profile location see Figure 20. See Table 3 for explanation of geologic legend.*

Lake gravity low, the Dome Stock gravity low, the Cochenour gravity high, and the Rathouse Lake gravity low. Two alternative models have been calculated for this profile.

Model 1 The metatexites of the Northern Supracrustal Domain have been interpreted (Figure 24a) to be dipping gently to the south in the immediate vicinity of the Sydney Lake Fault system and a few km south of the fault dip steeply to the south. A similar configuration has been arrived from Profiles AA' and BB' (Figures 21 and 22). The calculated depth extent of the metasediments on this profile is 10 km, the maximum reached until they are overlain by the Bluffy Lake Batholith in Profile JJ' (Figure 30).

The mafic to intermediate intrusive units between kilometres 25 to 30 have been modeled using a mean density of 2.92 g/cm^3. The causative body which takes the form of a flat-lying sill has a limited depth extent of only 0.6 km.

The 25 mgal residual negative anomaly coinciding with Bug Lake-Stone Lake gravity low correlates on the surface with granodioritic and trondhjemitic rocks. The density measurements in this region, however, indicate lighter granitic rocks of mean density 2.64 g/cm^3. Using this density, the causative body has a depth extent of 4 km with vertically dipping sides.

A prominent circular gravity low centred about kilometre 60 is caused by the granodioritic rocks of the Dome Stock. The mean density of the rocks contained in the stock is 2.70 g/cm^3. On the basis of gravity modeling, the 2.6 km thick Dome Stock appears to be entirely enclosed within the Red Lake Greenstone Belt. Both to the north and south, the stock is in contact with 1 km deep felsic to intermediate metavolcanic units of density 2.73 g/cm^3.

A major part of the 23 mgal amplitude positive residual anomaly (the Cochenour gravity high) between kilometres 50 to 75, has been accounted for mostly by the underlying folded mafic metavolcanics. These rocks have limited surface exposure in the form of narrow bands. All lower density rocks of limited depth extent (0.5 to 1.8 km) are underlain, along this profile, by mafic metavolcanics whose bottom topography assumes anticlinal and synclinal shapes. Near kilometre 58, south of the Dome Stock, the modeled mafic metavolcanics represent an anticlinal form with a thickness of <2 km. The location of the interpreted anticlinal axis coincides with a mapped anticline. Near kilometre 63, north of the Dome Stock, the shape of the modeled mafic metavolcanics suggests a synclinal form with a maximum thickness of <6 km. The location of the interpreted synclinal axis is found to be under the Dome Stock and perhaps therefore there is no expression of it at the surface. It is obvious from the gravity anomaly that the folded metavolcanics have their greatest concentration of mass and thickness directly below the peak of the residual gravity anomaly.

North of the Cochenour gravity high, the rocks of the Alford Lake area, perhaps constituting a smaller denser phase (mean density 2.75 g/cm^3) of the Rathouse Lake Batholith, have been modeled to a thickness of 0.5 km. The main Rathouse Lake batholith has a depth extent of 3 km based on using a uniform mean density of 2.64 g/cm^3.

Model 2 A second model (Figure 24b) was calculated for the Cochenour gravity high between kilometres 50 to 75. In this simplified model, many of the smaller surface geological units have been lumped together by averaging their mean densities.

Also, different mean density values were used for both the mafic metavolcanics (2.87 g/cm^3 against 2.89 g/cm^3 used in Model 1) and Dome Stock (2.69 g/cm^3 against 2.70 g/cm^3 used in Model 1). In Model 2, the overall shapes of the causative bodies remain similar to those in Model 1 except that their thicknesses are somewhat different.

This illustrates the non-uniqueness of the solution where the interpretation process is purely subjective and a number of models can be fitted to the same anomaly.

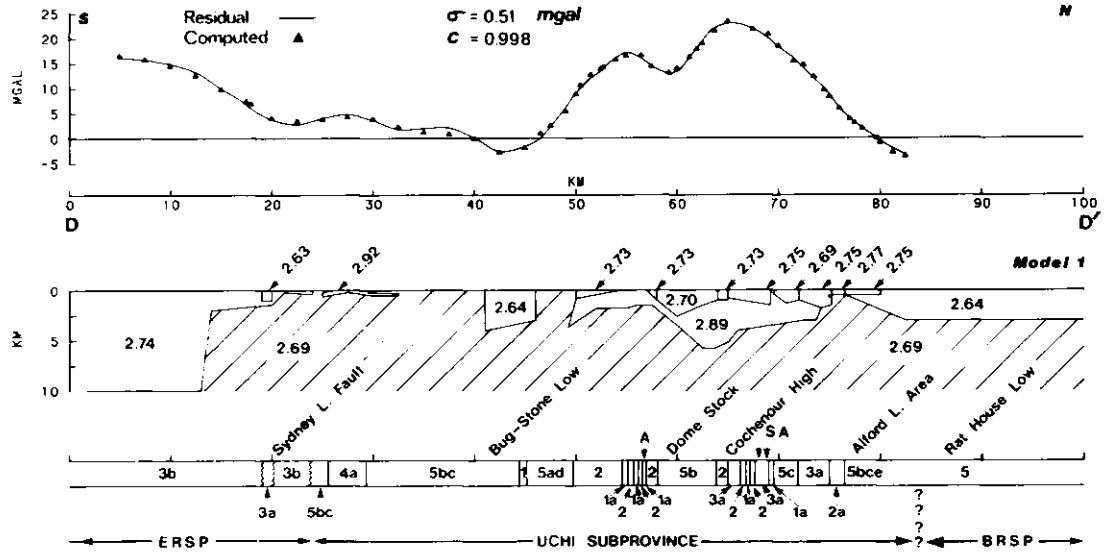

Figure 24a. *Profile DD' (Model 1), showing the graphical residual and computed gravity anomalies, interpreted gravity models and surface geology. Densities in g/cm³. For profile location see Figure 20. See Table 3 for explanation of geological legend.*

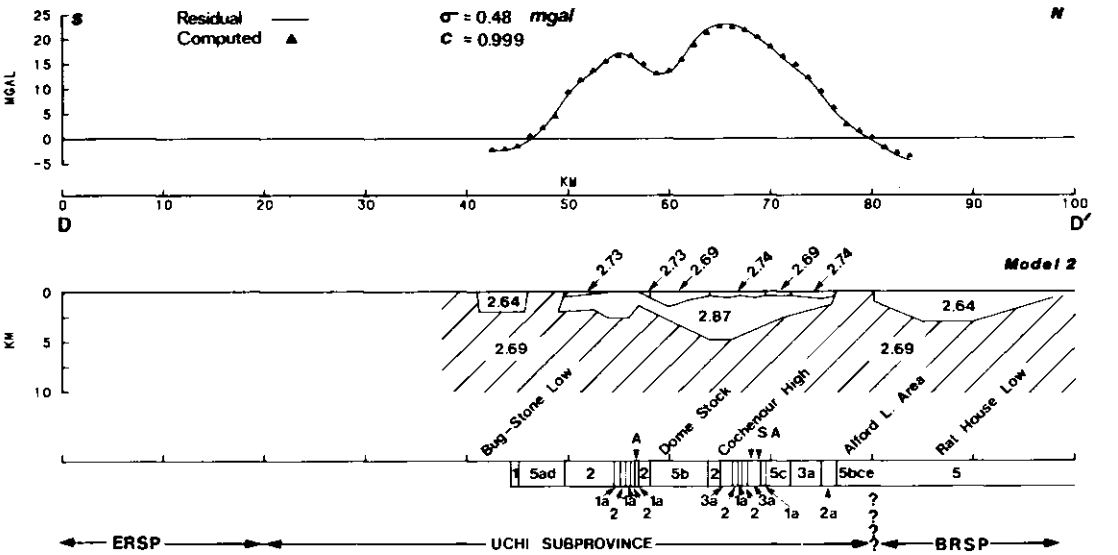

Figure 24b. *Profile DD' (Model 2), showing the graphical residual and computed gravity anomalies, interpreted gravity models and surface geology. Densities in g/cm³. For profile location see Figure 20. See Table 3 for explanation of geological legend.*

Profile EE′

This 90 km long, approximately northward-trending profile (Figure 25) passes through the Northern Supracrustal Domain, the Bug Lake-Stone Lake gravity low, the "Howey Diorite" gravity high, the Cochenour gravity high, and the Rathouse Lake gravity low. The coefficient of correlation between the observed and calculated anomalies is 0.999 and the estimate of standard deviation is 0.44 mgal.

The interpreted characteristics of the metasedimentary trough of the Northern Supracrustal Domain are similar to those found in earlier profiles. These are a 14 to 16 mgal residual positive anomaly, a gentle southerly dip with limited depth extent in the vicinity of the Sydney Lake Fault System, and a steep dip with a 8 to 10 km depth extent a few kilometres south of the fault. On the present profile, the depth extent of the trough is about 9 km. The 2 mgal negative residual anomaly, at kilometre 29, coincides on the surface with granodioritic and trondhjemitic rocks. This small anomaly is also quite distinct on the the Bouguer anomaly map. To model this anomaly, lighter rocks are required whose mean density is less than the background density. Therefore, a mean density of 2.64 g/cm^3 was chosen to model a 3.5 km deep intrusive body which partly underlies the mafic intrusive rocks (2.8 g/cm^3) outcropping near kilometre 31.

The Bug Lake-Stone Lake gravity low has been modeled using a mean density of 2.64 g/cm^3. The intrusive body is interpreted as having a depth extent of less than 2 km. The northern edge of this intrusive body comes into contact with the steeply dipping Red Lake Greenstone Belt. A 27 mgal amplitude positive residual anomaly, known as the Cochenour gravity high, coincides with the eastern part of the Red Lake Greenstone Belt. It has been shown from the model (Figure 25) that the major contribution of the anomaly is due to the mafic metavolcanics which are exposed in a few locations. The outcropping felsic to intermediate metavolcanic, metasedimentary, and intrusive units including the "Howey Diorite" are all contained within the mafic metavolcanics. Most of these units with the exception of the "Howey Diorite" are <1 km thick. The steeply dipping rocks of the "Howey Diorite" have a depth extent of about 2 km. The bottom topography of the mafic metavolcanics takes the form of a homocline structure between kilometres 50 to 65 where its depth-extent varies between 1 to 3 km. The deepest section (4 km) of the mafic metavolcanics sequence is interpreted at kilometre 70 where a synclinal axis has also been mapped at the surface.

In the Alford Lake area, the positive residual anomaly has been explained by the limited depth extent, 0.5 km, mafic phases (mean density 2.75 g/cm^3) of the Rathouse Lake Batholith (mean density 2.64 g/cm^3) which has a depth extent of about 3 km.

Profile FF′

This profile (Figure 26) runs north-northwest from the English River metasediments across the Trout Lake granitic area approximately 20 km to the east of the Red Lake Greenstone Belt.

The English River metasediments attain a maximum depth extent of 9 km and the subprovince boundary models with a southerly 45 degree dip. The reliability of this interpretation is moderated by the proximity of a low density (2.63 g/cm^3) diatexite unit, although Profile GG′ (*see* Figure 27) lends credibility to this interpretation.

The interpretation between kilometres 17 and 45, covering Sandy Creek gravity low, the Bruce Stock gravity low, and the Ten Mile Creek gravity high is highly qualitative both from the lack of density data and structural ambiguity. These units are modeled as thinning out north of the Sydney Lake Fault and are less than 1 km thick.

The structure shown for the granitic areas of the Trout River and Trout Lake gravity lows suffers from the lack of surface detail. The interpreted model shows that the Trout River and the Trout Lake Batholiths are interconnected and their limited depth extent suggest that they are probably extensive sheets.

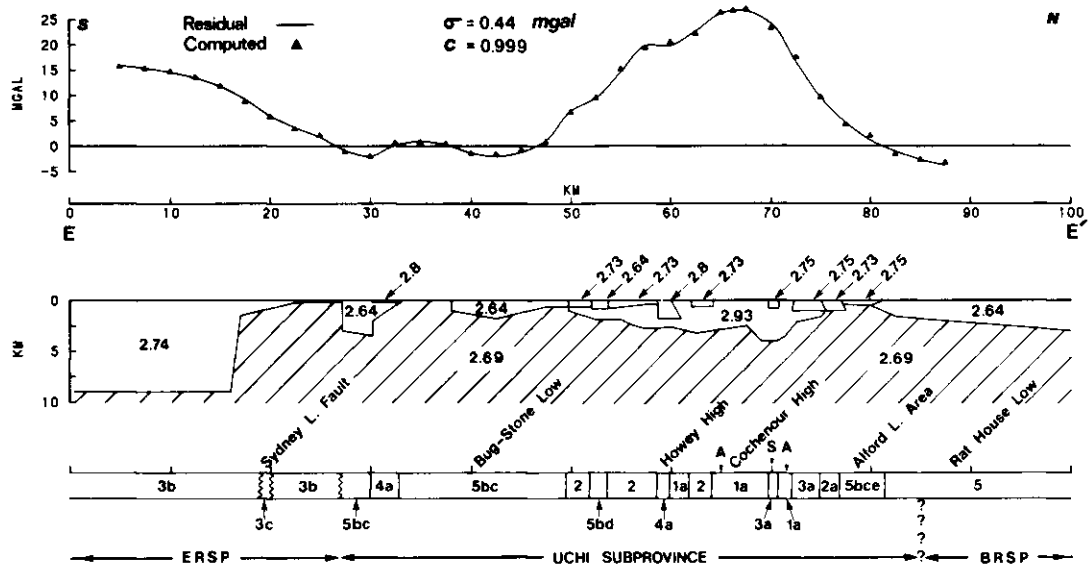

Figure 25. *Profile EE', showing the graphical residual and computed gravity anomalies, interpreted gravity models and surface geology. Densities in g/cm³. For profile location see Figure 20. See Table 3 for explanation of geological legend.*

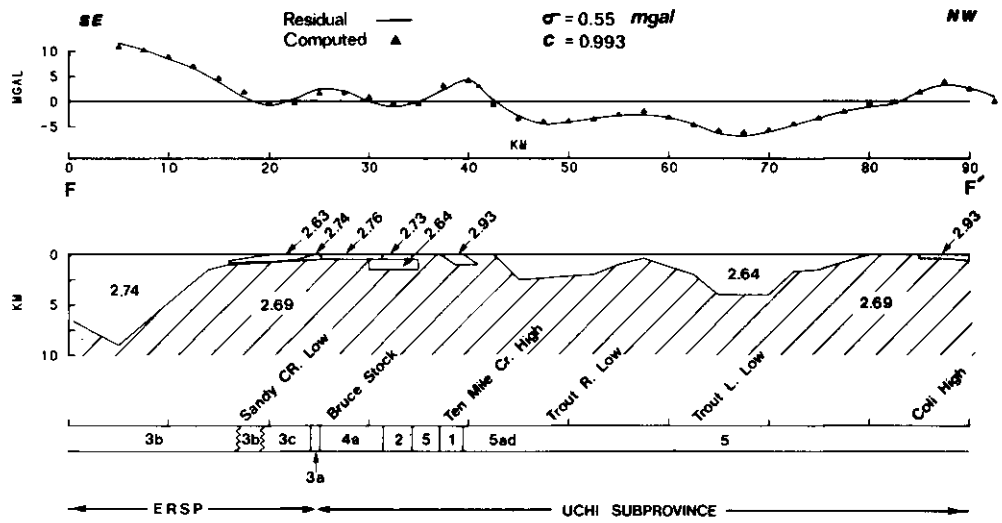

Figure 26. *Profile FF', showing the graphical residual and computed gravity anomalies, interpreted gravity models and surface geology. Densities in g/cm^3. For profile location see Figure 20. See Table 3 for explanation of geological legend.*

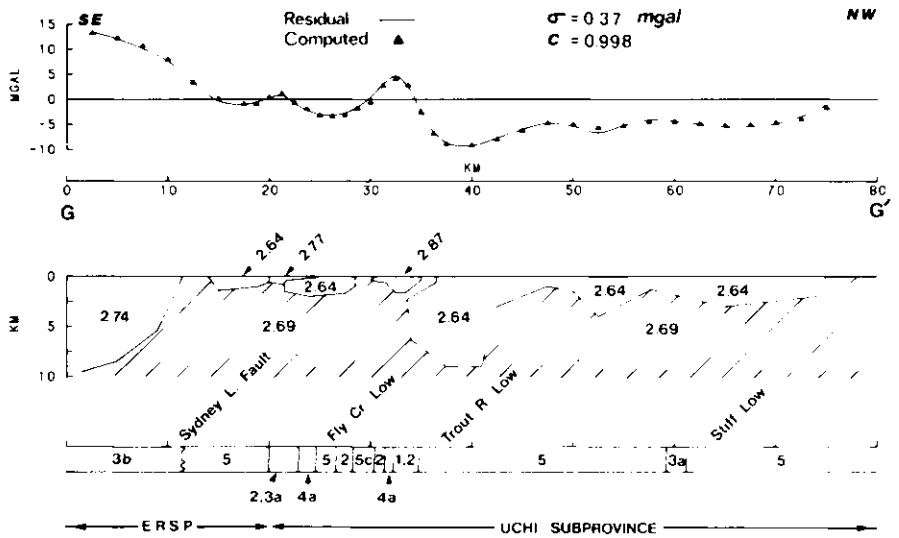

Figure 27. *Profile GG', showing the graphical residual and computed gravity anomalies, interpreted gravity models and surface geology. Densities in g/cm³. For profile location see Figure 20. See Table 3 for explanation of geological legend.*

Near its northwestern end, the profile passes through the eastern end of the Coli Lake gravity high which has been modeled using a mean density of 2.93 g/cm³. The Coli Lake Belt appears to be <1.0 km thick. A better model of this belt is discussed in profile WW'.

Profile GG'

The profile (Figure 27) runs parallel to, and approximately 17 km east of profile FF', and about 17 km to the west of the Birch-Uchi Greenstone Belt. It passes through the Northern Supracrustal Domain and extends across the granitic terrain of the Fly Creek, Trout River, and Stiff Lake areas.

The geological section shows more detail than is warranted by the station spacing, and as a result densities have been averaged over several units in certain areas.

The English River metasediments in this profile model to a depth-extent of 10 km, and the south dipping structure agrees well with the extrapolated position of the Sydney Lake cataclastic zone at kilometre 12. This interpretation is considered fairly reliable as there are no additional surface units to create ambiguity.

The granitic unit between kilometres 12 and 20, which forms part of the Bluffy Lake Batholith, has been modeled with a density of 2.64 g/cm³, although the average over the entire exposure is 2.69 g/cm³. This light density is dictated primarily by the regional-residual separation, which may be in error by 1 to 2 mgal. It can also be justified by the difference in gravity response between this part and the remainder of the batholith, indicating different phases of intrusive material.

The Fly Creek granite, mean density 2.64 g/cm³, underlies much of the felsic to intermediate metavolcanics and metasediments of mean density 2.77 g/cm³ near kilometre 23. The Trout River granitic area is characterized by a prominent 9 mgal amplitude negative residual anomaly which gives a depth extent of 9 km to the granites of mean density 2.64 g/cm³. The Stiff Lake granitic area models as a sheet-like structure, <3 km in depth-extent (it is at its deepest on Profile RR') and joins the Trout River Batholith.

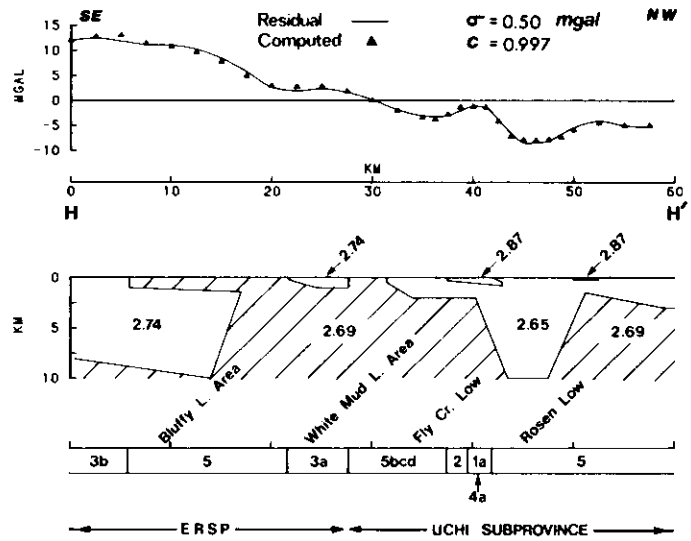

Figure 28. *Profile HH', showing the graphical residual and computed gravity anomalies, interpreted gravity models and surface geology. Densities in g/cm³. For profile location see Figure 20. See Table 3 for explanation of geological legend.*

The interpreted structure of the granitic rocks implies that these rocks "welled up" from the Trout River and Rosen Lake areas, then spread laterally in thin sheets. The Bluffy Lake, Fly Creek, and Trout River units have all been modeled discretely, but they could be joined at depth.

The Fredart Lake arm (mean density 2.87 g/cm³) of the Birch-Uchi Belt, at kilometre 33, possibly represents a homocline, but the contouring interval is not sufficient for a more detailed interpretation.

Profile HH'

This profile (Figure 28) runs north-northwest across the Bluffy Lake Batholith, the Whitemud Lake area, the Rosen Lake Batholith, and across the Fredart Lake arm of the Birch-Uchi Belt. The geological feature of primary interest in this profile is the Bluffy Lake Batholith.

The Bluffy Lake Batholith (mean density 2.69 g/cm³), an extensive body of trondhjemite-granodiorite, is clearly outlined on the aeromagnetic maps, but due to a lack of density contrast, little correlation is possible with the gravity except in the immediate vicinity of Bluffy Lake. In modeling this body, the Northern Supracrustal Domain metasediments were preassigned a thickness of 10 km (from previous profiles), and the depth of the Bluffy Lake Batholith was adjusted accordingly. The resulting interpretation shows the batholith to be a relatively thin sheet of less than 1.5 km thickness which has possibly intruded the metasediments from the north. This would be in conformity with the structures interpreted in Profile II' (*see* Figure 29). Unfortunately, the dips of the contacts are not known, so greater accuracy is not possible.

The English River-Uchi Subprovince boundary is, again, represented by a steeply dipping discontinuity, with metasediments to the south and granitoids to the north. The angle of contact is approximate.

The Rosen Lake gravity low is characterized by an 8.5 mgal negative residual anomaly which is interpreted due to a granite batholith having a mean density 2.65 g/cm³.

Although some trondhjemite and granodiorite has been mapped in the batholith region, the surface sampling implies a more granitic composition of mean density of 2.65 g/cm^3. The shape of the Rosen Lake Batholith which extends to a depth of 10 km strongly indicates that the granites welled up to the surface and then spread out laterally in a thin sheet.

Profile II'

This northwest-trending profile (Figure 29) runs across the Bluffy Lake Batholith, the Whitemud Lake metasedimentary area, the Lost Bay gravity high, and terminates at the western limb of the Birch-Uchi Belt near Fly Creek.

The Bluffy Lake Batholith, though lacking in density contrast (mean density 2.69 g/cm^3), corresponds with a region having a positive residual anomaly. This may be caused by the dense metasediments (mean density 2.74 g/cm^3) of the English River Subprovince underlying the Bluffy Lake Batholith to a depth of about 12 km.

Due to a lack of density contrast, the batholith cannot be modeled directly, but the underlying metasediments indicate that the batholith is a thin sheet not more than 3 km in depth-extent. The Northern Supracrustal Domain metasediments of mean density 2.74 g/cm^3 belonging to the Whitemud Lake area, have depth-extents varying from less than 0.2 km to 3 km. A granitoid segment of 2 km depth-extent outcrops at kilometre 29.

Figure 29 shows a model of the various units of the Birch-Uchi Greenstone Belt, which satisfies the surface geology and the residual gravity. The Lost Bay gravity high has been modeled due to the mafic metavolcanics (mean density 2.93 g/cm^3) which are less than 3.5 km in depth extent. A mapped synclinal axis, near kilometre 46, does not agree with the gravity interpretation. The present interpretation shows that the greenstone belt is thinning (calculated thickness less than 0.5 km) rather than thickening at the mapped synclinal axis at kilometre 46. It is, therefore, suggested that the synclinal axis be moved 5 to 6 km to the south, near kilometre 40, where there is evidence of a prominent syncline from the model.

Profile JJ'

Profile JJ' (Figure 30) runs approximately in a northwest direction across Bluffy Lake Batholith, the Whitemud Lake metasedimentary area, the Lost Bay gravity high, the Fly Creek gravity low, the Mitchell gravity high, and the Rosen Lake gravity low.

As suggested in earlier models, the Bluffy Lake Batholith has a depth extent of about 3 km. The batholith is a sheet-like structure that is enclosed completely within the metasediments of the English River Subprovince; these rocks extend to a depth of about 12 km along this profile. The metasediments of the Whitemud Lake area have a depth-extent of less than 3 km, with their maximum depth to the north. The metavolcanics (mean density 2.80 g/cm^3) of the Lost Bay High have a depth-extent of about 3 km (*see* Profile II' Figure 29).

The Fly Creek and the Rosen Lake gravity lows are associated with low density granitic rocks (mean density 2.64 g/cm^3). Between kilometres 50 and 55, the shallow supracrustal units belonging to the Mitchell gravity high of the Birch-Uchi Greenstone Belt occur as shallow remnants (less than 1.5 km thick) in a granitic terrain. The Rosen Lake Batholith has a root which extends to a depth of 12 km. A 3 km deep body consisting of felsic metavolcanics (mean density 2.73 g/cm^3) is almost surrounded by granites, near kilometre 62.

Profile KK'

This northwest-trending profile (Figure 31) focuses primarily on the structure of the southwest part of the Birch-Uchi Greenstone Belt. Because of the complexity and abundance of numerous relatively thin geological units, a uniform density of 2.87 g/cm^3 has been assumed for most of the metavolcanic areas, with the

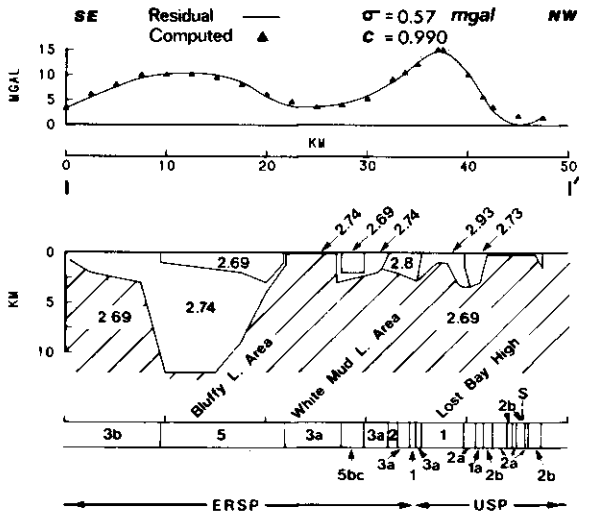

Figure 29. *Profile II', showing the graphical residual and computed gravity anomalies, interpreted gravity models and surface geology. Densities in g/cm³. For profile location see Figure 20. See Table 3 for explanation of geological legend.*

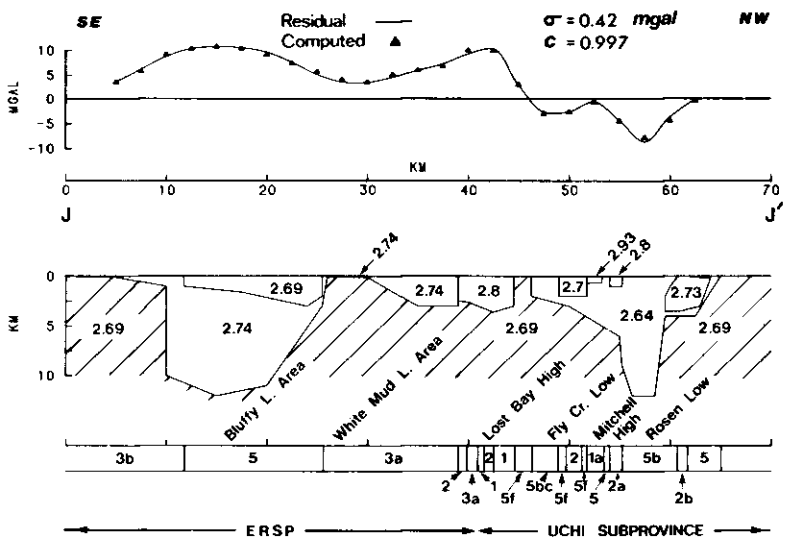

Figure 30. *Profile JJ', showing the graphical residual and computed gravity anomalies, interpreted gravity models and surface geology. Densities in g/cm³. For profile location see Figure 20. See Table 3 for explanation of geological legend.*

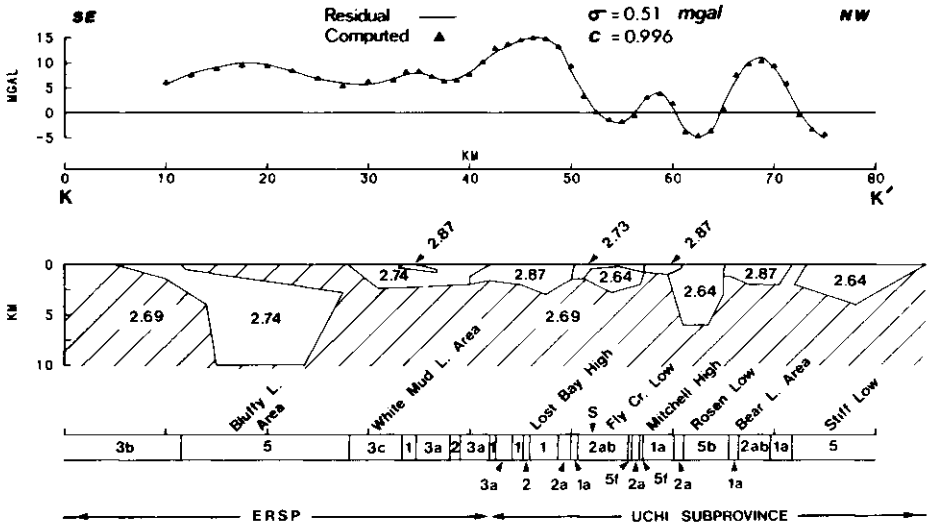

Figure 31. *Profile KK', showing the graphical residual and computed gravity anomalies, interpreted gravity models and surface geology. Densities in g/cm³. For profile location see Figure 20. See Table 3 for explanation of geologic legend.*

exception of the felsic to intermediate metavolcanic units between kilometres 51 to 57 which have a mean density of 2.73 g/cm³.

The Whitemud metasediments extend to a depth of 2 km, with a greenstone remnant at kilometre 34. The maximum depth-extent for the metavolcanics of the Lost Bay gravity high region is 3 km. A synclinal axis is suggested at kilometre 48, since this is the deepest part of the greenstone belt, along this profile. The mapped synclinal axis at kilometre 54 models, from the gravity data, as an anticlinal structure. This discrepancy also exists on Profiles II', MM', and RR' (Figures 29, 33, and 38).

The Fly Creek gravity low at kilometre 54 is interpreted to be caused by an intrusive feature, based on the mapped graben structure and extrapolation of the intrusive body which outcrops south of the anomaly. The intrusion has been modeled as a discreet body, but may be connected at depth with the Rosen Lake Batholith (as in Profile JJ' (Figure 30)) which may also be joined with the Stiff Lake Batholith (*see* Profile GG'; Figure 27). The Rosen Lake Batholith here extends to a depth of about 6 km, whilst the Stiff Lake Batholith is comparatively shallower as it extends to a depth of only 4 km.

Profile LL'

This north-trending profile (Figure 32) originates in the English River metasediments and runs across the Papaonga Lake gravity high, the Allison-Sesikinaga Lakes granitic area, the Seagrave Lake gravity high, the Gull Lake gravity low, the Casummit Lake gravity high, and terminates in the Shearstone-Kerswill Lakes granitic area. The profile shows poor correlation between the gravity field and the surface geology.

The English River-Uchi Subprovince boundary has been interpreted as a steeply south dipping interface with metasediments extending to a depth of 8 km. The diatexites (mean density 2.63 g/cm³) occurring within the metasediments are less than 1 km thick.

The Allison-Sesikinaga Lakes granitic area is characterized by an 8 mgal negative residual anomaly which has been modeled using a uniform density of

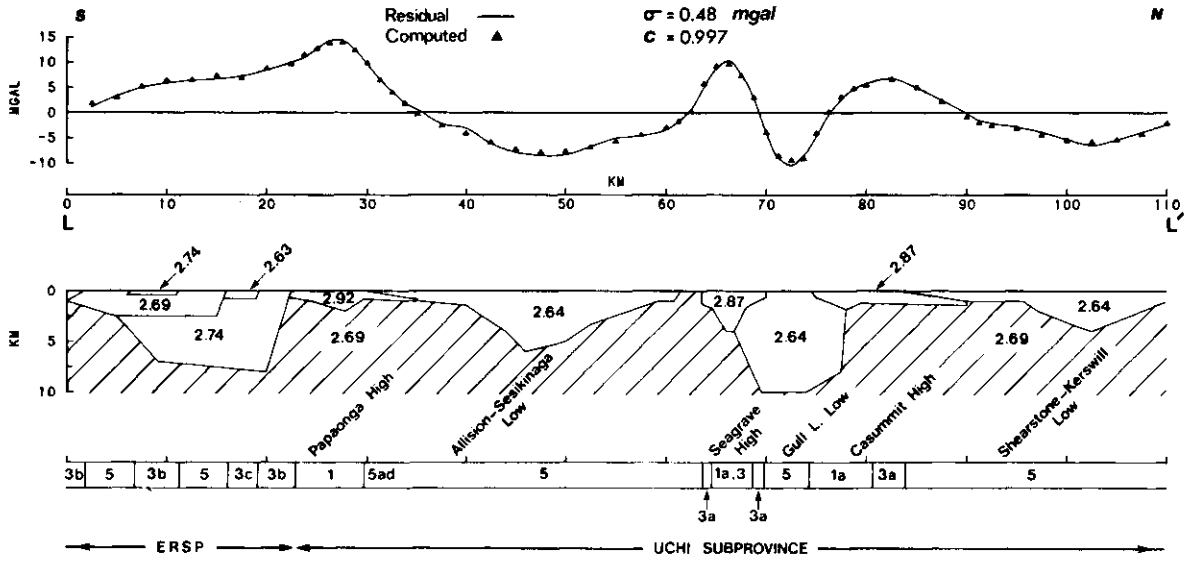

Figure 32. *Profile LL', showing the graphical residual and computed gravity anomalies, interpreted gravity models and surface geology. Densities in g/cm³. For profile location see Figure 20. See Table 3 for explanation of geological legend.*

2.64 g/cm^3. The batholith on this profile extends to a depth of 6 km below the surface. It reaches almost 8 km, its maximum, on Profile PP' (Figure 36).

In the Papaonga Lake and Casummit Lake gravity high regions, a major discrepancy exists in the residual gravity anomalies over the greenstone-granite contact. In the Casummit Lake gravity high region, the positive residual anomaly peaks almost at the metasediment-granite contact, near kilometre 83. However, the positive gravity region extends for another 6 km (up to kilometre 89) into the low density granitic terrain (mean density 2.64 g/cm^3). Although the density sampling north of location kilometre 83 is relatively sparse, there is no evidence to support the existence of denser granites which could explain the positive gravity anomaly. A similar correlation problem occurs at kilometre 30 in the Papaonga Lake area. In both areas, the mafic metavolcanics have been interpreted as relatively thin units (less than 2 km) with gentle dips and extending below the granites. This gives the granites a nappe structure overhanging from the north. In the Papaonga Lake area, near kilometre 30, an 80° dip has been recorded from surface mapping, but cannot be incorporated in the gravity interpretation. This poses a challenge to re-examine the supposed origin of vertical and subvertical dips which dominate most Archean greenstone belts (*see* Gupta *et al.* 1982).

The gravity interpretation indicates probable synclinal structures in the greenstone (mean density 2.87 g/cm^3) directly below the peak of the Seagrave Lake gravity high at kilometre 66, and possibly in the Casummit Lake gravity high region of the Springpole Lake arm at kilometre 78. It is suggested that between the two synclines a possible anticline structure is now intruded by the granites of the Gull Lake Batholith. The batholith, represented by a 10 mgal negative residual anomaly, extends to a depth of 10 km. The depth is approximate because of the effect of the main mass of the batholith lying to the east has not been taken into account.

The Shearstone-Kerswill Lakes granite body is a shallow dipping sheet-like mass which has been modeled using a mean density of 2.64 g/cm^3 to have a depth extent of 4 km.

Profile MM'

This profile (Figure 33) runs from the English River metasediments in a north-northwest direction across the central synclinal axis of the Birch-Uchi Greenstone Belt just to the south of the Perrigo and Okanse intrusive rocks and into the Berens River area. The profile intersects the two largest positive anomalies of the Birch-Uchi Greenstone Belt, the Lost Bay gravity high (+22 mgal) and the Goodall gravity high (+27 mgal). Two possible models are shown in Figures 33a and 33b. The second model is a more detailed interpretation of the greenstone belt.

Model 1

The interpretation (Figure 33a) of the Northern Supracrustal Domain metasediments is considered least reliable because of the surface outcrops of trondhjemite and diatexites. The depth extent of the metasediments has been computed to be <6 km, which is the minimum depth computed compared to all the previous profiles.

The geological section shows a complex folded structure with several additional fold axes interpreted from the gravity data and supported by the surface relationships. In this model, a single uniform density of 2.87 g/cm^3 has been used for most of the greenstone belt.

The felsic to intermediate metavolcanics (mean density 2.73 g/cm^3) between kilometres 35 to 40, and the metasediments (mean density 2.75 g/cm^3) between kilometres 42 to 49, belonging to the Papaonga Lake area have been interpreted as shallow basins, less than 1 km deep. These units are underlain by mafic metavolcanics which outcrop extensively in the Lost Bay gravity high region and have depth-extents varying between 0.5 km to 4 km. The assumption of buried layered mafic metavolcanics in certain locations is necessary to generate sufficient gravity effect which is comparable to the residual anomaly. This is justified on the basis of the mapped geological configuration and is also shown by Profile PP' in the

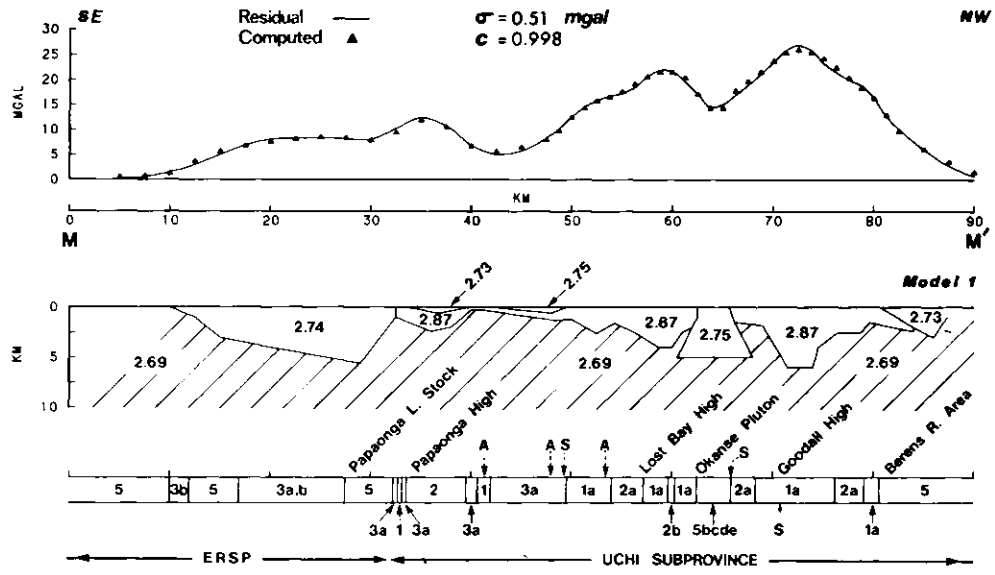

Figure 33a. *Profile MM' (Model 1), showing the graphical residual and computed gravity anomalies, interpreted gravity models and surface geology. Densities in g/cm³. For profile location see Figure 20. See Table 3 for explanation of geologic legend.*

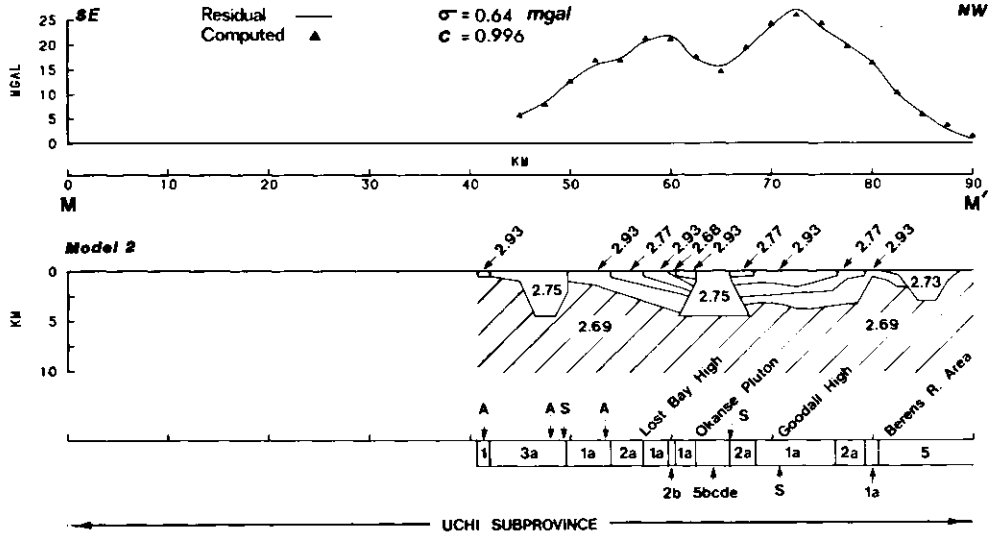

Figure 33b. *Profile MM' (Model 2), showing the graphical residual and computed gravity anomalies, interpreted gravity models and surface geology. Densities in g/cm³. For profile location see Figure 20. See Table 3 for explanation of geological legend.*

Grace Lake area. The interpreted depth-extents and fold axis locations are only approximate because of the inherent ambiguity of the potential field.

The inverted funnel-shaped Okanse intrusive extending to a depth of 5 km, centred at kilometre 64, is flanked to the south by the Lost Bay gravity high and to the north by the Goodall gravity high. The Okanse intrusive, which is wider at its base than at its top, has been interpreted as a diapiric structure having a mean density of 2.75 g/cm^3. The intrusion is possibly intruding an anticlinal structure to the south-southeast of the mapped syncline.

The Goodall gravity high produces the largest residual anomaly (+27 mgal) of the entire Birch-Uchi Belt. The anomaly has been explained by metavolcanics of mean density 2.87 g/cm^3 having a depth-extent of 6 km.

The 2.73 g/cm^3 density rocks of the Berens River area extend to a depth varying from 2 to 3 km depending on the shape and proportion of the underlying rocks. The metavolcanics belonging to the Goodall gravity high grade into the granitic terrain of the Berens River area near kilometre 80 and underlie them for some distance. Similar marginal subsidence has been postulated by Gorman *et al.* (1978) based on Romberg's experiments.

Model 2 In this model (Figure 33b) all the exposed geological units have been assigned observed mean densities unlike the first model where the greenstone belt was assigned a single mean density. The model also takes into account the three mafic to felsic cycles of volcanism and the central synclinal axis about which the folding took place (Thurston *et al.* 1978). From gravity interpretation, the calculated depth-extent of the greenstone belt is <5 km in the Lost Bay gravity high region. The model shows that the mapped volcanic cycles are not continuous at depth as they have been interrupted by the intrusion of the Okanse Pluton which has a depth extent of 5 km. The mafic metavolcanic units are generally deeper than the felsic or intermediate metavolcanic units to produce the large positive anomaly. Between kilometres 42 to 50, a sedimentary basin with a depth-extent of 4.5 km is required to satisfy the residual anomaly, unlike in Model 1 (Figure 33a) where metasediments of 0.5 km depth-extent were underlain by mafic metavolcanics.

Profile NN'

This profile (Figure 34) runs northerly along the eastern edge of the survey area and intersects the Snelgrove Lake gravity low, the Moon Lake gravity high, and the Gull Lake gravity low. Two alternate interpretations have been provided for this profile, the second based on the residual anomaly obtained from the upward continuation method.

Model 1 The Snelgrove Lake Batholith is associated with a 9 mgal negative residual anomaly (Figure 34a). The batholith extends to a depth of 5 km and could be a southward extension of the much larger Gull Lake Batholith. The Gull Lake Batholith produces the lowest Bouguer contour (-78 mgal) of the entire survey area with a negative residual anomaly of -19 mgal amplitude. The batholith has been considered as one single body of uniform density 2.64 g/cm^3. The residual anomaly closely follows the general outline of the granitic area with some minor deviations. A granitic batholith with a root extending to a depth of 16 km has been modeled. However, two factors should be noted:

1. The interpretation is extremely sensitive to the density contrast. For example, changing the density contrast by -0.01 mgal (well within the standard error) would result in a depth extent of only 13 km from the present 16 km.
2. The present profile runs along the edge of the survey area where there is little control on regional residual separation. Therefore, the computed depth extent of the Gull Lake Batholith is highly qualitative.

From the shape of the calculated bodies the Snelgrove Lake and Gull Lake Batholiths appear to thin out substantially into sheet-like structures on their southern and northern interfaces, respectively. It is speculated that the sheet-like bodies near the margins of the batholiths probably "spread out" from the main mass. The

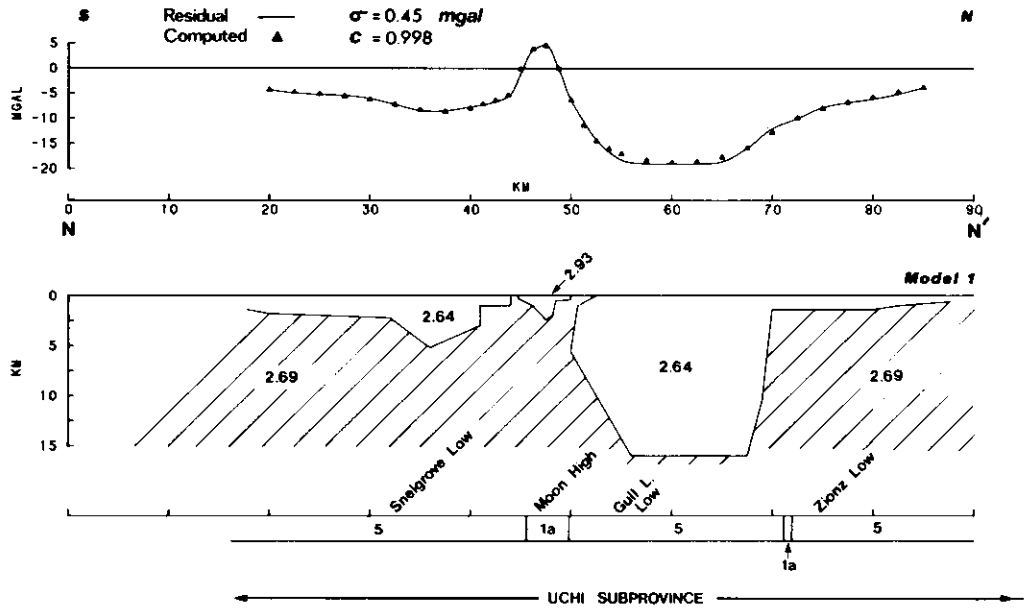

Figure 34a. *Profile NN' (Model 1), showing the graphical residual and computed gravity anomalies, interpreted gravity models and surface geology. Densities in g/cm³. For profile location see Figure 20. See Table 3 for explanation of geological legend.*

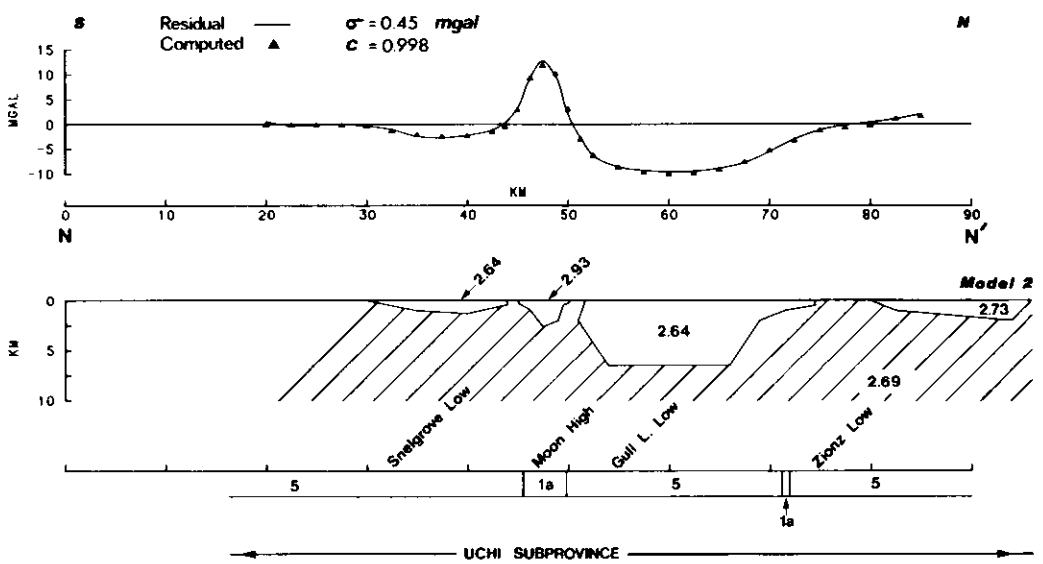

Figure 34b. *Profile NN' (Model 2), showing the 16.09 km upward continuation based residual and computed gravity anomalies, interpreted gravity models and surface geology. Densities in g/cm³. For profile location see Figure 20. See Table 3 for explanation of geological legend.*

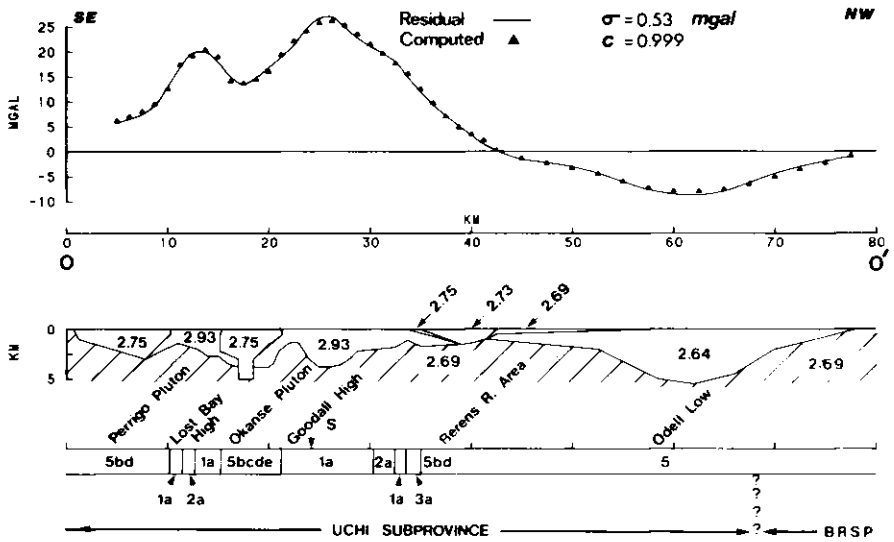

Figure 35. *Profile OO', showing the graphical residual and computed gravity anomalies, interpreted gravity models and surface geology. Densities in g/cm³. For profile location see Figure 20. See Table 3 for explanation of geological legend.*

two batholiths have been interpreted as separate bodies with the Moon Lake metavolcanics body lying between them (also *see* Profile QQ', Figure 37). However, they could also be modeled as a single batholith continuing below the metavolcanics.

The Moon Lake gravity high coincides with mafic metavolcanics that are less than 2.5 km in depth-extent.

Model 2 To obtain a more moderate depth extent for the Gull Lake Batholith than that calculated from Model 1, the 16.09 km upward continuation based residual anomaly with a 6.5 mgal base level shift was used for two-dimensional interpretation (Figure 34b). A 6.5 km depth extent for this batholith is obtained using a mean density of 2.64 g/cm³, whereas the Snelgrove Batholith has a depth-extent of 1 km instead of 5 km as in Model 1. The discrepancy between the differing depths obtained from the two models points to the problem of regional and residual separation. The models are thus heavily dependent on the regional background level chosen.

Profile OO'

This northwest-trending profile (Figure 35) almost passes through the centre of the Birch-Uchi Greenstone Belt. It starts in the region of the Perrigo Pluton, catches the northern end of the Lost Bay gravity high, through the Okanse Pluton and the Goodall gravity high, into the Berens River area where it finally ends in the batholithic region of the Odell Lake gravity low.

The inward dipping Perrigo Pluton of mean density 2.75 g/cm³ extends to a depth of about 3 km. As in Profile MM', the northern part of the Lost Bay gravity high has a 4 km depth-extent for the metavolcanic units. The Okanse Pluton of mean density 2.75 g/cm³ extends to a depth of 5 km,but here models with a root at the bottom. The depth-extent of the mafic metavolcanics in the Goodall gravity high region is about 4 km. The bottom topography of the metavolcanics shows the form of anticlinal, synclinal, and homoclinal structures. The mapped synclinal axis,

near kilometre 24, is offset by 1 km southeast of the deepest part of the greenstones.

The granitic area of the Odell Lake region has been modeled using a mean density of 2.64 g/cm^3. The gentle inward dipping bowl-shaped granitic body extends to a depth of less than 6 km, as with Profile PP' (Figure 36).

Profile PP'

This profile (Figure 36) runs northwest perpendicular to the main trend of the north-central part of the Birch-Uchi Greenstone Belt. It intersects the Allison-Sesikinaga Lakes gravity low, the positive anomalies of the Grace Lake area, the Shabumeni Lake gravity high, and the Odell Lake gravity low. Two models have been computed, using different density values for the metavolcanics.

Geological details in the granitic areas are sparse, particularly in the Berens River and Odell Lake areas.

Model 1 The Allison-Sesikinaga Lakes Batholith (Figure 36a) (mean density 2.64 g/cm^3) appears to deepen toward the greenstone granite contact, attaining a maximum depth-extent of about 7.5 km (this deepens slightly in Model 2). The gravity modeling requires that the granite extend beneath the greenstone belt for at least 4 km, while the overlying Grace Lake metasediments (mean density 2.75 g/cm^3) are shallow. This implies that the Costello Lake, Cook Lake, Bertha Lake, and Deaddog Lake intrusive rocks all lie along an anticlinal axis.

A mapped anticlinal axis near kilometre 55 is flanked to the north by a mapped syncline. Both are located in the metasediments of the Grace Lake area and correspond with the gravity interpretation. The magnitude of the residual anomaly associated with the metasedimentary rocks and the mapped fold patterns indicate that the Grace Lake metasediments are underlain by mafic metavolcanic rocks (mean density 2.93 g/cm^3) as for Profile MM' (Figure 33), Model 1 in the Papaonga area. Models with varying proportions of metasediments to metavolcanics give a total depth-extent of between 2.0 to 2.5 km. This implies that the metasediments are probably at most, 2 km thick.

On the basis of gravity modeling, a synclinal axis is proposed near kilometre 70, along the Shabumeni Lake arm of the Birch-Uchi Greenstone Belt, possibly flanked to the northwest by a marginal homocline. The latter carries the metavolcanics beneath the granitic rocks of the Berens River area. The syncline could be an extension of the major fold which controls the structure of the south-central area of the Birch-Uchi Belt. The 4 km thick metavolcanics corresponding with the Shabumeni Lake gravity high region have been modeled with a weighted mean density of 2.87 g/cm^3. The metavolcanics near kilometre 58 in the Grace Lake area, underlying the 2.75 g/cm^3 metasediments, have a depth-extent of 2 km.

This profile, in particular, suggests that the vertical dips observed at the surface of the greenstone belts are often due to a "crumpling" of the rocks, rather than a "standing of the unit on end" (*see* Gupta *et al.* 1982).

The density sampling northwest of the Birch-Uchi Greenstone Belt indicates two different lithologies in the Berens River and Odell Lake granitic areas, the corresponding mean densities being 2.73 and 2.64 g/cm^3, respectively. The exact composition of the rocks in these areas is uncertain, however, and there is little difference in their aeromagnetic expression. The lack of geological mapping makes the presented interpretation highly tentative.

Model 2 In this model, (Figure 36b) the mafic and intermediate metavolcanics have been modeled using mean densities of 2.93 and 2.77 g/cm^3, respectively. Here, the interpreted depth-extent of the greenstone belt is <3 km compared to 4 km from Model 1. The general shape of the greenstone belt obtained from Model 2 is similar to that in Model 1. However, the syncline at kilometre 70 has disappeared in Model 2. It is, therefore, imperative to accurately define the lithologies and their mean densities.

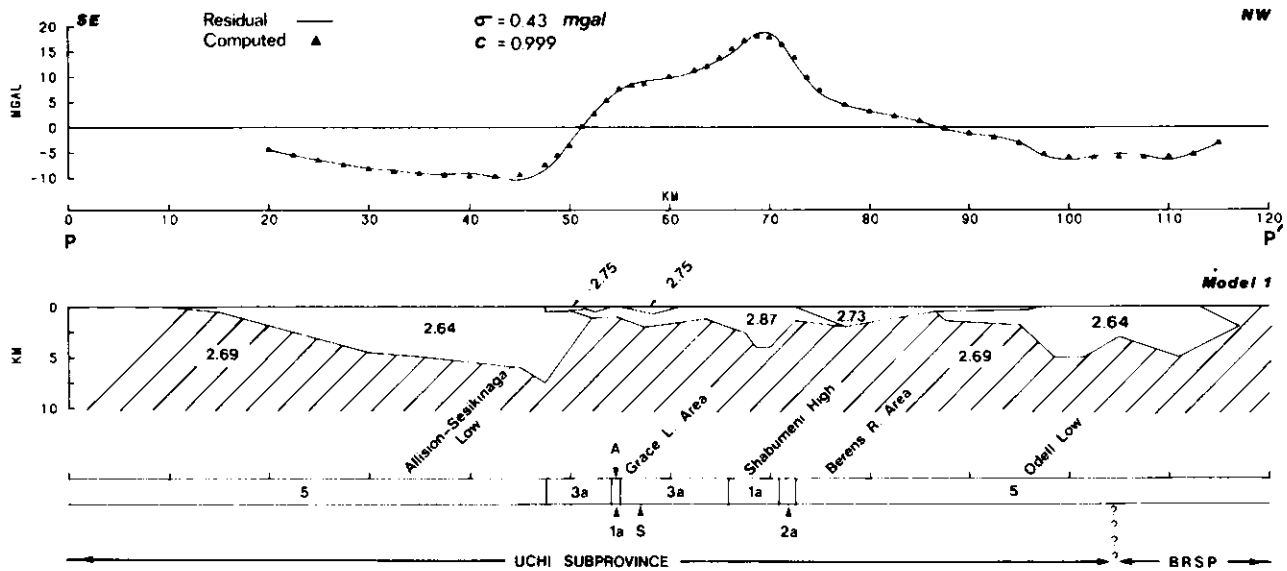

Figure 36a. *Profile PP' (Model 1), showing the graphical residual and computed gravity anomalies, interpreted gravity models and surface geology. Densities in g/cm³. For profile location see Figure 20. See Table 3 for explanation of geological legend.*

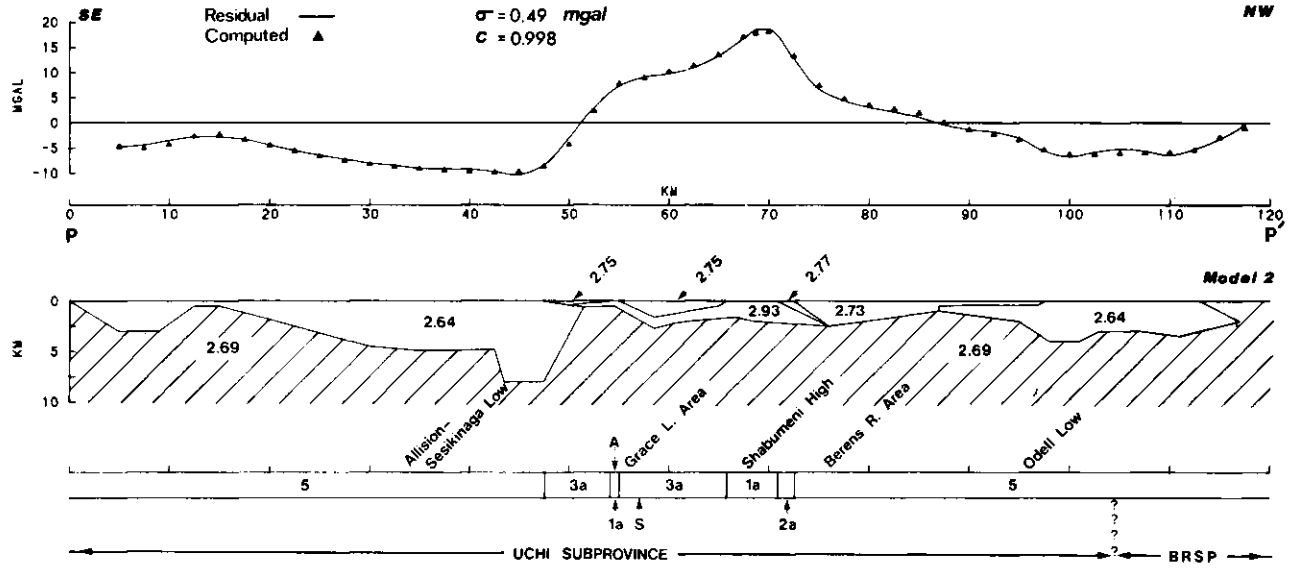

Figure 36b. *Profile PP' (Model 2), showing the graphical residual and computed gravity anomalies, interpreted gravity models and surface geology. Densities in g/cm^3. For profile location see Figure 20. See Table 3 for explanation of geological legend.*

Profile QQ'

Profile QQ' (Figure 37) is approximately 100 km long and trends northwest. It crosses through the Snelgrove Lake granite area, the Moon Lake gravity high, the Gull Lake Batholith, the Zionz Lake gravity low, the Jackpine Lake area and finally, the Shearstone-Kerswill Lakes gravity low. A uniform surface density of 2.64 g/cm^3 has been used in the modeling of the granitic bodies.

The Snelgrove Lake granitic body has a depth extent of 5 km. The Gull Lake Batholith has a relatively flat base and steep, inward dipping interfaces which extend to a depth of 13 km. Near kilometre 58, the northern contact of this batholith connects with the sheet-like granitic body of Zionz Lake which is probably connected at depth with the Shearstone-Kerswill Lakes Batholith. The Shearstone Kerswill Lakes Batholith is a thin (less than 4 km depth-extent) inward dipping body (*see* also Profile XX').

The Moon Lake mafic metavolcanic unit separates the Snelgrove Lake and Gull Lake Batholiths. The metavolcanics have been modeled using a mean density of 2.93 g/cm^3 which resulted in a 1.5 km depth-extent. The supracrustal unit, mean density 2.73 g/cm^3, of the Jackpine Lake area has a depth-extent of about 2 km. Other minor greenstone bodies form remnants within the granite.

Profile RR'

This profile (Figure 38) runs easterly across the centre of the Birch-Uchi greenstone belt and intersects most geological units at 90°. Some of the noticeable anomalies along this profile are the Snelgrove Lake gravity low, the Allison-Sesikinaga Lakes gravity low, the Perrigo Pluton, the Lost Bay gravity high, the Okanse Pluton, the Goodall gravity high, and the Stiff Lake gravity low. Three models of the residual gravity field have been considered for this profile. The first is a simplified version, the other two show variations of the greenstone belt.

The geological section shows three mafic to felsic cycles of metavolcanics comprising a geologically measured 9 km thick sequence of greenstone rocks which are folded about a central synclinal axis (Thurston and Jackson 1978). To the west, the structure has been mapped as a homocline with a steeply dipping, east-facing succession. To the east is a more complicated sequence of steeply plunging, north-trending isoclinal folds, developed on both limbs of a proposed regional anticline (Thurston and Jackson 1978). In this profile, the isoclinal folds are cut by the intrusion of the Perrigo Pluton. To the east and west, the greenstone belt is in contact with the Stiff Lake and Allison Sesikinaga Lakes granitic areas, respectively.

The Allison-Sesikinaga Lakes gravity low is a broad region of negative residual anomalies lying east of the Birch-Uchi Belt. The anomaly which is open to the east, suggests that this batholith extends beyond the eastern boundary of the survey area. Using a mean density of 2.64 g/cm^3, a wedge-shaped inward sloping body extending to a depth of 6.5 km has been calculated to represent the batholith (*see* also Profiles LL' and PP'; Figures 32 and 36). The Stiff Lake Batholith extends to 7 km (*see* Profiles VV' which crosses the centre of this batholith).

Model 1 (Figure 38a) The greenstone belt with a positive residual anomaly of more than 23 mgal has been modeled with an assigned mean density of 2.87 g/cm^3 (Figure 38a). This density value is based on mapped mafic, intermediate, and felsic metavolcanic proportions in the Birch-Uchi Belt (Thurston 1978; Goodwin 1972, 1977). The maximum depth-extent for the greenstones, in this model, is 5.5 km which is obtained directly beneath the peak of the Lost Bay gravity high. A synclinal axis is mapped adjacent to this modeled body which suggests an anticline shape. It implies that the mapped syncline is in the surface rocks only with very limited depth-extent.

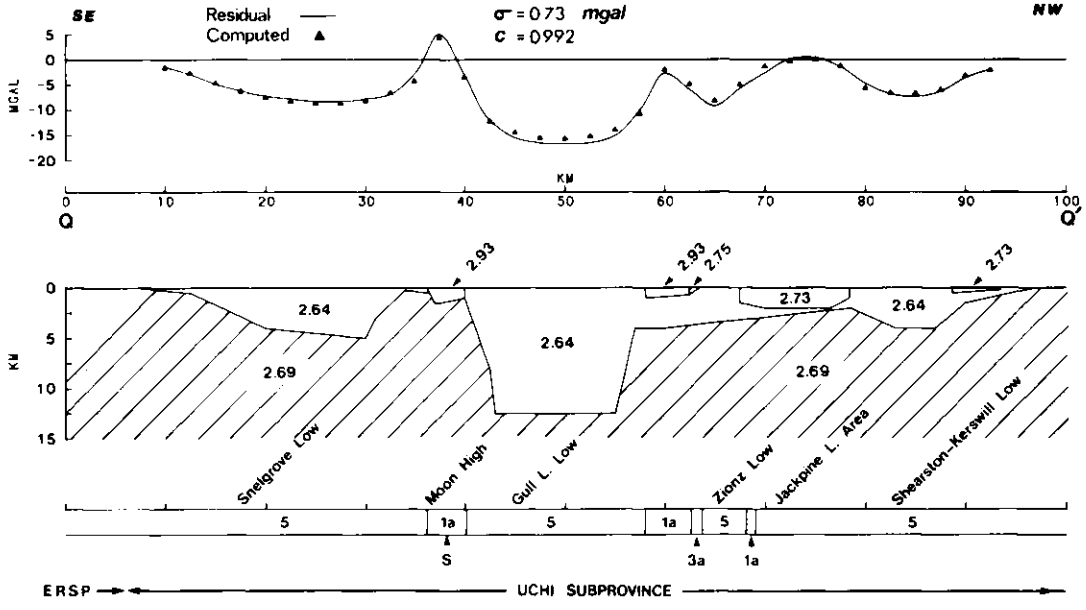

Figure 37. *Profile QQ', showing the graphic residual and computed gravity anomalies, interpreted gravity models and surface geology. Densities in g/cm^3. For profile location see Figure 20. See Table 3 for explanation of geological legend.*

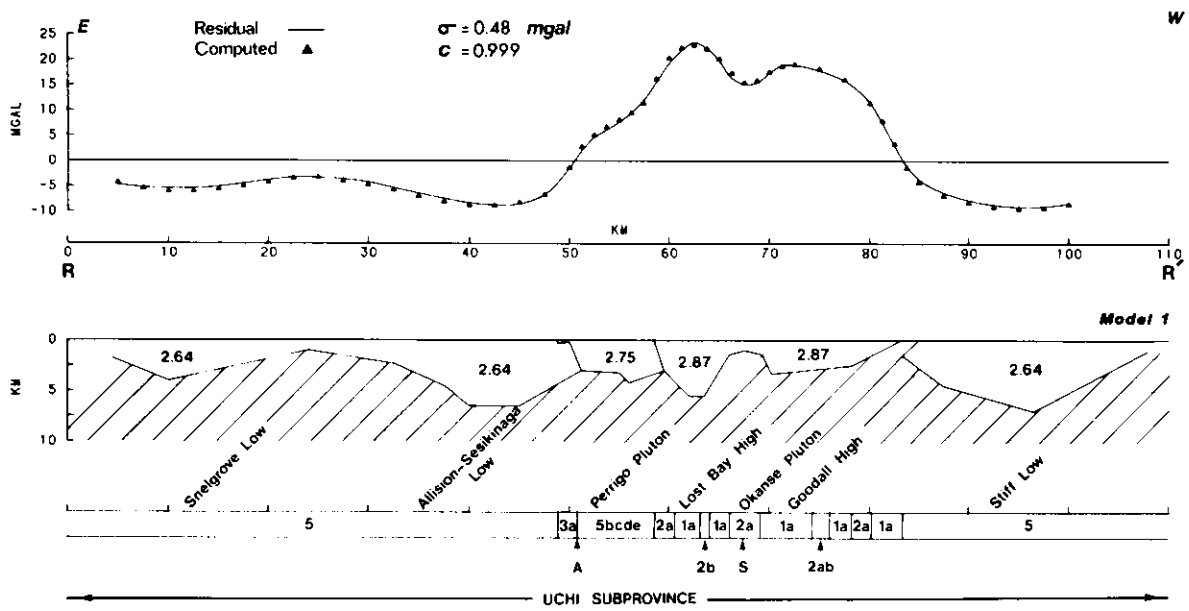

Figure 38a. *Profile RR' (Model 1), showing the graphical residual and computed gravity anomalies, interpreted gravity models and surface geology. Densities in g/cm^3. For profile location see Figure 20. See Table 3 for explanation of geological legend.*

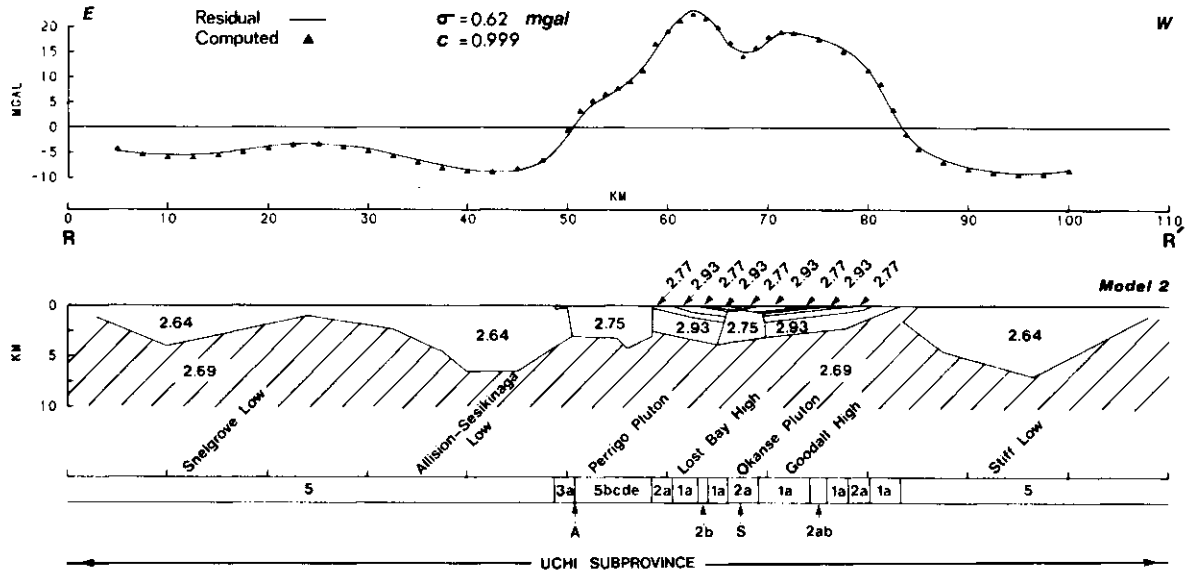

Figure 38b. *Profile RR' (Model 2), showing the graphical residual and computed gravity anomalies, interpreted gravity models and surface geology. Densities in g/cm^3. For profile location see Figure 20. See Table 3 for explanation of geological legend.*

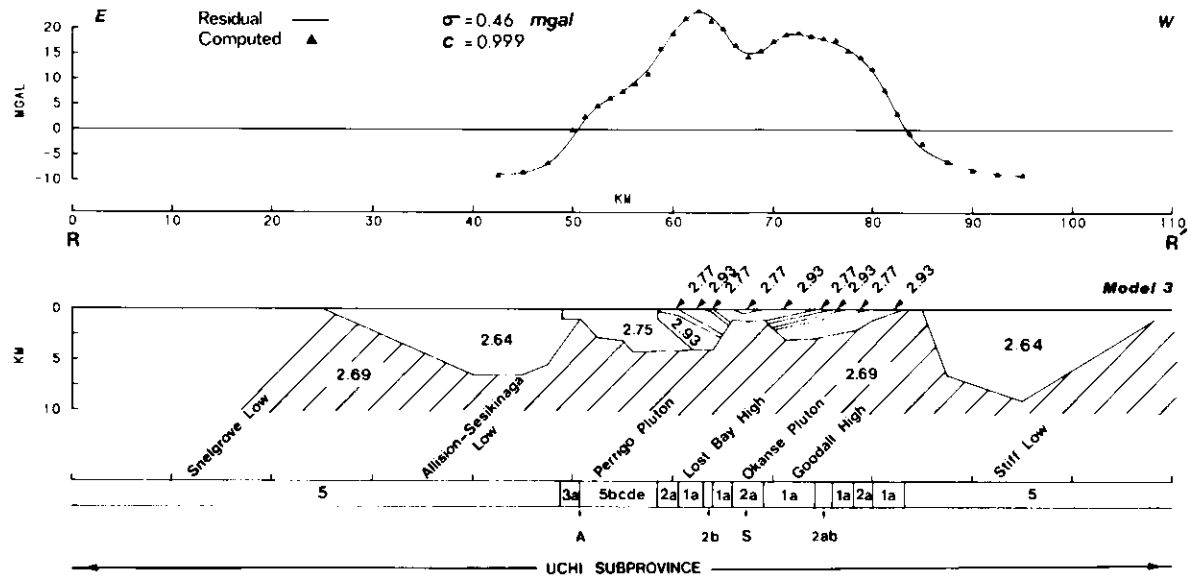

Figure 38c. *Profile RR' (Model 3), showing the graphical residual and computed gravity anomalies, interpreted gravity models and surface geology. Densities in g/cm³. For profile location see Figure 20. See Table 3 for explanation of geological legend.*

Model 2 The three volcanic cycles with their mafic and intermediate members as proposed by Thurston *et al.* (1978), have been retained (Figure 38b). The calculated depth-extent of the greenstone belt along this profile is less than 4 km. A gravity low near kilometre 68 coincides with a mapped synclinal axis which is located in volcanic cycle 3. A buried intrusive body of mean density 2.75 g/cm^3 which comes to within 0.5 km of the surface is required to model the gravity low. The depth-extent of the buried intrusive body is about 3 km. On the residual gravity map (Map 2494), this low runs along the entire length of the synclinal axis, from the Fly Creek gravity low area in the southwest to the Okanse Pluton in the north. A graben fault system (Thurston 1978) at kilometre 68 gives credibility to this intrusive hypothesis.

Model 3 The gravity low at kilometre 68 has been modeled (Figure 38c) by adjusting the thickness and the geometry of the various metavolcanic units which retain all the three cycles of volcanism and eliminating the proposed intrusion. The greenstone belt retained a depth-extent of 4 km. The gravity interpretation near kilometre 68 suggests a thinning rather than a thickening of the greenstone belt to coincide with the mapped synclinal axis.

In general, the structure of the greenstone belt interpreted from the gravity data is much more complex than the geological mapping indicates. The depth-extent (about 4 to 5 km) of the greenstones calculated from the gravity modeling is almost half of what Thurston (1978) and Pryslak (1971) have measured from the surface evidence. Also, here the volcanic cycles are not continuous at depth. Discrepancies between surface exposures and estimated stratigraphic thicknesses may indicate that additional fold structures or thrust faulting may be present.

The surrounding Allison-Sesikinaga Lakes and Stiff granites have been modeled with a maximum depth extent of about 6.5 to 7 km. Areas where these granitic bodies are not shown in direct contact with the metavolcanics are intended as transition zones rather than "basement". It is difficult to determine the extent to which these granites underlie the greenstone belt. Schematic drawings (Baragar and McGlynn 1976) frequently show the metavolcanics completely enveloped in granite which has intruded the margin between the volcanic rocks and "basement" upon which they were originally deposited. The apparent thickening of the granites toward the metavolcanic boundary rather than away from it (for example, kilometre 35 to kilometre 45) implies that the greenstone belt may indeed be underlain by substantial granitic rock, which would also affect the interpreted depth. However, the lack of control over what exists below the metavolcanics makes it necessary to restrict the interpretation to the margins of the belt.

Profile SS'

This profile (Figure 39a) strikes north-northeast and runs across the metasedimentary sequence of the Seagrave Lake area, the mafic metavolcanic sequence of the Casummit Lake area, and terminates in the Shearstone-Kerswill Lakes granitic area. Two interpretations have been shown, the first a simplified version of the second.

Model 1 The metavolcanic units were assigned a weighted mean density of 2.87 g/cm^3 and give a modeled depth-extent of 2.2 km. The interpreted metavolcanics structure suggests two synclinal shaped troughs whose axes on the surface are probably located at kilometre 10 and kilometre 28. The mapped anticlinal axis near kilometre 21 is thus flanked on both sides by the suggested synclines. The metasediments (mean density 2.75 g/cm^3) have underlying mafic metavolcanics which thin toward the anticlinal axis, near kilometre 21. The gravity interpretation also suggests that the metavolcanics extend below the granites for a short distance to the north.

The Shearstone-Kerswill granite is a lopolith-shaped body with a depth-extent of about 2 km (*see* also Profiles LL', QQ', and VV'; Figures 32, 37, and 42a).

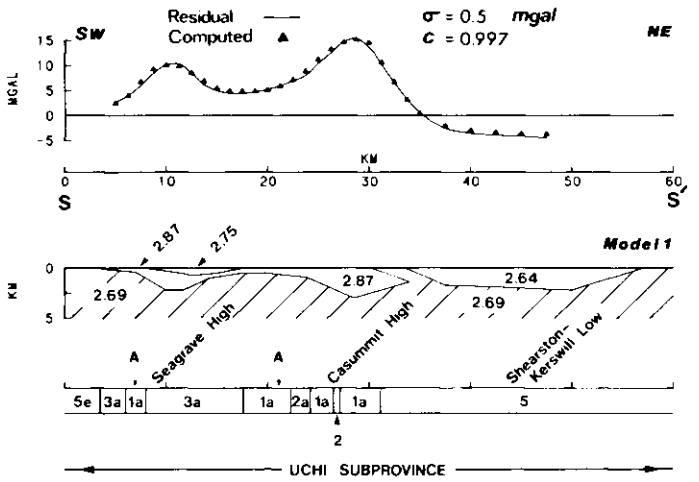

Figure 39a. *Profile SS' (Model 1), showing the graphical residual and computed gravity anomalies, interpreted gravity models and surface geology. Densities in g/cm³. For profile location see Figure 20. See Table 3 for explanation of geological legend.*

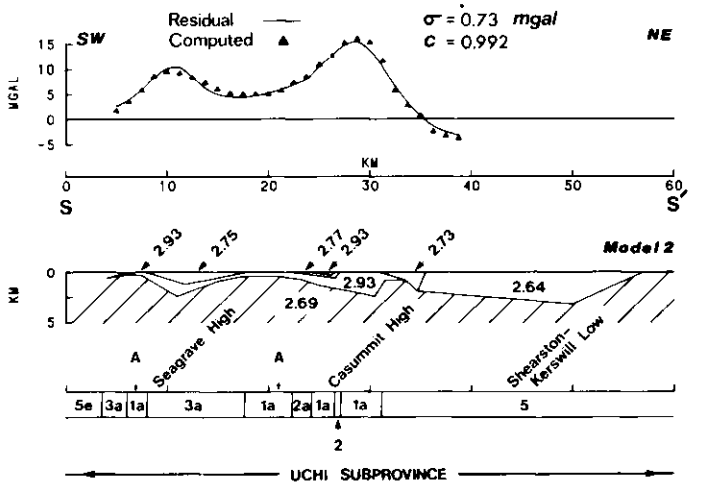

Figure 39b. *Profile SS' (Model 2), showing the graphical residual and computed gravity models and surface geology. Densities in g/cm³. For profile location see Figure 20. See Table 3 for explanation of geological legend.*

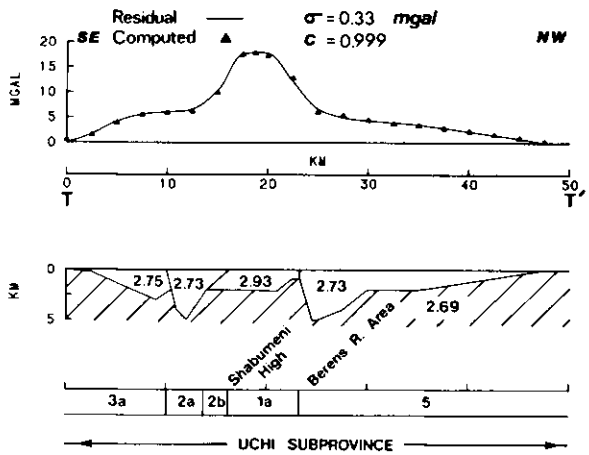

Figure 40. *Profile TT', showing the graphical residual and computed gravity anomalies, interpreted gravity models and surface geology. Densities in g/cm³. For profile location see Figure 20. See Table 3 for explanation of geological legend.*

Model 2 This model (Figure 39b) is different from the first model in terms of the densities assigned to the various metavolcanic units. The mafic and felsic to intermediate metavolcanics were assigned densities of 2.93 and 2.77 g/cm³, respectively. Using these density values, the greenstone sequence is calculated to be of 2.5 km depth-extent. The metasediments and the batholith have slightly more depth-extent but the overall shape of the bodies are similar to that in Model 1.

Profile TT'

This northwest-trending profile (Figure 40) cuts across the northern part of the Birch-Uchi Greenstone Belt. The most prominent anomaly on this profile is an 18 mgal positive residual anomaly called the Shabumeni gravity high. Using the outcrop locations from the surface geology, the positive anomaly can be explained by the mafic to intermediate metavolcanics and felsic to intermediate metavolcanics of mean density 2.93 and 2.73 g/cm³, respectively. The rectangular and almost flat bottom shaped mafic metavolcanics have a depth-extent of only 2 km, whilst the intermediate metavolcanics have a depth-extent of 5 km. The anomaly could also be modeled as mafic metavolcanics underlying the intermediate metavolcanics. This would have resulted in a shallower intermediate metavolcanics than the present 5 km.

The rocks of the unmapped Berens River area were assigned a mean density of 2.73 g/cm³, as determined from an average of the density sampling in this region. The steeply north dipping body is about 5 km deep and beyond kilometre 30 assumes a depth limited sheet-like structure.

Profile UU'

This north-northeast trending profile (Figure 41) runs across the Trout River gravity low, the Stiff Lake gravity low, the Skinner gravity high, and up to the Berens River area. Two different models have been computed for this profile. In the first model, the anomaly has been explained by a downward extension of the mapped geological units. In the second model, mafic metavolcanics underlie mapped units.

Model 1 The Stiff Lake Batholith (Figure 41a) (mean density 2.65 g/cm³) extends to a depth of 7 km (*see* also Profile GG', Figure 27). The Skinner gravity high has been explained in terms of mafic metavolcanics (mean density 2.93 g/cm³), minor amounts of intermediate metavolcanics (mean density 2.77 g/cm³), and metasedi-

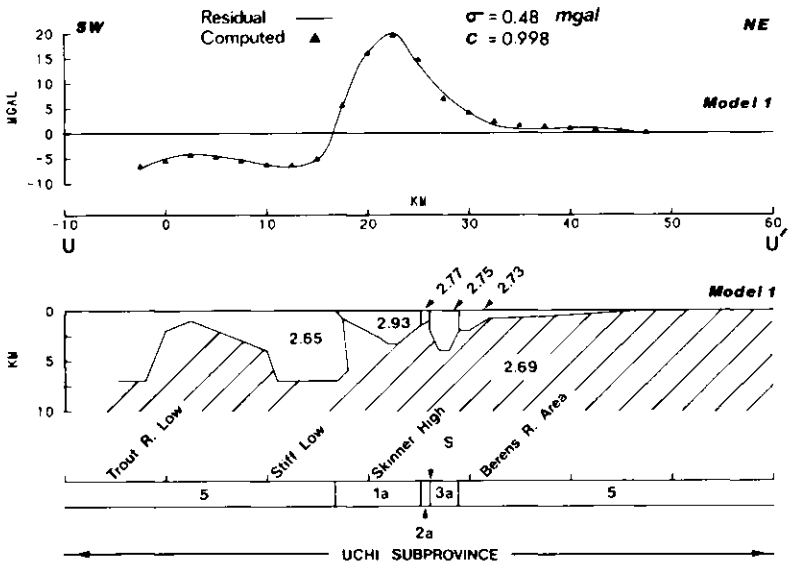

Figure 41a. *Profile UU' (Model 1), showing the graphical residual and computed gravity anomalies, interpreted gravity models and surface geology. Densities in g/cm³. For profile location see Figure 20. See Table 3 for explanation of geologic legend.*

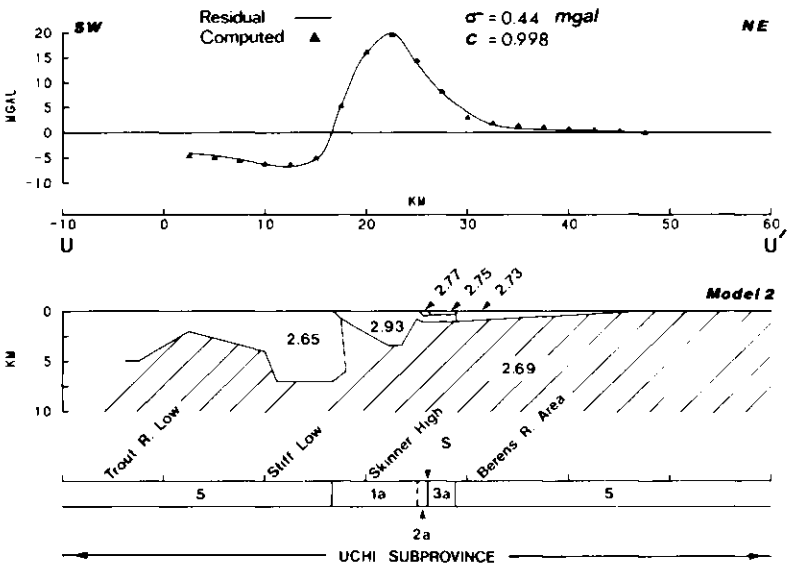

Figure 41b. *Profile UU' (Model 2), showing the graphical residual and computed gravity anomalies, interpreted gravity models and surface geology. Densities in g/cm³. For profile location see Figure 20. See Table 3 for explanation of geological legend.*

ments (mean density 2.75 g/cm^3). The depth-extent of the mafic metavolcanics, having a synformal shape, is about 3 km. The vertically dipping metasediments are modeled to a depth-extent of 4 km. The interpretation in the Berens River area is highly questionable since the profile is almost parallel to the residual gravity contours.

Model 2 The mafic metavolcanics of the Skinner gravity high region are assumed to be overlain by the intermediate metavolcanics and the metasediments. This reduces the thickness of the metasediments to only 0.5 km, compared to the thickness of 4 km obtained in Model 1.

In the models presented, the deepest part of the greenstone belt occurs either at kilometre 28 (in the metasediments of Model 1) or at kilometre 23 (in the mafic metavolcanics of Model 2). From surface geology, a synclinal axis has been mapped at kilometre 26 that coincides with the thinnest part of the greenstone belt presented in the two models. The location of the mapped synclinal axis is offset either 2 km to the northeast if Model 1 is preferred, or 3 km to the southwest if Model 2 is preferred.

Profile VV'

The profile (Figure 42) strikes northeast and runs perpendicular to the Trout Lake-Stiff Lake granitic areas, the Skinner gravity high, the Berens River area, the Blondin Lake gravity high, and finally through the Shearstone-Kerswill Lakes granitic area. As already explained in previously mentioned profiles, the granitic areas have not been mapped in detail, and thus various granitic phases have been interpreted on the basis of density sampling. Two gravity models have been calculated for this profile.

Model 1 The Stiff Lake Batholith (Figure 42a), mean density 2.65 g/cm^3, extends to a depth of 7 km for the main body. The batholith thins to the south to less than 2 km in the form of an extensive sheet which finally joins with the Trout Lake Batholith to the southwest.

The mafic metavolcanic units coinciding with the edge of the Skinner gravity high have been modeled as two separate bodies of less than 2 km depth-extent, both of mean density 2.93 g/cm^3.

The Berens River terrain (mean density 2.73 g/cm^3) gives an average depth-extent of about 2.5 km, as does the Shearstone-Kerswill Lakes area (mean density 2.64 g/cm^3). Because the geological mapping and the surface data are sparse, structural details shown for the bottom topography are tentative.

In the Blondin Lake area of the Birch-Uchi Greenstone Belt, the gravity interpretation confirms the mapped synclinal structure (better shown in Model 2) which is located directly under the peak of the Blondin Lake gravity high, near kilometre 78. The model suggests a depth-extent of 4 km for the metavolcanics.

Model 2 The mafic metavolcanic and metasedimentary units near the western end of the Skinner gravity high are assumed to be underlain by the Stiff Lake granitic rocks (Figure 42b). The metavolcanic-metasedimentary units of <2.5 km depth-extent are considered as remnants of the Birch-Uchi Greenstone Belt. A mean density of 2.66 g/cm^3 for the Stiff Lake and Trout Lake Batholiths produced a depth extent of 13 km for the Stiff Lake Batholith and 5 km for the Trout Lake Batholith. The two differing models illustrate the non-uniqueness of gravity interpretation.

Profile WW'

The 30 km long, east-northeast trending profile WW' crosses the western end of the Nungesser Road gravity low and through the centre of the positive residual anomaly of the Coli Lake Greenstone Belt.

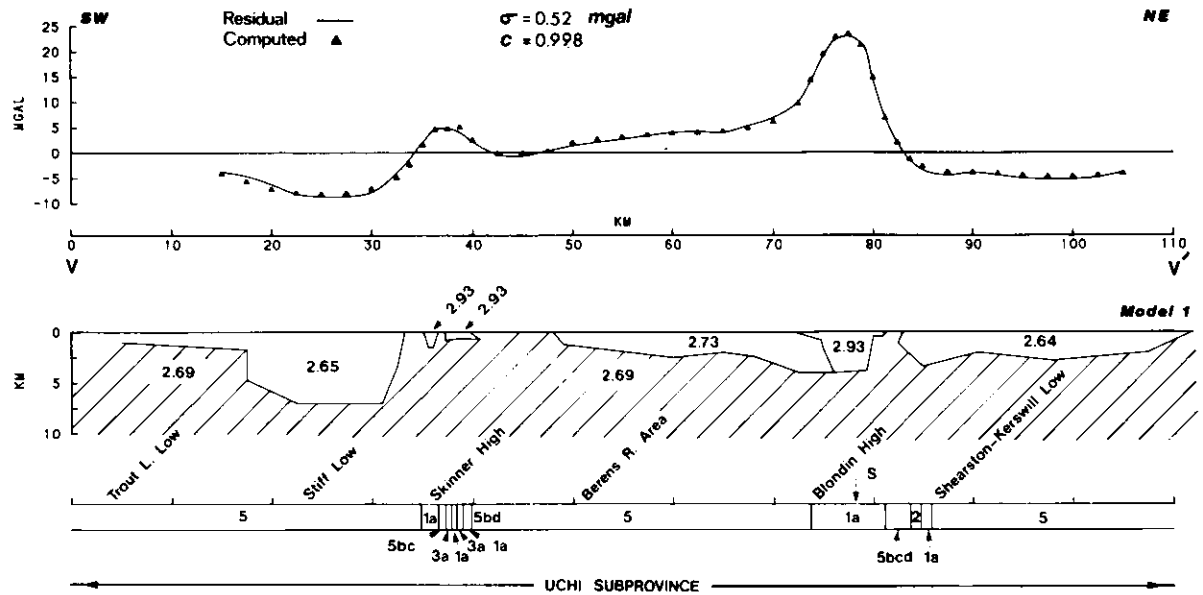

Figure 42a. *Profile VV' (Model 1), showing the graphical residual and computed gravity anomalies, interpreted gravity models and surface geology. Densities in g/cm³. For profile location see Figure 20. See Table 3 for explanation of geological legend.*

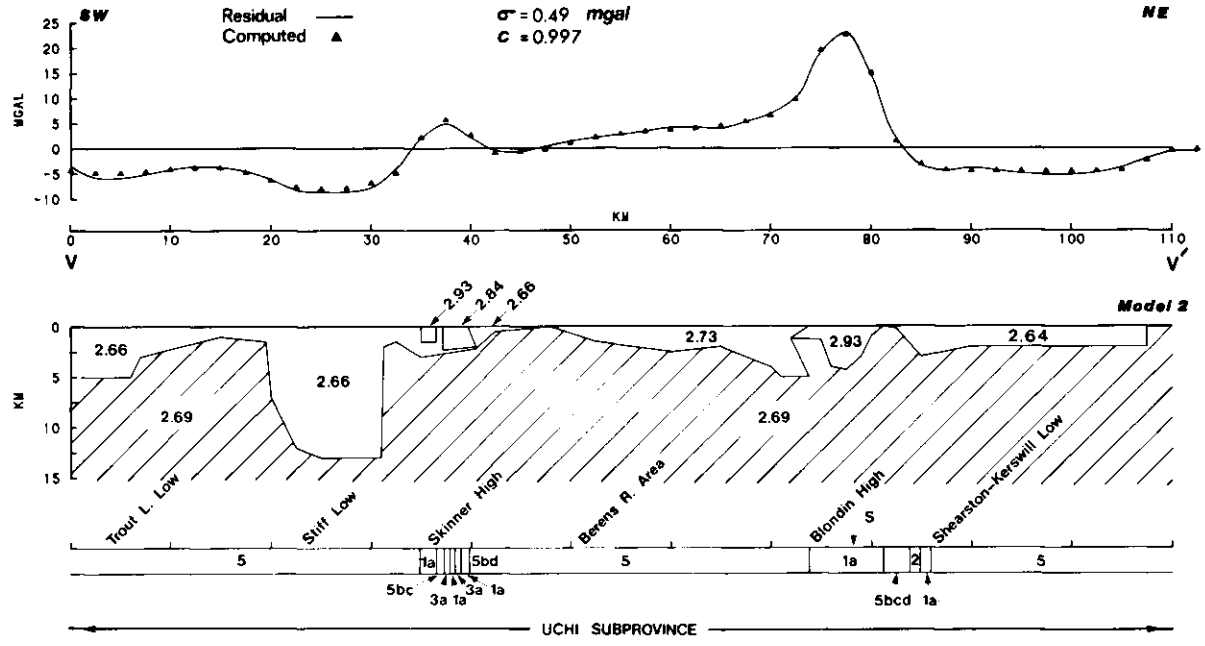

Figure 42b. *Profile VV' (Model 2), showing the graphical residual and computed gravity anomalies, interpreted gravity, models and surface geology. Densities in g/cm^3. For profile location see Figure 20. See Table 3 for explanation of geological legend.*

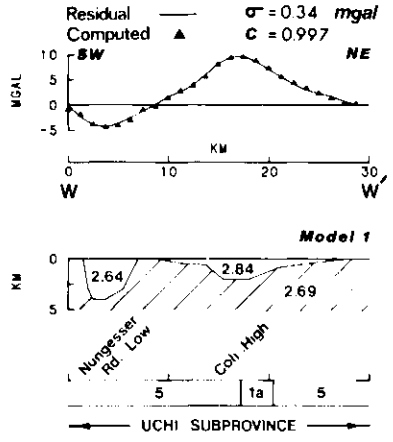

Figure 43a. *Profile WW' (Model 1), showing the graphical residual and computed gravity anomalies, interpreted gravity models and surface geology. Densities in g/cm³. For profile location see Figure 20. See Table 3 for explanation of geological legend.*

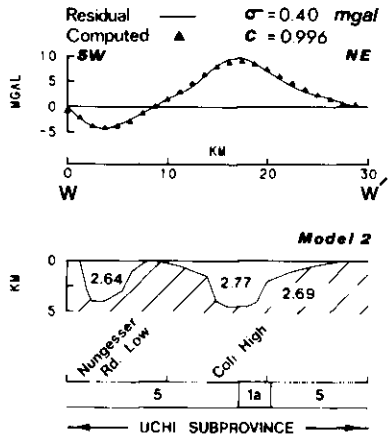

Figure 43b. *Profile WW' (Model 2), showing the graphical residual and computed gra vity anomalies, interpreted gravity models and surface geology. Densities in g/cm³. For profile location see Figure 20. See Table 3 for explanation of geological legend.*

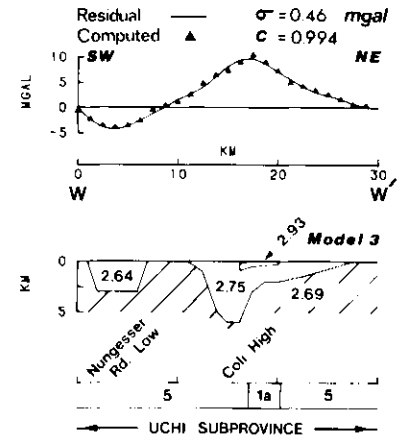

Figure 43c. *Profile WW' (Model 3), showing the graphical residual and computed gravity anomalies, interpreted gravity models and surface geology. Densities in g/cm³. For profile location see Figure 20. See Table 3 for explanation of geological legend.*

The 4 mgal amplitude negative residual anomaly coincident with the Nungesser Road gravity low has been explained by a granitic body of mean density 2.64 g/cm^3. The inverted cone-shaped body extends to a depth of about 4 km, having steeply dipping inward slopes on either side.

Density sampling in the Coli Lake gravity high region shows a predominance of 2.75 g/cm^3 density rocks. These rocks flank the mafic metavolcanics (mean density 2.93 g/cm^3) on both sides. As the area is still largely unmapped, three different densities have been used on three models to explain the geometry of the Coli Lake Greenstone Belt.

Model 1 A simple arithmetic mean of 2.84 g/cm^3 was calculated from the 2.75 and 2.93 g/cm^3 density rocks (Figure 43a). This assumes that the entire positive residual anomaly area of the Coli Lake Greenstone Belt is underlain by a mass of mean density 2.84 g/cm^3. A basin-shaped body with gently dipping margins was modeled from the gravity data. The deepest part of the basin has a depth-extent of about 2 km.

Model 2 A weighted mean density of 2.77 g/cm^3 was calculated based on the proportions of the exposed metavolcanic and the granitoid rocks under the positive residual anomaly region. This was modeled to a 4.5 km depth-extent body having a basin-like shape.

Model 3 The mafic metavolcanics (mean density 2.93 g/cm^3) and the surrounding 2.75 g/cm^3 density rocks are assumed to be responsible for the positive residual anomaly of the Coli Lake Greenstone Belt (Figure 43c). Both of these units have been modeled individually. The model shows a depth-extent of 1 km for the mafic metavolcanics which dip to the south. The 2.75 g/cm^3 density body extends to a depth of about 6 km with inward dipping slopes and thinning to the north.

Profile XX'

This north-trending profile (Figure 44) passes through the Snelgrove Lake and Gull Lake Batholiths, the Casummit Lake gravity high, the Zionz Lake Batholith, the Jackpine Lake area, and ends in the Shearstone-Kerswill Lakes Batholith. This profile was drawn from the residual map obtained from the upward continuation method as explained in an earlier section (*see* Profile NN', Model 2, Figure 34b). Most of the residual anomalies under the profile are negative and have been explained by granitic bodies of mean density 2.64 g/cm^3.

The Snelgrove Lake Batholith extends to a depth of about 5 km. The Gull Lake Batholith extending to a depth of 10 km thins to the north where it reaches to a depth of only 5 km to join up with the Zionz Lake Batholith. The rocks of the Jackpine Lake area (mean density 2.73 g/cm^3) which comes into contact with the Zionz Lake Batholith (*see* Profile QQ'; Figure 37) dip to the north and have a depth-extent of only 2 km.

The profile crosses the eastern tail of the Casummit Lake gravity high; it is represented by a small positive residual anomaly <3 mgal in amplitude. The 2 km depth-extent mafic metavolcanics and the sliver of metasediments causing this anomaly have been modeled entirely within the Gull Lake Batholith.

Profile YY'

The northwest-trending profile YY' (Figure 45) passes through the Allison-Sesikinaga Lakes gravity low, the metasedimentary area of the Grace Lake region, the Shabumeni Lake gravity high, and finally the Berens River area. Three gravity models have been calculated for this profile (*see* also Profile PP', Figure 36).

Model 1 The interface of the Allison-Sesikinaga Lakes Batholith (mean density 2.64 g/cm^3) which comes into contact with the rocks of the Birch-Uchi Greenstone Belt is steeply dipping to the southeast (Figure 45a). The batholith extends to a depth of about 8 km. Between kilometres 7 to 12, the thin (0.5 km) metasediments

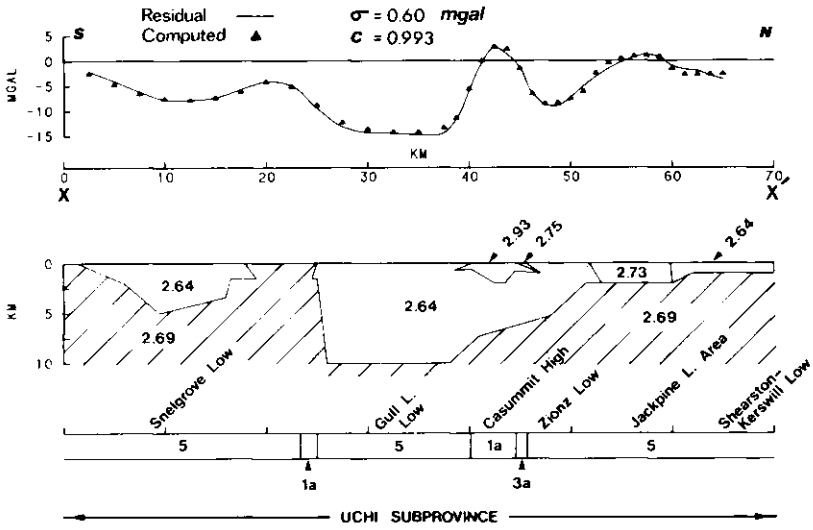

Figure 44. *Profile XX', showing the 16.09 km upward continuation based residual and computed gravity anomalies, interpreted gravity models and surface geology. Densities in g/cm³. For profile location see Figure 20. See Table 3 for explanation of geological legend.*

(mean density 2.75 g/cm³) of the Grace Lake area overlie the granitic rocks forming the batholith. The metasediments deepen towards the northwest, attaining a maximum thickness of 5 km. The Shabumeni Lake gravity high has been modeled by the metavolcanics of mean densities 2.93 and 2.77 g/cm>3 which are less than 3 km in depth-extent. Beyond kilometre 30 (as with Model 2), the metavolcanics are dipping to the northwest. The depth extent of the 2.73 g/cm³ density rocks of the Berens River area is about 4 km near the contact with the metavolcanics. Away from this contact, towards the northwest the Berens River area rocks attain a depth extent of less than 2.5 km.

Model 2 This model (Figure 45b) differs from Model 1 between kilometres 10 to 28 where unlike Model 1, the Grace Lake metasediments are flanked on both sides by the mafic metavolcanics. This configuration reduces the depth-extent of the Grace Lake metasediments to 3.4 km compared to 5 km calculated from Model 1. The shape of the bodies suggests an anticlinal axis near kilometre 27.

Model 3 The mafic metavolcanics of mean density 2.93 g/cm³ have been brought under the Grace Lake metasediments which overlie the metavolcanics (Figure 45c). Also, the 2 km thick Grace Lake metasediments have been folded, near kilometre 30, along a proposed synclinal axis located in the mafic metavolcanics. The Berens River granitoids are slightly thinner in this model than in the above two models.

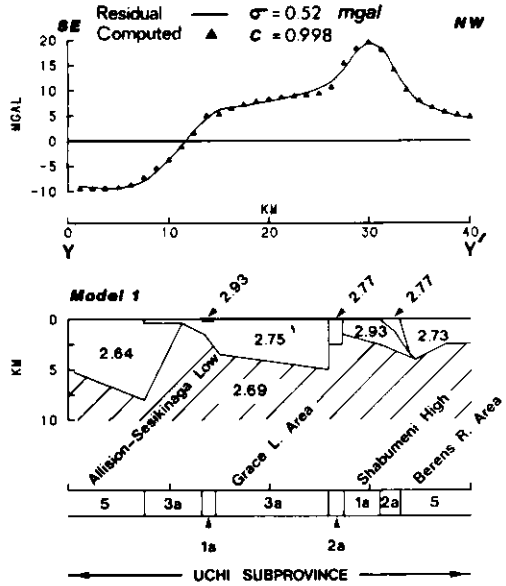

Figure 45a. *Profile YY' (Model 1), showing the graphical residual and computed gravity anomalies, interpreted gravity models and surface geology. Densities in g/cm³. For profile location see Figure 20. See Table 3 for explanation of geological legend.*

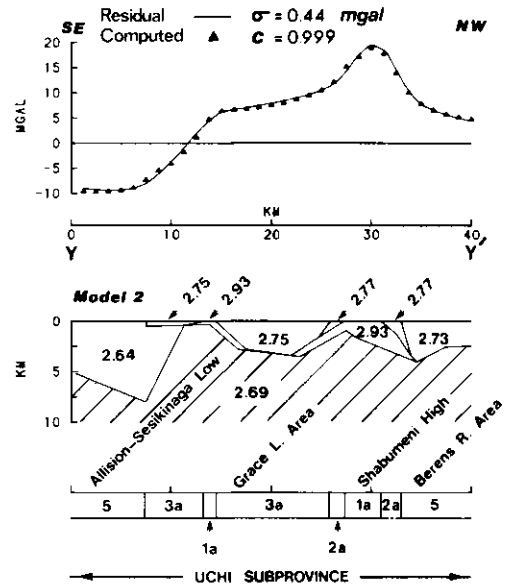

Figure 45b. *Profile YY' (Model 2), showing the graphical residual and computed gravity anomalies, interpreted gravity models and surface geology. Densities in g/cm³. For profile location see Figure 20. See Table 3 for explanation of geological legend.*

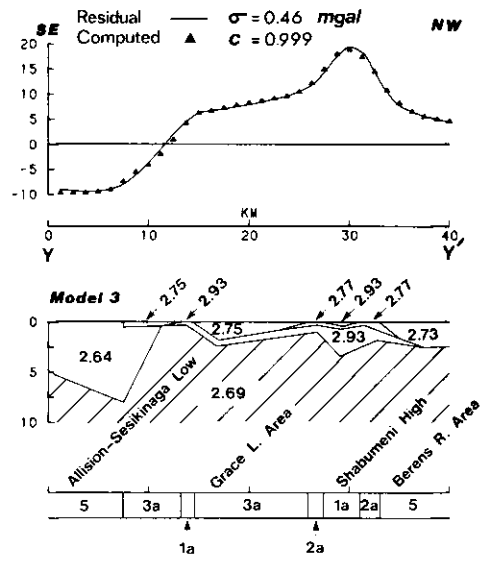

Figure 45c. *Profile YY' (Model 3), showing the graphical residual and computed gravity anomalies, interpreted gravity models and surface geology. Densities in g/cm³. For profile location see Figure 20. See Table 3 for explanation of geological legend.*

Regional Anomaly Maps

Regional separation of the Bouguer anomaly field was carried out using three different methods. These were: upward continuation filters, optimum filters designed from an analysis of the energy spectrum, and visual graphical smoothing. As explained earlier in the section entitled Pattern Recognition and Data Treatment, the graphical regional field (Figure 15; Map 2493) was found to be the most satisfactory as it seems to represent only the variations at the Riel and Mohorovicic discontinuities. Moreover, it is also in good agreement with the regional map of Innes (1960).

The graphically separated regional anomaly (Figure 15; Map 2493) depicted by an east-west trending gravity low is open to the east and takes the general form of concentric ellipses, occupying the entire area. The regional field varies from -38 mgal over the English River Subprovince near the southern border of the map area, decreasing gradually northward towards the Uchi Subprovince to <-60 mgal, just east of the Birch-Uchi Belt (Map 2493). The east-west trending linear gravity contours, coinciding with the boundary between the Uchi and English River Subprovince, probably indicate a thin crust along this boundary.

According to Wilson (1971), the depth to the Riel discontinuity is deeper in the English River Subprovince (22 km) than in the Uchi Subprovince (20 km) or the Berens River Subprovince (18 km). In contrast, the depth to the Mohorovicic discontinuity interface (that is, the thickness of the total crust) is shallower in the English River Subprovince (30 km) than in the Uchi Subprovince (34 km) or the Berens River Subprovince (36 km). This implies that the total crust is thinnest under the English River Subprovince and thickest under the Berens River Subprovince. A regional gravity interpretation, based on the gravity data collected during this survey, across the English River Subprovince is given by Gupta and Barlow (1984).

Summary

The results of the interpretation of the gravitational field over the Birch-Uchi and Red Lake Greenstone Belts and the surrounding areas have been discussed. During the survey, covering an area of about 21 100 km^2, 5180 gravity stations were established and over 2800 density measurements were made.

The Bouguer anomaly field was digitized at a regular grid spacing of 1.609 km. This field was divided into its regional and residual components, using spectrum-based optimum filters, upward continuation filters, and graphical smoothing techniques. The filtered maps were compared with the local geology for the purpose of selecting suitable maps which could be used for two-dimensional gravity modeling.

The spectrum-based regional-residual maps were considered least applicable since two of the large gravity highs on the regional map can be explained better by the upper crustal greenstone densities rather than by undulations at the deeper Riel and Mohorovicic discontinuities. The upward continuation based regional map shows less correlation with the surface geology than the spectrum-based regional map, but the greenstone belts are still discernible. The graphically smoothed regional field which produces a single gravity low for the study area was found to be the most satisfactory. The map is devoid of any upper crustal geological features and therefore seems to represent entirely, the variations at the Riel and Mohorovicic discontinuities.

A comparison of the various residual maps has shown that, in many areas, negative residual anomalies of the spectrum and upward continuation based residual maps correspond on the surface with higher density anomalous rocks. This makes modeling of the residual anomalies a problem lacking in geological control. Artificial bodies of low density must be buried under the surface to account for the regional-residual separation discrepancy of negative anomalies, where the surface evidence clearly indicates high density rocks. The problem has been avoided in the graphically smoothed maps which were heavily biased towards the local geology. For these reasons, the graphically smoothed residual and regional maps were adopted for modeling work.

Major residual gravity anomalies have been discussed and, wherever possible, their significance has been explained in terms of geological structures and tectonics. A brief summary of the results is described below.

The residual gravity anomalies of near surface mass distribution have been explained by surface densities which were measured from the 2813 rock samples collected during the survey. A background density of 2.69 g/cm^3 was chosen for the granitoid terrain of the area.

The study objectives have been achieved in that the gravity interpretation has demonstrated the subsurface configurations of the greenstone belts and the surrounding granitoid areas. The modeled greenstone belts usually indicate broad synformal shapes with varying depth-extents, averaging 4 km for the Red Lake Belt, between 3.5 to 4 km for the Birch-Uchi Belt, 2.3 km for the Dixie Lake Belt, and about 1 km for the Coli Lake Belt.

The gravity data suggest that the thickest greenstone section of the Birch-Uchi Belt is present under the peak of the Goodall gravity high where the calculated depth-extent varies between 4 to 6 km depending on the choice of the density value used. The greenstone section then apparently thin towards the south, along the anomaly axis, reaching a depth-extent of about 3 km near the southern tip of the Goodall gravity high. Similarly, the greenstone section is thickest (depth-extent 5.5 km) directly below the peak of the Lost Bay high and then continues to thin, along the anomaly axis, both to the south and north producing depth-extents between 3 to 3.5 km. The greenstones in the northern part of the Birch-Uchi Belt, in the Blondin Lake and Casummit Lake gravity high regions, are about 4 km and 3 km in depth-extent, respectively. The depth-extent of the various associated arms of the Birch-Uchi Belt varies from 2 to 2.5 km in the Papaonga Lake area, 1.5 to 2.5 km in the Moon Lake area, 3 to 4 km in the Seagrave Lake area, and about 3.5 km in Skinner Township. The metasediments of the Grace Lake area vary in depth-extent between 0.5 to 4.5 km.

The gravity interpretation indicates that in the Red Lake Belt, the greenstone section producing the Todd-Fairlie and Cochenour gravity highs has a depth-extent of about 5 km, directly underneath a probable synclinal axis. In the Embryo-Telescope Lakes arm of the Red Lake Belt, the greenstone section is <1 km in depth-extent.

It is shown that a majority of the felsic metavolcanic and metasedimentary units of the Uchi Subprovince are of limited depth-extent, between 0.5 to 1.5 km, and usually underlain by the thick units of mafic metavolcanics.

The bottom topographies of the modeled greenstones reflect typical basin, ridge, or homocline-like structures (or a combination of them) whose vertical projection onto the surface, in many instances, coincide with the mapped structure. However, discrepancies between the interpreted and the mapped fold structures have also been noticed throughout the area.

Large gravity gradients occurring at the greenstone-granite boundaries have been explained primarily in terms of large density contrasts prevailing at the boundaries. The plutonic bodies of the study area have significant differences in their structural pattern and depth extents. The negative anomaly producing granitic batholiths show widely varying compositional differences, as evident from their densities which vary from 2.73 g/cm^3 near the greenstone-granitic contacts to 2.64 g/cm^3 in the centre of the batholiths. Most of the batholiths reach down to depths of between 4 and 7 km, the exceptions being the Gull Lake (between 13 to 16 km depth-extent), the Rosen Lake (between 10 to 12 km depth-extent), and the Trout River (about 9 km depth-extent) batholiths. The shallow depth extent and the two-dimensional configuration of some of these bodies indicate that they are probably sheet or sill-like structures. The Dome Stock intruding into the metavolcanics of the Red Lake Belt, characterized by a circular gravity low, is entirely enclosed within the greenstone belt and extends from the surface to a depth of 2.6 km. The Perrigo and Okanse Plutons of the Birch-Uchi Greenstone Belt have depth-extents of 4 and 5 km, respectively.

The residual gravity field in the areas away from the margins of the greenstone belts, that is, away from greenstone-granite boundary, show positive residual anomalies in areas of probable hybrid granitic rocks. Such anomalies, for example, in the Alford Lake and Berens River areas, have been explained in terms of probable granitized volcanic rocks of density 2.75 and 2.73 g/cm^3.

All along the southern border of the study area, a significant change in the anomaly level marked by a steep gravity gradient reveals the boundary between the Uchi and the English River Subprovinces. The 12 to 15 mgal amplitude residual positive anomaly associated with this boundary, indicates the existence of an east-west trending metasedimentary trough. In the immediate vicinity of the Sydney Lake Fault system, the trough is less than 2 km in depth-extent and dips gently to the south. A few kilometres south of the fault system, however, the trough dips steeply to the south, reaching depths varying between 8.5 to 12 km. The diatexite units of the Northern Supracrustal Domain north of the fault are less than 2 km in depth-extent.

The Bluffy Lake Batholith has been modeled to a depth-extent of about 1.5 to 3 km. The model shows that the batholith is a thin sheet or sill-like structure which has possibly intruded the underlying metasediments from the north.

It has been shown from the model of the regional gravity profile that the regional anomaly field in the study area can be explained by undulations on the Riel and Mohorovicic discontinuities.

The second derivative map shows a much sharper and closer relationship to the surface geology. This is evident in the centre of the Birch-Uchi Belt, where the geology is best known. Here, the bands of positive and negative second derivative anomalies, in the centre of the Birch-Uchi Belt, are clearly associated with the contrasting mafic to felsic cycles of volcanism. The second derivative map, in conjunction with geology, should prove to be an excellent tool in resolving stratigraphic and structural problems in poorly exposed Precambrian terrain.

Without doubt, many refinements of the interpretation and the interpretation method itself will be made in the future by geoscientists working in greenstone belts. However, the results of this work provide an important third dimension constraint to geologists that will assist them in generating realistic tectonic models for the evolution of the Archean greenstone belts.

References

Anhaeusser, C.R.
1971: Cyclic Volcanicity and Sedimentation in the Evolutionary Development of Archean Greenstone Belts of Shields Areas; p.57-70 *in* Geological Society of Australia, Special Publication 3, edited by J.E. Glover.

Ayres, L.D.
1974: Geology of the Trout Lakes Area, District of Kenora (Patricia Portion); Ontario Division of Mines, Geological Report 113, 197p. Accompanied by Map 2270, scale 1 inch to 1/2 mile.
1978: Metamorphism in the Superior Province of Northwestern Ontario and Its Relationship to Crustal Development; *in* Metamorphism in the Canadian Shield, Geological Survey of Canada, Paper 78-101.

Ayres, L.D., Lumbers, S.B., Milne, V.G., and Robeson, D.W.
1971: Ontario Geological Map; Ontario Department of Mines and Northern Affairs, Map 2196, scale 1 inch to 16 miles.

Ayres, L.D., Raudsepp, M., Averill, S.A., and Edwards, G.R.
1973: Favourable Lake-Berens Lake; Ontario Division of Mines, Map 2262, scale 1 inch to 4 miles.

Baragar, W.R.A., and McGlynn, J.C.
1976: Early Archean Basement in the Canadian Shield; A Review of the Evidence; Geological Survey of Canada, Paper 76-14, 20p.

Barlow, R.B., Gupta, V.K., and Wadge, D.R.
1976: Bouguer Gravity Map of the Birch-Uchi-Confederation Lakes Area, District of Kenora (Patricia Portion); Ontario Division of Mines, Preliminary Map P.1186, Geophysical Series, scale 1:126 720 or 1 inch to 2 miles.

Breaks, F.W., and Bond, W.D.
1977: Manifestations of Recent Reconnaissance Investigations in the English River Subprovince, Northern Ontario; p.170-210 *in* Proceedings of the 1977 Geotraverse Conference, University of Toronto.

Breaks, F.W., Bond, W.D., and Stone, D.
1978: Preliminary Geological Synthesis of the English River Subprovince Northwestern Ontario, and Its Bearing Upon Mineral Exploration; Ontario Geological Survey, Miscellaneous Paper 72, 55p. Accompanied by Map P.1971, scale 1:253 440.

Clarke, G.K.C.
1969: Optimum Second Derivative and Downward Continuation Filters; Geophysics, Volume 34, p.424-437.

Cooley, J.W., and Tukey, J.W.
1965: An Algorithm for the Machine Calculation of Complex Fourier Series; Math. Comput., Volume 19, p.297-301.

Darracott, B.W.
1976: On the Choice of a "2D" or "3D" Model in Gravity Interpretation; Geoexploration, Volume 14, p.143-146.

Dean, W.C.
1958: Frequency Analysis for Gravity and Magnetic Interpretation; Geophysics, Volume 23, p.97-127.

Ferguson, S.A.
1965a: Baird Township, Eastern Part, Kenora District; Ontario Department of Mines, Map 2072, scale 1 inch to 1000 feet.
1965b: Dome Township, Eastern Part, Kenora District; Ontario Department of Mines, Map 2074, scale 1 inch to 1000 feet.
1966: Red Lake Area, District of Kenora; Ontario Department of Mines, Preliminary Map P.338, scale 1 inch to 1 mile.
1972: Stratigraphy, Structure and Geological History of the Red Lake Area, Ontario; p.1-23 *in* Some Papers on the Geology of the Red Lake Area, District of Kenora, Patricia Portion, Ontario Division of Mines, Open File Report 5078, 106p.

Fuller, B.D.
1967: Two-Dimensional Frequency Analysis and Design of Grid Operators, p.658-708 *in* Mining Geophysics, Volume II, Society of Exploration Geophysicists, Tulsa.

Goodwin, A.M.
1967: Volcanic Studies in the Birch-Uchi Lakes Area of Ontario; Ontario Department of Mines, Miscellaneous Paper 6, 96p.
1972: The Superior Province; p.527-624 *in* Variations in Tectonic Styles in Canada, edited by R.A. Price and R.J.W. Douglas, Geological Association of Canada, Special Paper Number 11.
1977: Archean Volcanism in Superior Province, Canadian Shield; p.205-241 *in* Volcanic Regimes in Canada, edited by W.R.A. Baragar, L.C. Coleman and J.M. Hall, Geological Association of Canada, Special Paper Number 16.

Gorman, B.E., Pearce, T.H., and Birkett, T.C.
1978: On the Structure of Archean Greenstone Belts; Precambrian Research, Volume 6, p.23-41.

Grant, F.S., Gross, W.H., and Chinnery, M.A.
1965: The Shape and Thickness of an Archean Greenstone Belt by Gravity Methods; Canadian Journal of Earth Sciences, Volume 2, p.418-424.

Gupta, V.K., and Barlow, R.B.
1984: A Detailed Gravity Profile Across the English River Subprovince, Northwestern Ontario; Canadian Journal of Earth Sciences, Volume 21, p.145-151.

Gupta, V.K. and Ramani, N.
1978: Gravity Anomalies in Red Lake and Uchi Lake Areas of Northwest Ontario (Abstract); p.29 *in* Program with Abstracts, 1978, Fifth Annual Meeting, Canadian Geophysical Union.
1980: Some Aspects of Regional-Residual Separation of Gravity Anomalies in a Precambrian Terrain; Geophysics, Volume 45, p.1412-1426.

Gupta, V.K., Thurston, P.C., and Dusanowskyj, T.H.
1982: Constraints Upon Models of Greenstone Belt Evolution by Gravity Modelling, Birch-Uchi Greenstone Belt, Northern Ontario; Precambrian Research, Volume 16, p.233-255.

Gupta, V.K., and Wadge, D.R.
1978: Bouguer Gravity and Generalized Geologic Map Red Lake Area, District of Kenora (Patricia Portion); Ontario Geological Survey, Preliminary Map P.1248, Geophysical Series, scale 1:100 000.

Hall, D.H., and Hajnal, Z.
1969: Crustal Structure in Northwestern Ontario: Refraction Seismology; Canadian Journal of Earth Sciences, Volume 6, p.81-99.

Henderson, R.G.
1960: A Comprehensive System of Automatic Computation in Magnetic and Gravity Interpretation; Geophysics, Volume 25, p.569-585.

Innes, M.J.S.
1960: Gravity and Isostasy in Northern Ontario and Manitoba; Dominion Observatory Publication, Volume 21, Number 6, p.263-338.

James, F., and Ross, M.
1976: MINUIT, A System for Function Minimization and Analysis of the Parameter Errors and Correlations: Long-Write-Up; CERN Computer Centre Program Library.

Johns, G.W., and Thurston, P.C.
1975: Honeywell and McNaughton Townships, Kenora District; Ontario Geological Survey, Map 2404, scale 1 inch to 1/2 mile.

Ku, C.C., Telford, W.M., and Lim, S.H.
1971: The Use of Linear Filtering in Gravity Problems; Geophysics, Volume 36, p.1174-1203.

Meyer, F.D.
1974: Filter Techniques in Gravity Interpretation; Advances in Geophysics, Volume 17, p.187-261.

Milsom, J., and Worthington, G.A.
1977: Computer Programs for Rapid Computation of Gravity Effects of Two-Dimensional and Three-Dimensional Bodies; Computers and Geosciences, Volume 3, p.269-281.

Nagy, D.
1964: The Gravitational Effect of Two-Dimensional Masses of Arbitrary Cross Section; Unpublished Manuscript, Gravity Division, Department of Energy, Mines and Resources, Ottawa.

Observatories Branch, Department of Energy, Mines and Resources
1970: Gravity Map Series No. 29, Ottawa, Canada.
1973: Gravity Map Series Nos. 100 and 101, Ottawa, Canada.

Peters, L.J.
1949: The Direct Approach to Magnetic Interpretation and Its Practical Application; Geophysics, Volume 14, p.290-319.

Pirie, J.
1978: Geology of the Red Lake Area, District of Kenora; p.20-21 *in* Summary of Field Work, 1978, by the Ontario Geological Survey, edited by V.G. Milne, O.L. White, R.B. Barlow, and J.A. Robertson, Ontario Geological Survey, Miscellaneous Paper 82, 235p.

Pirie, J. and Grant, A.
1978a: Bateman Township, District of Kenora; Ontario Geological Survey, Preliminary Map P.1569, scale 1 inch to 1000 feet.
1978b: Balmer Township, District of Kenora; Ontario Geological Survey, Preliminary Map P.1976-A, scale 1 inch to 1000 feet.

Pirie, J. and Sawitzky, E.
1977: McDonough Township, District of Kenora; Ontario Geological Survey, Preliminary Map P.1240, scale 1 inch to 1000 feet.

Pryslak, A.P.
1971: Narrow Lake-Shabumeni River Area (Skinner and Goodall Townships), District of Kenora (Patricia Portion); *in* Summary of Field Work, 1971, by the Geological Branch, edited by E.G. Pye, Ontario Department of Mines and Northern Affairs, Miscellaneous Paper 49, 109p.

Riley, R.A.
1975: Ball Township, Kenora District; Ontario Division of Mines, Map 2265, scale 1 inch to 1000 feet.
1976: Mulcahy Township, District of Kenora; Ontario Division of Mines, Map 2295, scale 1 inch to 1000 feet.
1978a: Todd Township, District of Kenora; Ontario Division of Mines, Map 2406, scale 1 inch to 1000 feet.
1978b: Fairlie Township, District of Kenora; Ontario Division of Mines Map 2407, scale 1 inch to 1000 feet.

Runnalls, R.J.
1978: Gravity Modelling, Red Lake Region, Northwestern Ontario; Unpublished M.Sc. Thesis, University of Toronto.

Schwerdtner, W.M., and Goodwin, A.M.
1977: Structural Geology of Geotraverse Conference, Abstracts; University of Toronto, p.10-23.

Spector, A., and Grant, F.S.
1970: Statistical Models for Interpreting Aeromagnetic Data; Geophysics, Volume 25, p.293-302.

Stone, D.
1977: The Sydney Lake Fault Zone; p.94-108 *in* Proceedings of the 1977 Geotraverse Conference, University of Toronto.
1981: The Sydney Lake Fault Zone in Ontario and Manitoba, Canada. Unpublished Ph.D. thesis, University of Toronto.

Thurston, P.C.
1976: Confederation Lakes Synoptic Project, District of Kenora (Patricia Portion); p. 8-11 *in* Summary of Field Work, 1976, by the Geological Branch, edited by V.G. Milne, W.R. Cowan, K.D. Card, and J.A. Robertson, Ontario Division of Mines, Miscellaneous Paper 67, 183p.
1977: Birch Lake Area, District of Kenora, Patricia Portion; p. 9-11 *in* Summary of Field Work, 1977, by the Geological Branch, edited by V.G. Milne, O.L. White, R.B. Barlow, and J.A. Robertson, Ontario Geological Survey, Miscellaneous Paper 75, 208p.
1978: Geology of the Earngey-Costello Area, District of Kenora, Patricia Portion; Ontario Geological Survey, Open File Report 5240, 210p. Accompanied by Preliminary Maps P.932, P.1056, P.1057, P.1058, scale 1 inch to 1/4 mile.
1985: Physical Volcanology and Stratigraphy of the Confederation Lake Area, District of Kenora (Patricia Portion): Ontario Geological Survey, Report 236, 117p. Accompanied by Map 2498.

Thurston, P.C., and Breaks, F.W.
1978: Metamorphic and Tectonic Evolution of the Uchi-English River Subprovince; *in* Metamorphism in the Canadian Shield, Geological Survey of Canada, Paper 78-10.

Thurston, P.C., and Jackson, M.C.
1978: Confederation Lake Area, District of Kenora (Patricia Portion); Ontario Geological Survey, Preliminary Map P.1975, Geological Series, scale 1:63 360 or 1 inch to 1 mile.

Thurston, P.C., Raudsepp, M., and Wilson, B.C.
1974: Earngey Township and Part of Birkett Township, District of Kenora; Ontario Division of Mines, Preliminary Map P.932, scale 1 inch to 1/4 mile.

Thurston, P.C., Wan, J., Squair, H.S., Warburton, A.F., and Wierzbicki, V.W.
1978: Volcanology and Mineral Deposits of the Uchi- Confederation Lakes Area, Northwestern Ontario; *in* Toronto '78 Field Trips Guidebook, edited by A.L. Currie and W.C. Mackasey, Geological Society of America.

Wiener, N.
1949: Extrapolation, Interpolation and Smoothing of Stationary Time Series; J. Wiley and Sons, New York.

Wilson, H.D.B.
1971: The Superior Province in the Precambrian of Manitoba; Geological Association of Canada, Special Paper Number 9, p.41-49.

INDEX

Ministry of Northern Development and Mines

Ontario

Ontario Geological Survey

Map 2494

RED LAKE – BIRCH LAKE

DISTRICT OF KENORA

Residual Component of Bouguer Gravity

Scale 1:250 000

Scale, 1 inch to 200 miles

Aeromagnetic reference 7010G, 7011G, 7266G, 7122G, 7123G, 7124G.
NTS reference 52J,K,L,M,N,O.
Gravity map reference No. 100 (Energy, Mines & Resources, Canada).

SOURCES OF INFORMATION

Gravity survey and compilation by V.K. Gupta, D.R. Wadge and assistants, Ontario Geological Survey, 1976, 1977.

Gravity data reduction by Gravity Division, Earth Physics Branch, Energy, Mines and Resources, Canada, 1976.

Geology generalized by V.K. Gupta, D.R. Wadge from published maps of the Ontario Geological Survey.

Cartography by M.G. Sefton and assistants, Surveys and Mapping Branch, 1983.

Preliminary maps, Ontario Geological Survey,
P. 1196, Bouguer Gravity map, Birch-Uchi-Confederation Lakes Area, Scale 1 inch to 2 miles, 1976.
P. 1248, Bouguer Gravity and Generalized Geology, Red Lake Area, Scale 1:100 000, 1978.

Base map derived from NTS sheets 52J,K,L,M,N,O with additional information by V.K. Gupta.

Magnetic declination in the area was approximately 5°43'E, 1977.

Every possible effort has been made to ensure the accuracy of the information presented on this map, but the Ontario Ministry of Natural Resources does not assume any liability for errors that may occur. Source references are included and users may wish to verify critical information.

Parts of this publication may be quoted if credit is given. It is recommended that reference to this map be made in the following form:
Gupta, V.K. and Wadge, D.R.
1986: Residual Component of Bouguer Gravity, Red Lake-Birch Lake, District of Kenora; Ontario Geological Survey, Map 2494, Geophysical/Geochemical Series, Scale 1:250 000. Survey 1976, 1977.
This map is published with the permission of E.G. Pye, Director, Ontario Geological Survey.

LEGEND

PHANEROZOIC

CENOZOIC

QUATERNARY

RECENT

Organic mud, lacustrine and fluvial clay, silt and sand.

PLEISTOCENE

Glacial till, lacustrine varved clay, clay and silt, fluvial silt and sand.

UNCONFORMITY

PRECAMBRIAN*

EARLY PRECAMBRIAN

INTRUSIVE ROCKS

FELSIC TO INTERMEDIATE INTRUSIVE ROCKS

5 Undifferentiated.
5a Granite (in the strict sense).
5b Granodiorite.
5c Trondhjemite.
5d Quartz Monzonite.
5e Syenodiorite.
5f Subvolcanic Intrusives.

INTRUSIVE CONTACT

INTERMEDIATE TO ULTRAMAFIC INTRUSIVE ROCKS

4a Intermediate to mafic intrusives.
4b Serpentinized or carbonatized ultramafic intrusives.

INTRUSIVE CONTACT

METASEDIMENTARY ROCKS

3a Metasediments.
3b Migmatitic metasedimentary migmatite.
3c Diatexitic metasedimentary migmatite.

METAVOLCANIC ROCKS

FELSIC AND INTERMEDIATE METAVOLCANIC ROCKS

2 Undifferentiated.
2a Intermediate metavolcanics.
2b Felsic metavolcanics.

INTERMEDIATE AND MAFIC METAVOLCANICS ROCKS

1 Undifferentiated.
1a Mafic metavolcanics.

** These rock units are grouped lithologically and the order does not necessarily imply age relationship between groups.*

SYMBOLS

Geological boundary.

Anticline, syncline.

Fault.

Geological subprovince boundary, in places marked by fault zone.

Positive Contour.

Negative Contour.

Zero Contour.

Contour interval 20 gravity unit or 2 mgal.

TECHNICAL NOTES

The residual component was graphically separated from the Bouguer gravity map 2492.

Published 1986

Ministry of Northern Development and Mines
Ontario

Ontario Geological Survey

Map 2493

RED LAKE – BIRCH LAKE

DISTRICT OF KENORA

Regional Component of Bouguer Gravity

Scale 1:250 000

Aeromagnetic reference 7010G, 7011G, 7266G, 7122G, 7123G, 7124G.
NTS reference 52J/K,L,M,N,O.
Gravity map reference No. 100 (Energy, Mines & Resources, Canada).

SYMBOLS

Regional gravity low.

Contour interval is 20 gravity units (= 2 mgal).

TECHNICAL NOTES

The regional component was graphically separated from the Bouguer gravity map 2492.

SOURCES OF INFORMATION

Gravity survey and compilation by V.K. Gupta, D.R. Wadge and assistants, Ontario Geological Survey, 1976, 1977.

Gravity data reduction by Gravity Division, Earth Physics Branch, Energy, Mines and Resources, Canada, 1976.

Geology generalized by V.K. Gupta, D.R. Wadge from published maps of the Ontario Geological Survey.

Cartography by M.G. Sefton and assistants, Surveys and Mapping Branch, 1983.

Preliminary maps, Ontario Geological Survey:
P. 1186, Bouguer Gravity map, Bloch-Uchi-Confederation Lakes Area, Scale 1 inch to 2 miles, 1978.
P. 1248, Bouguer Gravity and Generalized Geology, Red Lake Area, Scale 1:100 000, 1978.

Base map derived from NTS sheets 52J/K,L,M,N,O with additional information by V.K. Gupta.

Magnetic declination in the area was approximately 9°43'E, 1977.

Every possible effort has been made to ensure the accuracy of the information presented on this map, but the Ontario Ministry of Natural Resources does not assume any liability for errors that may occur. Source references are included and users may wish to verify critical information.

Parts of this publication may be quoted if credit is given. It is recommended that reference to this map be made in the following form:
Gupta, V.K. and Wadge, D.R.
1980: Regional Component of Bouguer Gravity, Red Lake-Birch Lake, District of Kenora, Ontario; Geological Survey, Map 2493, Geophysical/Geochemical Series, Scale 1:250 000. Survey 1976, 1977.
This map is published with the permission of E.G. Pye, Director, Ontario Geological Survey.

Published 1980

Ministry of Northern Development and Mines

Ontario

Ontario Geological Survey

Map 2492

RED LAKE – BIRCH LAKE

DISTRICT OF KENORA

Bouguer Gravity

Scale 1:250 000

Aeromagnetic reference 7010G, 7011G, 7266G, 7122G, 7123G, 7124G.
NTS reference 52J,K,L,M,N,O.
Gravity map reference No. 100 (Energy, Mines & Resources, Canada).

SOURCES OF INFORMATION

Gravity survey and compilation by V.K. Gupta, D.R. Wadge and assistants, Ontario Geological Survey, 1976, 1977.

Gravity data reduction by Gravity Division, Earth Physics Branch, Energy, Mines and Resources, Canada, 1976.

Geology generalized by V.K. Gupta, D.R. Wadge from published maps of the Ontario Geological Survey.

Cartography by M.G. Sefton and assistants, Surveys and Mapping Branch, 1983.

Preliminary maps, Ontario Geological Survey, P. 1186, Bouguer Gravity map, Birch-Uchi-Confederation Lakes Area, Scale 1 inch to 2 miles, 1976. P. 1248, Bouguer Gravity and Generalized Geology, Red Lake Area, Scale 1:100 000, 1978.

Base map derived from NTS sheets 52J,K,L,M,N,O with additional information by V.K. Gupta.

Magnetic declination in the area was approximately 5°43' E. 1977.

Every possible effort has been made to ensure the accuracy of the information presented on this map, but the Ontario Ministry of Natural Resources does not assume any liability for errors that may occur. Source references are included and users may wish to verify critical information.

Parts of this publication may be quoted if credit is given. It is recommended that reference to this map be made in the following form:
Gupta, V.K. and Wadge, D.R.
1980: Bouguer Gravity, Red Lake-Birch Lake, District of Kenora; Ontario Geological Survey, Map 2492, Geophysical-Geochemical Series, Scale 1:250 000. Survey 1976, 1977.

This map is published with the permission of E.G. Pye, Director, Ontario Geological Survey.

LEGEND

PHANEROZOIC

CENOZOIC

QUATERNARY

RECENT

Organic mud, lacustrine and fluvial clay, silt and sand.

PLEISTOCENE

Glacial till, lacustrine varved clay, clay and silt, fluvial silt and sand.

UNCONFORMITY

PRECAMBRIAN*

EARLY PRECAMBRIAN

INTRUSIVE ROCKS

FELSIC TO INTERMEDIATE INTRUSIVE ROCKS

5 Undifferentiated.
5a Granite (in the strict sense).
5b Granodiorite.
5c Trondhjemite.
5d Quartz Monzonite.
5e Syenodiorite.
5f Subvolcanic intrusives.

INTRUSIVE CONTACT

INTERMEDIATE TO ULTRAMAFIC INTRUSIVE ROCKS

4a Intermediate to mafic intrusives.
4b Serpentinized or carbonatized ultramafic intrusives.

INTRUSIVE CONTACT

METASEDIMENTARY ROCKS

3a Metasediments.
3b Migmatitic metasedimentary migmatite.
3c Diatexitic metasedimentary migmatite.

METAVOLCANIC ROCKS

FELSIC AND INTERMEDIATE METAVOLCANIC ROCKS

2 Undifferentiated.
2a Intermediate metavolcanics.
2b Felsic metavolcanics.

INTERMEDIATE AND MAFIC METAVOLCANICS ROCKS

1 Undifferentiated.
1a Mafic metavolcanics.

** Those rock units are grouped lithologically and the order does not necessarily imply age relationship between groups.*

SYMBOLS

Geological boundary.

Anticline, syncline.

Fault.

Geological subprovince boundary, in places marked by fault zone.

Gravity high.

Gravity low.

Contours of equal Bouguer anomalies at intervals of 20 gravity unit (20 gravity unit = 2 mgal).

TECHNICAL NOTES

Observed gravity values are based on the National Gravity Net which is consistent with the International Gravity Standardization Net 1971 (IGSN 71). Theoretical gravity values are computed using the Geodetic Reference System 1967 (GRS 67). Bouguer anomalies have been calculated assuming a vertical gravity gradient of 0.3086 mgal/m and a crustal density of 2.67 g/cm³.

The randomly spaced Bouguer gravity data were interpolated to a 1.609 km grid-cell size for machine contouring. A smoothing window was applied to the final contours.

Published 1980.

Ministry of Northern Development and Mines

Ontario

Ontario Geological Survey

Map 2495

RED LAKE – BIRCH LAKE

DISTRICT OF KENORA

Second Vertical Derivative of Bouguer Gravity

Scale 1:250 000

Scale, 1 inch to 200 miles

Aeromagnetic reference 7010G, 7011G, 7266G, 7122G, 7123G, 7124G.
NTS reference 52J,K,L,M,N,O.
Gravity map reference No. 100 (Energy, Mines & Resources, Canada).

SOURCES OF INFORMATION

Gravity survey and compilation by V.K. Gupta, D.R. Wadge and assistants, Ontario Geological Survey, 1976, 1977.

Gravity data reduction by Gravity Division, Earth Physics Branch, Energy, Mines and Resources, Canada, 1976.

Geology generalized by V.K. Gupta, D.R. Wadge from published maps of the Ontario Geological Survey.

Cartography by M.G. Sefton and assistants, Surveys and Mapping Branch, 1983.

Preliminary maps, Ontario Geological Survey:
P. 1186, Bouguer Gravity map, Birch-Uchi-Confederation Lakes Area, Scale 1 inch to 2 miles, 1976.
P. 1248, Bouguer Gravity and Generalized Geology, Red Lake Area, Scale 1:100 000, 1978.

Base map derived from NTS sheets 52J,K,L,M,N,O with additional information by V.K. Gupta.

Magnetic declination in the area was approximately 5°43'E, 1977.

Every possible effort has been made to ensure the accuracy of the information presented on this map, but the Ontario Ministry of Natural Resources does not assume any liability for errors that may occur. Source references are included and users may wish to verify critical information.

Parts of this publication may be quoted if credit is given. It is recommended that reference to this map be made in the following form:
Gupta, V.K. and Wadge, D.R.
1986 Second Vertical Derivative of Bouguer Gravity, Red Lake-Birch Lake, District of Kenora, Ontario Geological Survey, Map 2495, Geophysical/Geochemical Series, Scale 1:250 000. Survey 1976, 1977.
This map is published with the permission of E.G. Pye, Director, Ontario Geological Survey.

LEGEND

PHANEROZOIC

CENOZOIC

QUATERNARY

RECENT

Organic mud, lacustrine and fluvial clay, silt and sand.

PLEISTOCENE

Glacial till, lacustrine varved clay, clay and silt, fluvial silt and sand.

UNCONFORMITY

PRECAMBRIAN*

EARLY PRECAMBRIAN

INTRUSIVE ROCKS

FELSIC TO INTERMEDIATE INTRUSIVE ROCKS

5 Undifferentiated.
5a Granite (in the strict sense).
5b Granodiorite.
5c Trondhjemite.
5d Quartz Monzonite.
5e Syenodiorite.
5f Subvolcanic Intrusives.

INTRUSIVE CONTACT

INTERMEDIATE TO ULTRAMAFIC INTRUSIVE ROCKS

4a Intermediate to mafic intrusives.
4b Serpentinized or carbonatized ultramafic intrusives.

INTRUSIVE CONTACT

METASEDIMENTARY ROCKS

3a Metasediments.
3b Metatextic metasedimentary migmatite.
3c Diatexitic metasedimentary migmatite.

METAVOLCANIC ROCKS

FELSIC AND INTERMEDIATE METAVOLCANIC ROCKS

2 Undifferentiated.
2a Intermediate metavolcanics.
2b Felsic metavolcanics.

INTERMEDIATE AND MAFIC METAVOLCANICS ROCKS

1 Undifferentiated.
1a Mafic metavolcanics.

**These rock units are grouped lithologically and the order does not necessarily imply age relationship between groups.*

SYMBOLS

Geological boundary.

Anticline, syncline.

Fault.

Geological subprovince boundary, in places marked by fault zone.

Positive Contour.

Negative Contour.

Zero Contour.

Contour interval 0.5 mgal/km²

TECHNICAL NOTES

The Second Vertical derivative map was computed utilizing an optimum Second Vertical derivative matched filter designed on the basis of Wiener filter theory. The positive and negative second Vertical derivative anomalies generally correspond with mafic and felsic rock units respectively. The zero contours of the Second Vertical derivative usually coincide with density boundaries.

Published 1986